Application of Light Detection and Ranging (Lidar) and Multi-temporal Landsat for Mapping and Monitoring Wetlands

Nilam Kayastha

Dissertation submitted to the faculty of the Virginia Polytechnic Institute and State University in partial fulfillment of the requirements for the degree of

Doctor of Philosophy

In

Geospatial and Environmental Analysis

Valerie A. Thomas, Co-Chair

John M. Galbraith, Co-Chair

Megan W. Lang

Randolph H. Wynne

December 19 2013

Blacksburg, VA

Keywords: wetlands, lidar, Landsat, multi-temporal,change detection, terrain analysis

Application of Light Detection and Ranging (Lidar) and Multi-temporal Landsat for Mapping and Monitoring Wetlands

Nilam Kayastha

ABSTRACT

To successfully protect and manage wetlands, efficient and accurate tools are needed to identify where wetlands are located, the wetland type, what condition they are in, what are the stressors present, and the trend in their condition. Wetland mapping and monitoring are useful to accomplish these tasks. Wetland mapping and monitoring with optical remote sensing data has mainly focused on using a single image or using image acquired over two seasons within the same year. Now that Landsat data are available freely, a multi-temporal approach utilizing images that span multiple seasons and multiple years can potentially be used to characterize wetland dynamics in more detail. In addition, newer remote sensing techniques such as Light Detection and Ranging (lidar) can provide highly detailed and accurate topographic information, which can improve our ability to discriminate wetlands. Thus, the overall objective of this study was to investigate the utility of lidar and multi-temporal Landsat data for mapping and monitoring of wetlands. My research is presented as three independent studies related to wetland mapping and monitoring. In the first study, inter-annual time series of Landsat data from 1985 to 2009 was used to map changes in wetland ecosystems in northern Virginia. Z-scores calculated on tasseled cap images were used to develop temporal profile for wetlands delineated by the National Wetland Inventory. A change threshold was derived based on the Chi-square distribution of the Z-scores. The accuracy of a change/no change map produced was 89% with a

kappa value of 0.79. Assessment of the change map showed that the method used was able to detect complete wetland loss together with other subtle changes resulting from development, harvesting, thinning and farming practices. The objective of the second study was to characterize differences in spectro-temporal profile of forested upland and wetland using intra and inter annual time series of Landsat data (1999-2012). The results show that the spector-temporal metrics derived from Landsat can accurately discriminate between forested upland and wetland (accuracy of 88.5%). The objective of the third study was to investigate the ability of topographic variables derived from lidar to map wetlands. Different topographic variables were derived from a high resolution lidar digital elevation model. Random forest model was used to assess the ability of these variables in mapping wetlands and uplands area. The result shows that lidar data can discriminate between wetlands and uplands with an accuracy of 72%. In summary, because of its spatial, spectral, temporal resolution, availability and cost Landsat data will be a primary data source for mapping and monitoring wetlands. The multi-temporal approach presented in this study has great potential for significantly improving our ability to detect and monitor wetlands. In addition, synergistic use of multi-temporal analysis of Landsat data combined with lidar data may be superior to using either data alone for future wetland mapping and monitoring approaches.

.

ACKNOWLEDGEMENTS

I would like to thank my advisors, Dr. Valerie Thomas and Dr. John Galbraith for providing me with this opportunity to conduct this research. This research would not have been possible without their guidance, insight and support. I am especially grateful for their encouragement and for trusting my commitment to finishing the dissertation. I would also like to thank my committee members, Dr. Randolph Wynne and Dr. Megan Lang for their guidance and suggestions, which have been instrumental in successful completion of this dissertation.

This research would not have been possible without help and input from many other people and organization. I would also like to thank Kevin McGuckin and Brian Diggs from Conservation Management Institute at Virginia Tech for their help in interpreting the aerial photos. I am especially grateful to Ms. Alison Rogerson at Delaware Department of Natural Resources and Environmental Control for providing me with the field data collected for comprehensive assessment of wetlands in Delaware.

I would also like to express my thanks to all my friends in Blacksburg for making my stay memorable and enjoyable. I would especially like to acknowledge Jessica Walker for her technical help in my research.

I am grateful to my parents for their sacrifice and recognizing the importance of education. Finally, I would like to thank my husband Asim for his love and encouragement.

ATTRIBUTION

One of the chapter presented as part of this dissertation was published in the journal Wetlands. The paper was the results of a collaborative effort of the author and advisors Dr. Valerie Thomas and Dr. John Galbraith, as well as Dr. Asim Banskota.

Chapter 2: Monitoring Wetland Change using Inter-Annual Landsat Time-Series

Chapter 2 was published in Wetlands, volume 32, October 2012, pages 1149–1162.

Dr. Valerie Thomas is assistant professor in the Department of Forest Resources and Environmental Conservation at Virginia Polytechnic Institute and State University.

Dr. John Galbraith is associate professor in the Department of Crop & Soil Environmental Sciences at Virginia Polytechnic Institute and State University.

Dr. Asim Banskota is currently a research associate in the Department of Forest Resources at University of Minnesota.

Table of Contents

ABSTRACT ii
ACKNOWLEDGEMENTS iv
ATTRIBUTION v
Table of Contents vi
List of Figures ix
List of Tables xii
CHAPTER 1: General Introduction and Objective 1
1. Introduction: Research background and justification 1
1.1 Wetland: Definition and importance 1
1.2 Remote sensing for mapping and monitoring wetlands 2
1.3 Multi-temporal analysis for mapping and monitoring wetlands 7
1.4 Objectives 11
References 13
CHAPTER 2: Monitoring Wetland Change using Inter-Annual Landsat Time-Series 16
Abstract 17
1. Introduction 17
1.1 Background 17
1.2 National wetland inventory data 19
2. Data and Methods 19
2.1 Study area 19
2.2 Landsat time series development 19
2.3 Aggregation of NWI class 20
2.4 Identification of reference wetland samples 21
2.5 Z-score calculation 21
2.6 Determining change/no-change 22
2.6 Flagging false change 22
2.7 Validation 23
3. Results 24

3.1 Z-score profile of reference wetlands 24
3.2 Accuracy assessment 24
4. Discussion 25
5. Conclusion 28
Acknowledgement 29
References 29
CHAPTER 3: Discriminating Forested Wetlands and Uplands Using Temporal Metrics Derived From Landsat Time Series 31
Abstract 32
1. Introduction 33
2. Methods 37
2.1 Study area 37
2.2 Field data 39
2.3 Landsat data and indices calculation 41
2.4 Smoothing and curve fitting 42
2.5 Extraction of temporal metrics 44
2.6 Random forest classification 46
3. Results 48
3.1 Time series profile of wetland and upland forests 48
3.2 Random forest classification 50
4. Discussion 56
5. Conclusion 60
Acknowledgement 60
References 61
CHAPTER 4: Utility of Lidar Derived Topographic Metrics for Improved Wetland Mapping 66
Abstract 66
1. Introduction 67
2. Methods 73
2.1 Study area 73
2.2 Lidar data and preprocessing 74

2.3 Computation of terrain variables 74
2.4 Field data collection 76
2.5 Random forest classification 76
2.6 Depression identification 77
3. Results 78
3.1 Wetness indices from different flow routing algorithm 78
3.2 Wetland classification accuracy 80
3.3 Accuracy of depression identification 85
4. Discussion 86
5. Conclusion 92
References 94
CHAPTER 5: Conclusions **99**

List of Figures

CHAPTER 2: Monitoring Wetland Change using Inter-Annual Landsat Time-Series **16**

Fig. 1. Study area: (a) State of Virginia showing study area and (b) study area overlaid on a false color composite of 2008 Landsat scene (red: near-infrared band; green: green band; blue: red band). Stafford county is highlighted in yellow. In a standard false color composite green vegetation appears in shades of red and urban areas in shades of cyan 20

Fig. 2. Example of Z-Score profile of a changed location.The profile highlights the importance of threshold selection for change detection. The actual change for this example occurred in the year 2000 (circled in solid line). Increasing the threshold value (α 00.001) will not identify this point as changed. Change is only identified in the year 2002 23

Fig. 3. Validation points used for accuracy assessment..... 24

Fig. 4. Z-score profiles of different wetland types in the region produced using leaf on Landsat images. The X-axis represents different years (1985-2009) in the image time series 24

Fig. 5. Disturbance events occurring in the study area between 1985 and 2009 as captured by the Landsat time series 26

Fig. 6. Disturbance year map produced from Landsat time series..... 26

Fig. 7. Examples of Z-score trajectory of different disturbance events: (a) complete vegetation removal, (b) conversion to a suburban development, (c) thinning of a forested wetland, (d) conversion to open water 27

CHAPTER 3: Discriminating Forested Wetlands and Uplands Using Temporal Metrics Derived From Landsat Time Series **31**

Fig. 1. Comparison of MODIS (a) and Landsat (b) spatial scale overlaid with the wetland layer. National Wetland Inventory wetlands in the study area occur in small, narrow patches and are fragmented. The resolution of MODIS pixels in (a) is too coarse to capture the spatial detail required 37

Fig. 2. The state of Delaware showing distribution of non-tidal forested wetlands derived from National Wetland Inventory data (http://www.fws.gov/wetlands/Data/Mapper.html)..... 39

Fig. 3. An example of temporal profile of wetland (a) and upland (b) from NDVI time series, with the fitted curve from rlowess (solid line) 48

Fig. 4. An example of temporal profile of wetland (a) and upland (b) from NDMI time series, with the fitted curve from rlowess (solid line) 48

Fig. 5. An example of temporal profile of wetland (a) and upland (b) from TCW time series, with the fitted curve from rlowess (solid line) 49

Fig. 6. An example of rlowess fit (black line) with 95% confidence interval bound (red dashed line) 50

Fig. 7. Variable importance plot for a three-class random forest model developed with NDMI temporal metric. Units are percent reduction in classification accuracy which would results when a given variable is removed from the classification model. See Table 1 for variable definition 52

Fig. 8. Variable importance plot for two class random forest model developed with NDMI temporal metrics. Units are percent reduction in classification accuracy which would result when a given variable is removed from classification model. See Table 1 for variable definition 53

Fig. 9. Scatter plot of two most important variable identified by random forest in discriminating between wetlands (plus sign) and uplands (triangle sign). TAUC is total area under the curve and Min05L is 5th percentile of the left hand side of the curve 54

Fig. 10. Variable importance plot for classification of flat vs. riverine wetland types developed with NDVI temporal metrics. Units are percent reduction in classification accuracy which would results when a given variable is removed from classification model. See Table 1 for variable definition 55

CHAPTER 4: Utility of Lidar Derived Topographic Metrics for Improved Wetland Mapping 66

Fig. 1. Map of the study area showing location within the Commonwealth of Virginia. The grey shaded area represents Prince William and Faquier County and the red box represents the approximate location of our study area 74

Fig. 2. Wetness index calculated from different flow routing methods D8 (a), D∞ (b), MFD (c), and SAGA (d) 79

Fig. 3. Classification output of the most accurate random forest model overlaid with NWI wetlands. This model included wetness index calculated from distributed flow routing method and other terrain variables. The red circle indicates the general location of wetland mitigation site in the study area 82

Fig. 4. Classification output of the least accurate random forest model, overlaid with NWI wetlands. This model included wetness index calculated from single direction flow routing method and other terrain variables. The red circle indicates the general location of wetland mitigation site in the study area 83

Fig. 5. Sinks identified in red polygons using depression filling technique (a) and examples of identified sinks (b). On the left is a new wetland site created for wetland mitigation, which is not mapped as wetlands in NWI and on the right are sinks identified in a forested area impounded by the road, which are mapped as wetlands in NWI.....86

Fig. 6. Liner man-made drainage features aerial photo (top) and lidar DEM (bottom.....91

List of Tables

CHAPTER 2: Monitoring Wetland Change using Inter-Annual Landsat Time-Series 16

Table 1 List of Landsat Thematic Mapper (TM) and Enhanced Thematic Mapper Plus (ETM+) image date, sensor types and assigned number in the time series 20

Table 2 Aerial photo dates used and corresponding percentage of NWI mapped in the study area 20

Table 3 Coefficients used for tasseled cap transformation of Landsat data based on Crist (1985) 22

Table 4 Error matrix for the change detection analysis 25

Table 5 Summary of wetland disturbance in the study area 25

Table 6 Descriptive statistics for the change example. The statistics includes mean and standard deviation of the Z-score values before and after the change and change magnitude (difference between the Z-score value before and after the change) 27

CHAPTER 3: Discriminating Forested Wetlands and Uplands Using Temporal Metrics Derived From Landsat Time Series 31

Table 1. List and description of temporal metrics derived from Landsat time series data 44

Table 2. Accuracy statistics for three class classification (wetland forest, upland forest and mixed wetland) 51

Table 3. Accuracy statistics for two class classification (wetland forest and upland forest) 53

Table 4. Accuracy statistics for classification of flat and riverine wetland types 55

CHAPTER 4: Utility of Lidar Derived Topographic Metrics for Improved Wetland Mapping 66

Table 1. Difference in mean index value of TWI generated using different flow routing method between wetlands and uplands 80

Table 2 Wetland Classification accuracy with TWI_{SAGA} 81
Table 3 Wetland Classification accuracy with TWI_{MFD} 81
Table 4 Wetland Classification accuracy with $TWI_{D\infty}$ 81
Table 5 Wetland Classification accuracy with TWI_{D8} 81
Table 6 Summary table of variable importance for random forest classification 84
Table 7 Comparison of sinks with the NWI wetland and hydric/non-hydric soils 85

CHAPTER 1

General Introduction and Objective

1. Introduction: Research background and justification

1.1 Wetland: Definition and importance

"Wetlands" is a generic term that groups a wide range of habitats that share a common feature of seasonal, continuous, or periodic standing water or saturated soils, and a dominance of hydrophytic vegetation. All wetland definitions are based on hydrologic condition (Zedler and Kercher, 2005). However, there is no single universally accepted definition of wetlands (Heimlich et al., 1998), primarily due to the large variability in the frequency, depth and duration of flooding from year to year (Mitsch and Gosselink, 2000). Wetlands vary widely because of regional and local differences in soils, topography, climate, hydrology, water chemistry, vegetation, and other factors, including human disturbance.

Two of the most widely used wetland definitions include Clean Water Act regulatory definitions and the definition by Cowardin et al. (1979). Section 404 of the Clean Water Act is the major federal regulation aimed at protecting wetlands: wetlands identified under this regulation are termed as "jurisdictional wetlands" (Messina and Connor, 2000). The Clean Water Act defines wetlands as "areas that are inundated or saturated by surface or ground water at a frequency and duration sufficient to support, and that under normal circumstances do support, a prevalence of vegetation typically adapted for life in saturated soil conditions" (U.S.E.P.A., 1977). Cowardin et al. (1979), defines wetlands as "land transitional between terrestrial and aquatic systems, where the water table is usually at or near the surface, or the land is covered by shallow water". For purposes of the Cowardin et al. (1979) classification, wetlands must have one or more of the following three attributes: (a) at least periodically, the land supports

hydrophytes, (b) the substrate is predominantly undrained hydric soil, and (c) the substrate is non-soil and is saturated with water or covered by shallow water at some time during the growing season of each year.

Historically, wetlands were regarded as wasteland and were drained, filled or manipulated to improve their worth and contribution to society (Mitsch and Gosselink, 2000). Some were drained to lessen the chance of mosquito-carried disease. Although there is no database on the historical distribution of wetlands, it is estimated that 50% of the global wetland area has been lost to human activities (Dudgeon, 2003). It is believed that overall 53% of the wetlands in the conterminous United States were lost from the 1780s to the 1980s (Mitsch and Gosselink, 2000).

The biologic, aesthetic, and economic values of wetlands are now known to be disproportionately large compared to the often small percentage of the landscape they occupy (Lang et al., 2008), which has led to efforts at local, national and international level for conservation of these ecosystem. Some of the important functions wetlands provide are habitat for diverse flora and fauna, groundwater recharge, flood attenuation, sediment retention, pollutant removal and carbon sequestration. Despite the national and international recognition of the importance of these ecosystem and ongoing efforts and legislation for protection of these ecosystems, wetlands worldwide are threatened due to human activities that include conversion of wetlands to other land use, urbanization, agricultural and silvicultural activities and hydrological alteration. Accurate mapping and monitoring of wetlands is essential for successful conservation and management efforts.

1.2 Remote sensing for mapping and monitoring wetlands

Manual interpretation of aerial photographs has been a widely used technique for wetland mapping. In the United States, the US Fish and Wildlife Service National Wetland Inventory

(NWI) program has produced a nationwide wetland distribution map, with ongoing updates (http://www.fws.gov/wetlands/Data/Mapper.html). NWI wetland maps are produced using mid-to-high altitude aerial photographs, usually taken during early spring. Aerial photographs at scales from 1:40,000 to 1:80,000 (or 1:133,000 for earlier maps) are used. Manual photo-interpretation techniques coupled with field verification, topographic maps and soil information are used for identification and classification of wetlands (Dahl and Watmough, 2007). Studies have shown varying levels of accuracies of NWI maps. In general they have been reported to have low commission error and in many cases high omission error (Wright and Gallant, 2007). Low commission error indicates that an area classified as wetland by NWI exists or existed at the time when photograph was taken. However, the high omission error indicates that many wetland areas are possibly not mapped by NWI. Stolt and Baker (1995) reported omission error rates greater than 85% in the Blue Ridge Physiographic region of Central Virginia, while Werner (2003) reported that 42% of field surveyed Palustrine wetlands were not mapped by NWI. Morrissey and Sweeney (2006) reported that NWI underestimated forested wetlands in Vermont by 39%. Galbraith et al. (2003) found that NWI underestimated wetlands by about 90% in a study in central Virginia. However, the effectiveness of NWI in estimating wetland area nationwide is not precisely known due to variability in land use, disturbance, climate, soil and geology. For example, Kudray and Gale (2000) found an NWI accuracy of 90.7% for forested wetlands in the upper Great Lakes region.

Wetland delineation on an NWI map is generally accurate when there is an abrupt change in hydrology, soil or vegetation at the wetland boundary (National Research Council, 1995). However, the dynamic nature of wetland hydrology, especially their alternating dry and wet nature, poses a problem for accurate wetland mapping, especially in subtle-relief landscapes.

Wetlands occur along a continuum of soil moisture between permanently flooded and drier habitats. This makes many wetlands, especially the ones that are temporarily flooded or seasonally saturated, difficult to detect. Moreover, many wetlands are small or narrow, form in a variety of landforms and, their hydrology is affected by small changes in elevation. They are not only found in depressions but also in broad flats and gently sloping areas, which further complicates their identification. In many cases, vegetation communities of the drier wetlands are not dramatically different at wetland boundaries from adjacent uplands, making wetland delineation even more difficult.

More than half of the wetlands in the United States are forested. Forested wetlands are one of the most difficult wetland types to map due to presence of the canopy and ephemeral hydrology (Wright and Gallant, 2007 and Lang et al., 2008). Presence of dense canopy in the forested communities prevents observation of soil, hydrology and topographic features, which are important parameters for determining wetlands. Evergreen-forested wetlands are especially difficult to map as they retain their foliage year round. The biggest problem occurs when dense evergreen stands occur in both wetland and adjacent upland areas. In addition, topographic maps have too coarse vertical resolution to show the relatively small variations in topography that can cause forested wetland formation on flat, humid coastal plains, which further makes detection of these wetlands difficult.

Manual interpretation of aerial photographs heavily relies on the knowledge of the photo-interpreter for wetland identification. Thus photo-interpretation is highly subjective and the repeatability of the method is questionable. High costs associated with the acquisition of aerial photos decreases their viability for use in timely updates of wetland maps. In addition, uses of single-date images to produce wetland maps are not informative about the wetland dynamics

(Wright and Gallant, 2007), which results in the misclassification of or complete inability to detect many wetlands. There also exists a large gap in completion status and digital availability of high resolution wetland, soils and topographic maps, indicating a need for alternative approaches for wetland identification.

Satellite remote sensing, because of its repeatable and consistent measurement, has proven to be the most cost-effective data source for large-scale land-cover mapping. When using multispectral images for wetland classification, there is often a tradeoff between spectral and spatial resolution. While spatial resolution is important for the identification of wetland patches, spectral resolution is important for discriminating between wetland and upland vegetation communities with similar spectral responses. Sensors such as the Moderate Resolution Imaging Spectroradiometer (MODIS) have higher spectral resolutions compared to multispectral sensors such as Landsat, but are often unsuitable for wetland studies due to their coarse spatial resolution (MODIS-250 m pixels; Landsat-30 m pixels). High spatial resolution sensors, such as Systeme Pour l'Observation de la Terre SPOT (20 m) and Quickbird (2.5 m), are needed to identify small patches of wetland. However, these sensors often have low spectral resolution that limits their ability to discriminate different vegetation types. Multispectral satellite imagery, especially that collected by Landsat Thematic Mapper (TM) and Enhanced Thematic Mapper (ETM+), has been widely used for wetland inventorying and mapping. Sader et al. (1995) used unsupervised classification of Landsat data and classified forested wetlands with an overall accuracy of 72%. However, the user's accuracy for the forested wetland was very low (58%). Harvey and Hill (2001) compared wetland classification using aerial photos (1 m pixels), SPOT XS (20 m pixels), and Landsat (30 m pixels) and found that Landsat provided a more accurate classification than SPOT XS and comparable accuracy to that of aerial photographs. They reported superior

performance of Landsat compared to SPOT which resulted due to better spectral resolution and inclusion of middle infrared bands not available in SPOT.

Topography plays a key role in wetland formation. Lidar data can provide detailed and accurate ground elevation information for the identification of topographic features that indicate the presence of wetlands that would otherwise be undetected. Fine-scale elevation data are particularly helpful in flat, wetland-rich areas such as coastal plains where complex interspersion of uplands and lowlands may cause mapping confusion and inaccuracy (Maxa and Bolstad, 2007). Lidar is a relatively new technology and its full potential in wetland related studies is yet to be realized. Hogg and Holland (2008) compared the use of a digital elevation model (DEM) derived from lidar to DEMs derived from point elevation data in the Canadian National Topographic Series at 1:20,000 and 1:50,000 scales to detect wetlands in the Turkey Lakes region of Ontario, Canada. Wetland classification with the lidar-derived DEM was more accurate and identified 35% more wetland area than classification using the other two DEMs. Richardson et al. (2009) used a DEM derived from lidar and terrain analysis to delineate wetland boundaries with 80% spatial agreement between the field validated and mapped wetlands. However, the study was only validated in a small area the authors did not specify the relief gradient in the area. However, the authors indicate the area being characterized by pronounced depression area indicating that substantial relief gradient was present in the study area. Various information derived from lidar data in combination with optical data has the potential for improving wetland mapping. Specifically, studies have utilized lidar-derived DEMs to calculate topographic wetness index (TWI) (Sorensen and Seiber, 2007, Murphy et al., 2009 and Richardson et al., 2009) that can be used as an indicator of wetland distribution. Topographic wetness index, which indicates the potential of an area to accumulate water, can quantify the effect of topography on runoff

generation approximating the location of zones of saturation (Murphy et al., 2009). In addition to topographic information the intensity of lidar signal has also been used in detection of inundation beneath the forested canopies (Lang et al., 2008). Forested wetlands are one of the most difficult wetland types to detect with remote sensing as their canopies obscure underlying hydrology and topography. High resolution DEMs derived from lidar coupled with optical data can improve mapping of forested wetlands (Lang et al., 2013). However, lidar data are not available worldwide at free cost, and little repetition of data collection in the same place over time has occurred because of its expense.

1.3 Multi-temporal analysis for mapping and monitoring wetlands

The temporal resolution of images used has been found to be very important in wetland mapping and monitoring. Many wetland species have overlapping reflectance at peak biomass (Schmidt and Skidmore, 2003), and often, vegetation species occurring in wetlands are similar to vegetation occurring in the neighboring uplands. Accuracies of methods using single image in wetland mapping such as NWI are affected by the timing of image acquisition (eg, drier condition during drought, extremely wet season, foliation condition). Use of multi-season images help in discriminating between wetland types by detecting hydrological and phenological changes characteristic of those types (Wolter et al., 2005 and Baker et al., 2006). The basic approach is the use of leaf-off and leaf-on images from a single growing season. Leaf-on images are used for discrimination among vegetation communities while leaf-off images are used to detect wetland hydrology. The accuracy of wetland maps produced from multi-season images has shown to be superior compared to a single date image. Mackey (1990) noted that satellite imagery collected during different seasons enhances phenological, hydrological, and compositional changes across seasons and between years, which improves the ability to

discriminate between wetland vegetation types. Using Landsat images from two dates, Lunetta and Balogh (2000) improved the accuracy of wetland maps to 88% compared to 69% from a single date image. Pantaleoni et al. (2009) used two dates of ASTER images during a single growing season to discriminate between uplands, woody wetlands, emergent wetlands and open water. They reported that their detection accuracy was comparable to that of NWI. The authors also suggested use of inter-annual images to better characterize the phenological differences between wetland and upland vegetation communities. Townsend and Walsh (2001) used Landsat TM data from March to August in a single year and produced a detailed classification of vegetation communities, although an overall accuracy of 92% was achieved, the individual accuracy for wetland communities was only 72%.

Most of the studies utilizing multi-temporal data use imagery from relatively few dates and a single growing season. In recent years, multi-year seasonal time-series data has been used for improved land-cover classification. These studies have utilized longer time series (greater than 10 years) representing seasonal and inter-annual variability between land cover classes for improved discrimination (Bradley and Mustard, 2008 and Zoffoli et al., 2008). Time series data provide information that are directly linked to key aspects of vegetation functions, such as seasonality, productivity and inter-annual variability and therefore have tremendous potential for characterizing, classifying and mapping vegetation (Wessels et al., 2010). Inter-annual variability derived from time series data can be a useful metric when land cover types show amplified response to differences in environment condition. When several years of data are combined, characteristic temporal patterns can be observed which can be used to classify land cover (Liang, 2001 and Moody & Johnson, 2001). Data collected by sensors such as Advanced Very High Resolution Radiometer (AVHRR) and MODIS provide daily observation. Numerous studies

have utilized the rich temporal information provided by these sensors to study vegetation dynamics at global and regional level. However, the coarser spatial resolution (MODIS-250 m pixels; AVHRR-1 km pixels) makes them less reliable in local scales and in heterogeneous landscape. Especially in wetland environment, these coarser scale sensors may not detect fine spatial structure that results due to the variability of vegetation, soil and water in wetlands.

Recently, Landsat data has become available free of cost. At the spatial resolution of 30 m and images dating back to 1972, the opening of Landsat archive provides an opportunity to study land cover dynamics at higher spatial and temporal resolution. The Landsat archive can be used to assess the temporal pattern of different vegetation communities to improve discrimination which would otherwise not be possible using few images taken at different dates. Few studies have utilized Landsat time series data to assess vegetation dynamics. Most of these studies have focused on characterizing long-term averages and inter-annual variability in vegetation phenology (Fisher et al., 2006, Elmore et al., 2012 and Melaas et al., 2013). In these studies Landsat time series images are arranged by Julian dates, discarding the year of acquisition, to create temporal profiles indicative of average phenology curve. Some studies (Walker et al., 2012) have utilized data fusion techniques which downscale MODIS data to spatial resolution of Landsat to characterize phenology at annual scale. However, information derived from such fused techniques is complicated by land cover heterogeneity below the coarse spatial resolution of MODIS and uncertainty introduced by the data fusion algorithm (Melaas et al., 2013).

Landsat time series data has also been widely used in spectral trajectory analysis to identify changes in land cover. Traditional land cover change detection methods, known as bi-temporal techniques, utilizes images taken at two time periods to detect change in land cover. Selection of optimal scenes is very important in bi-temporal change detection techniques to minimize

variability in spectral properties that is induced due to changes in phenology (Coppin et al., 2004). In addition, if the gaps between the images are long, the discontinuities resulting from disturbance events may be indistinguishable (de Beurs and Henebry, 2005).

Trajectory analysis utilizes multiple images taken over same area over a longer time period to monitor changes. This technique compares temporal trajectories of spectral values (or derived indices) of land cover change characteristics throughout the monitoring period (Coppin et al., 2004). Use of longer time series offers sufficient temporal sampling in terms of duration and frequency to allow detection of changes amidst substantial variation (de Beurs and Henebry 2005). Kennedy et al. (2007) used a trajectory-based method using 19 annual Landsat scenes to detect forest disturbances. They used four idealized temporal trajectories (disturbance, disturbance and revegetation, revegetation, and revegetation to stable state) of spectral values to characterize disturbances. Using a least squares fit method they analyzed how well the spectral trajectory of an area fit the four models to detect disturbance event. Huang et al. (2010) developed a vegetation change tracker (VCT) model using the spectral temporal information to detect areas of forest disturbance. The model used a cross-correlation approach using Z-statistics to identify disturbance. Accuracy of 80% in detecting forest disturbance was achieved in the study. Kennedy et al (2010) introduced a new algorithm, Landsat-based detection of trends in disturbance and recovery (LandTrendr). The method uses temporal segmentation of the trajectory to identify pattern in the time series that is indicative of different disturbance events and recovery trajectory of forests after disturbance. These disturbance events include; abrupt events such as deforestation and fire as well as subtle changes in vegetation community due to insects and diseases. Most of these studies using trajectory analysis is aimed at detecting forest disturbance and do not make distinction of forested wetlands. In these studies, non-forest

wetlands were a major source of error as they were either mapped as forested or disturbed forest. All of these studies using dense Landsat time series till date have focused only on identifying disturbance in forested communities. Utility of these techniques to monitor disturbances in other ecosystem should be assessed.

Trajectory analysis provides a unique and improved opportunity for monitoring disturbance and recovery changes in wetlands. Most of the wetland change detection studies are bi-temporal in nature (Ramsey and Laine, 1997 and Rebelo et al., 2009). Because wetlands demonstrate high level of natural temporal variability, the use of coarse temporal resolution images pose significant constraints in wetland change studies (Nielsen et al., 2008). Changes due to vegetation phenology can be minimized to some extent by using images acquired at anniversary dates but variability due to abnormal hydrologic conditions, such as flooding or drought can make determination of wetland change more difficult. Nielsen et al. (2008) utilized images from spring, summer and fall dates for wetland change monitoring. Despite the use of multi-season imagery, many of the flooded wetlands (natural occurrence at that time in the area) were classified as having high probability of change. Misinterpretation of wetland loss or gain can also result from factors such as farming of wetlands during dry cycles, drought conditions, excess surface water or flooding (Dahl, 2006). Use of dense time series of images will increase our ability to characterize the temporal variability of wetland and detect wetland change with greater accuracy.

1.4 Objectives

As discussed in previous sections, remote sensing data is inherent tool for wetland mapping and monitoring. Out of the different remote sensing sensors available, Landsat data because of its spatial coverage, spatial resolution of 30 meter, spectral bands in visible and near infrared region

and free availability will be one of the major data source for large scale and routine mapping and monitoring of wetland. Limitations of optical data, which is mainly associated with inability to directly observe soil saturation or flooding can be compensated using multi-temporal images. In recent years, the paradigm of multi-temporal analysis has shifted from analyzing two images in a year to multiple images spanning different seasons in a year and through multiple years. Now that all the past and future Landsat data is freely available, multi-temporal analysis can be extended to study land surface dynamics, such as wetlands, which was not possible due to coarser spatial resolution of available sensors. In addition to Landsat, newer remote sensing technology such as lidar that can provide detailed and accurate information on topography should be explored for mapping wetlands. The overall goal of this study was to assess the utility of lidar and time series Landsat data for mapping and monitoring of wetlands. The specific objectives are summarized below and are discussed as independent research papers.

- Evaluate the performance of use of inter-annual time series Landsat data in detecting disturbance in wetlands (Chapter 2).
- Assess the performance of time-series Landsat data (intra and inter annual) in discriminating between wetland and upland forests (Chapter 3).
- Assess the performance of topographic information derived from lidar in mapping wetlands (Chapter 4).

References

Baker, C., Lawrence, R., Montagne, C., & Patten, D. (2006). Mapping wetlands and riparian areas using Landsat ETM+ imagery and decision-tree-based models. Wetlands, 26, 465-474

Bradley B.A., & Mustard, J.F. (2005). Identifying land cover variability distinct from land cover change: cheatgrass in the Great Basin. Remote Sensing of Environment, 94, 204–213

Coppin, P., Jonckheere, I., Nackaerts, K., Muys, B., & Lambin, E. (2004). Digital change detection methods in ecosystem monitoring: A review. International Journal of Remote Sensing, 25, 1565−1596

Cowardin, L. M., Carter,V., Golet, F. C., & Laroe, E. T. (1979). Classification of wetlands and deepwater habitats of the United States. Washington, DC: U.S. Fish and Wildlife Service

Dahl T. E. (2006). Status and trends of wetlands in the conterminous United States, 1998–2004. U.S. Fish and Wildlife Service, Washington, DC

Dahl, T. E., & Watmough, M. D. (2007). Current approaches to wetland status and trends monitoring in prairie Canada and the continental United States of America. Canadian Journal of Remote Sensing, 33, S17–S27

de Beurs, K. M., & Henebry, G. M. (2005). A statistical framework for the analysis of long image time series. International Journal of Remote Sensing, 26, 1551−1573

Dudgeon, D. (2003). The contribution of scientific information to the conservation and management of freshwater biodiversity in tropical Asia. Hydrobiologia, 500, 295–14

Elmore, A.J., Guinn, S.M., Minsley, B.J., & Richardson, A.D. (2012). Landscape controls on the timing of spring, autumn, and growing season length in mid-Atlantic forests. Global Change Biology, 18, 656-674

Fisher, J.I., Mustard, J.F., & Vadeboncoeur, M.A. (2006). Green leaf phenology at Landsat resolution: Scaling from the field to the satellite. Remote Sensing of Environment, 100, 265-279

Galbraith, J.M., Donovan, P.F., Smith, K.M., & Zipper, C.E. (2003). Using public domain data to aid in field identification of hydric soils. Soil Science, 168, 563-575

Harvey, K.R. &. Hill, G.J.E. (2001). Vegetation mapping of a tropical freshwater swamp in the Northern Territory, Australia: a comparison of aerial photography, Landsat TM and SPOT satellite imagery. International Journal of Remote Sensing, 22, 2911-2925

Hogg, A.R., & Holland, J. (2008). An evaluation of DEMs derived from LiDAR and photogrammetry for wetland mapping. The Forestry Chronicle, 84, 840-849

Huang, C., Goward, S.N., Masek, J.G., Thomas, N., Zhu, Z., & Vogelmann, J.E. (2010). An automated approach for reconstructing recent forest disturbance history using dense Landsat time series stacks. Remote Sensing of Environment, 114, 183-198

Kennedy, R. E., Cohen, W. B., & Schroeder, T. A. (2007). Trajectory-based change detection for automated characterization of forest disturbance dynamics. Remote Sensing of Environment, 110, 370−386

Kennedy, R. E., Yang, Z. G., & Cohen, W. B. (2010). Detecting trends in forest disturbance and recovery using yearly Landsat time series: 1. LandTrendr - Temporal segmentation algorithms. Remote Sensing of Environment 114, 2897-2910

Kudray, G. M., & Gale, M. R. (2000). Evaluation of national wetland inventory maps in a heavily forested region in the upper great lakes. Wetlands, 20, 581-587

Lang, M., McCarty, G., Oesterling, R., & Yeo, I.-Y. (2013). Topographic metrics for improved mapping of forested wetlands. Wetlands, 33, 141-155

Lang, M.W., Kasischke, E.S., Prince, S.D., & Pittman, K.W. (2008) Assessment of C-band synthetic aperture radar data for mapping coastal plain forested wetlands in the mid-Atlantic region USA. Remote Sensing of Environment, 112, 4120–4130

Liang, S. (2001). Land-cover classification methods for multi-year AVHRR data. International Journal of Remote Sensing, 22, 1479−1493

Lunetta, R., & Balogh, M. (1999). Application of multi-temporal Landsat 5 TM imagery for wetland identification. Photogrammetric Engineering and Remote Sensing, 65, 1303-1310

Mackey, H.E. (1990). Monitoring seasonal and annual wetland changes in a freshwater marsh with SPOT HRV data. In Proceedings of the American Society for Photogrammetry and Remote Sensing, 4, 283-292

Maxa M., & Bolstad, P. (2009). Mapping northern wetlands with high resolution satellite images and Lidar. Wetlands, 29: 248–260

Messina, M.G, & Conner, W.H. (2000). Southern Forested Wetlands: Ecology and Management. (Boca Raton, FL: Lewis Publishers/CRC Press)

Mitsch, W.J., & Gosselink, J.G. (2000). Wetlands, 3rd ed. John Wiley & Sons, Inc., New York

Moody, A., & Johnson, D. M. (2001). Land-surface phenologies from AVHRR using the discrete Fourier transform. Remote Sensing of Environment, 75, 305−323

Morrissey, L. A., & Sweeney, W. R. (2006). Geographic information systems and water resources IV 2006 AWRA spring specialty conference May 8-10. In assessment of the national wetlands inventory: implications for wetland protection

Murphy, P.N.C., Ogilvie, J., & Arp, P. (2009). Topographic modeling of soil moisture conditions: a comparison and verification of two models. European Journal of Soil Science, 60, 94–109

National Research Council, Committee on the Characterization of Wetlands. (1995). Wetlands: Characteristics and Boundaries. National Academy Press, Washington, DC.

Nielsen, E.M., Prince, S.D., & Koeln, G.T. (2008). Wetland change mapping for the U.S. Mid-Atlantic Region using an outlier detection technique. Remote Sensing of Environment, 112, 3993–3995

Pantaleoni, E., Wynne, R.H. Galbraith, J.M. & Campbell, J.B. (2009). Mapping wetlands using ASTER data: a comparison between classification trees and logistic regression. International Journal of Remote Sensing, 30, 3423-3440

Ramsey, E.W., & Laine, S.C. (1997). Comparison of Landsat Thematic Mapper and high resolution aerial photography to identify change in complex coastal wetlands. Journal of Coastal Research, 13, 281–92

Rebelo, L.M., Finlayson, M., & Nagabhatla, N. (2009). Remote sensing and GIS for wetland inventory, mapping and change analysis. Journal of Environment Management, 90, 2234–2242

Richardson, M. C., Fortin, M. J., & Branfireun, B. A. (2009). Hydrogeomorphic edge-detection and delineation of landscape functional units from LIDAR DEMs. Water Resources Research, 45,W10441

Sader, S.A., Ahl, D., & Liou, W.S. (1995). Accuracy of Landsat-TM and GIS rule-based methods for forest wetland classification in Maine. Remote Sensing of Environment, 53,133-144.

Schmidt, K.S., & Skidmore, A.K. (2003). Spectral discrimination of vegetation types in a coastal wetland. Remote Sensing of Environment, 85, 92-108

Sørensen, R., & Seibert, J. (2007). Effects of DEM resolution on the calculation of topographical indices: TWI and its components. Journal of Hydrology, 347, 79-89

Stolt, M.H., & Baker, J.C. (1995). Evaluation of national wetland inventory maps to inventory wetlands in the southern Blue Ridge of Virginia. Wetlands, 15, 346–353

Townsend, P.A., & Walsh, S.J. (2001). Remote sensing of forested wetlands: application of multitemporal and multispectral satellite imagery to determine plant community composition and structure in southeastern USA. Plant Ecology, 157, 129-149

U.S.E.P.A. (1977). Federal water pollution control. Guidelines for specification of disposal sites for dredged or fill material. Act. 40 CFR Part 230 Section 404(b)(1)

Walker, J.J., de Beurs, K.M., Wynne, R.H., & Gao, F. (2012). Evaluation of Landsat and MODIS data fusion products for analysis of dryland forest phenology. Remote Sensing of Environment, 117, 381-393

Wessels, K., Steenkamp, K., Graham, von M., & Archibald. S. (2010). Remotely sensed vegetation phenology for describing and predicting the biomes of South Africa. Applied Vegetation Science, 14, 1–19

Wolter, P. T., Johnston, C. A., & Niemi, G. J. (2005). Mapping submergent aquatic vegetation in the US. Great Lakes using Quickbird satellite data. International Journal of Remote Sensing, 26, 5255–5274

Wright, C., & Gallant, A. (2007). Improved wetland remote sensing in Yellowstone National Park using classification trees to combine TM imagery and ancillary environmental data. Remote Sensing of Environment, 107:582-605

Zedler, J. B. & Kercher, S. (2005). Wetland resources: status, trends, ecosystem services, and restorability. Annual Review of Environment and Resources, 30: 39–74

Zoffoli, M.L., Kandus, P., Madanes, N., & Calvo, D.H. (2008). Seasonal and interannual analysis of wetlands in South America using NOAA-AVHRR NDVI time series: the case of the Parana Delta Region. Landscape Ecology, 23, 833-48

CHAPTER 2

Monitoring Wetland Change using Inter-Annual Landsat Time-Series

Nilam Kayastha[a], Valerie Thomas[b], John Galbraith[c] &Asim Banskota[d]

[a]Geospatial and Environmental Analysis Program, Virginia Polytechnic Institute and State University, Blacksburg, VA, 24061

[b]Department of Forest Resources and Environmental Conservation, Virginia Polytechnic Institute and State University, Blacksburg, VA, 24061

[c]Department of Crop & Soil Environmental Sciences, Virginia Polytechnic Institute and State University, Blacksburg, VA, 24061

[d]Department of Forest Resources and Environment Science, Michigan Tech University, Houghton, MI, 49931

Published in Wetlands, volume 32, October 2012, pages 1149–1162, available via http://link.springer.com/article/10.1007%2Fs13157-012-0345-1#page-1

Wetlands (2012) 32:1149–1162
DOI 10.1007/s13157-012-0345-1

ARTICLE

Monitoring Wetland Change Using Inter-Annual Landsat Time-Series Data

Nilam Kayastha · Valerie Thomas · John Galbraith · Asim Banskota

Received: 22 February 2012 / Accepted: 9 October 2012 / Published online: 30 October 2012

Abstract Successful conservation and management of wetlands requires up-to-date and accurate information on wetland location, size, condition, functionality, type, services provided, stressors and net change in extent. Most change detection studies utilize two date images to provide information on wetland dynamics. Comparison of infrequent imagery might not sufficiently capture natural variability in wetlands. Use of longer time series of images might increase our ability to characterize the temporal variability of wetland and detect changes with greater accuracy. We used inter-annual time series of Landsat data from 1985 to 2009 to map changes in wetland ecosystems in northern Virginia. Z-scores calculated on tasseled cap images were used to develop temporal profile for wetlands delineated by the National Wetland Inventory. A change threshold was derived based on the Chi-square distribution of the Z-scores. The accuracy of a change/no change map produced was 89 % with a kappa value of 0.79. Assessment of the change map showed that the method was able to detect complete wetland loss together with other subtle changes resulting from development, harvesting, thinning and farming practices. With additional research on attributing the change events, the method may provide more detailed information on status and the trends of wetland loss and functioning.

Keywords Wetland · Change detection · Landsat time series · Z-score

N. Kayastha (✉)
Geospatial and Environmental Analysis Program,
Virginia Polytechnic Institute and State University,
Blacksburg, VA 24061, USA
e-mail: nilamk@vt.edu

V. Thomas
Department of Forest Resources and Environmental Conservation,
Virginia Polytechnic Institute and State University,
Blacksburg, VA 24061, USA

J. Galbraith
Department of Crop & Soil Environmental Sciences,
Virginia Polytechnic Institute and State University,
Blacksburg, VA 24061, USA

A. Banskota
Department of Forest Resources and Environment Science,
Michigan Tech University,
1400 Townsend Dr. Houghton, MI 49931-1295, USA

Introduction

Background

Wetlands are one of the most valuable ecosystems in the world because of the numerous ecosystem services they provide, including flood attenuation, carbon sequestration, groundwater recharge, water purification and habitats for biodiversity. Successful conservation and management of wetlands requires up-to-date and accurate information on wetland location, size, condition, functionality, and type of wetlands and the rate of any changes (Murphy et al. 2007). Satellite remote sensing data provide consistent and repeatable measurements of landscape condition and have been extensively used for detecting and classifying changes in land surface condition over time (Kennedy et al. 2009). Most of the wetland monitoring studies have focused exclusively on wetland loss or gain and are focused on identifying wetland areas completely converted to other land use types (Syphard and Garcia 2001). However, other disturbance activities in wetland areas such as development, silviculture, farming activities or conversion of one wetland type to another will have significant effect on the functioning of the wetland and the monitoring efforts should be able to capture and characterize these changes.

Change detection methods can be categorized into two basic approaches: bi-temporal change detection and temporal trajectory analysis methods (Coppin et al. 2004). Bi-temporal techniques, which are the most common change detection technique, utilize images taken at two different time periods to assess changes in land cover. They utilize images taken at anniversary dates or anniversary windows to minimize the variability in spectral properties due to vegetation phenology and sun angle differences. However, even at anniversary dates or within anniversary windows, phenological inconsistencies due to local precipitation and temperature variation result in problems identifying real change from seasonal change (Coppin et al. 2004). In addition, when the gaps between the images are long, the discontinuities resulting from disturbance events may be indistinguishable from the trend (de Beurs and Henebry 2005).

Temporal trajectory analysis methods utilize time series of images to monitor indicators of land surface attributes. This technique compares temporal trajectories of spectral values (or derived indices) of land cover change characteristics throughout the monitoring period (Coppin et al. 2004). Use of longer time series offers sufficient temporal sampling in terms of duration and frequency that allow detection of changes amidst substantial variation (de Beurs and Henebry 2005). Typically, temporal trajectory analysis utilizes image from sensors with high temporal frequency but typically with coarse spatial resolution such as Advanced Very High Resolution Radiometer (AVHRR: 1 km), Moderate-Resolution Imaging Spectroradiometer (MODIS: 250 m to 1 km), and Systeme Probatoire de l'Observation de laTerre Vegetation (SPOT VGT: 1 km). There are different MODIS products with different temporal frequency and spatial resolution. The MODIS daily surface reflectance product has spatial resolution of 500 to 1,000 m. The 8 day surface reflectance composite has the spatial resolution of 500 m. Although the temporal frequency of these datasets is better, the spatial resolution is too coarse for wetlands studies.

Most of the wetland change detection studies are bi-temporal in nature (Ramsey and Laine 1997; Rebelo et al. 2009). National Oceanic and Atmospheric Administration's (NOAA) Coastal Change Analysis Program (C-CAP) has produced a national standard geospatial database to track coastal land cover change. C-CAP employs Landsat as primary data sources and uses images from two dates to produce land cover change every 5 years (NOAA-CSC 2008). Seasonal and inter-annual environmental changes such as precipitation and temperature create high level of variability in wetlands (Pavri and Aber 2004). Use of coarse temporal resolution images poses significant constraints in wetland change studies (Nielsen et al. 2008). These change detection techniques are mainly affected by the dynamic nature of wetland hydroperiod, which has a significant influence on the wetland formation as well as wetland biogeochemistry, soils and vegetation. Wetland vegetation phenology greatly complicates the process of detecting changes in wetlands, especially in seasonal and diurnal ephemeral features such as the presence and absence of floating vegetation, the flooding and exposure of tidal and inland mud flats, and the raising and lowering of water levels under the wetland canopy (Ramsey and Laine 1997). Change monitoring of inland fresh water wetland is a challenge because their types and spatial distribution of wetlands can change dramatically from season to season, especially when non-persistent species are present (Mackey 1990). Tuxen et al. (2008) utilized imagery acquired roughly the same seasonal time each year to assess vegetation colonization in a restoring marsh and experienced false changes due to phenological changes in vegetation resulting from differences in growth cycle due to changing climate condition. Changes due to vegetation phenology can be minimized to some extent by using images acquired at anniversary dates but variability due to abnormal hydrologic conditions, such as flooding or drought can make determination of wetland change more difficult. Nielsen et al. (2008) utilized images from spring, summer and fall dates for wetland change monitoring. Despite the use of multi-season imagery, many of the flooded wetlands (natural occurrence at that time in the area) were classified as having high probability of change. Misinterpretation of wetland loss or gain can also result from factors such as farming of wetlands during dry cycles, drought conditions, excess surface water or flooding (Dahl 2006). Ramsey et al. (2001) found that the human activities that involved lumber industry and agricultural activities such as farming and grazing were major source of error both in wetland mapping and change analysis. The timing of image acquisition with human activities can further increase the error in change analysis. Although these land use changes do not result in loss of wetland, they may significantly alter the reflectance characteristics leading to ambiguity in the change detection procedure. Use of dense time series of images will increase our ability to characterize the temporal variability of wetland and detect wetland change with greater accuracy. Ramsey et al. (2011) used vegetation index trend derived from daily MODIS data to assess the damage and subsequent recovery in forested wetlands due to hurricane Katrina. Ramsey et al. (2009) also studied the impact and recovery of forested wetlands using the pre and post hurricane Landsat and Radarsat images. The MODIS vegetation index trend provided a more detailed description of pre hurricane phenologies and post hurricane damages and recovery compared to snapshot information provided through Landsat and Radarsat.

Multispectral satellite imagery, especially that collected by Landsat Thematic Mapper (TM) and Enhanced Thematic Mapper (ETM+), has been widely used for wetland mapping and monitoring. Landsat data have been found to be preferable to other multispectral satellite data for wetland detection. The spatial resolution of Landsat (30 m) combined with its spectral resolution (7 bands) have been found to be preferable compared to other multispectral data such as SPOT which has higher spatial resolution but only four bands (Harvey and Hill 2001). Especially, the mid-infrared Landsat band (band 5, 1.55–1.75 μm) has been found to be useful to detection of water (Harvey and Hill 2001). In recent years, free release of the Landsat archive has resulted in growing number of temporal trajectory studies utilizing Landsat time series for characterizing ecological disturbance (Kennedy et al. 2007; Huang et al. 2010). These studies have exclusively focused on detecting and characterizing forest change and disturbance and do not differentiate between upland forest and forested wetlands. Non-forested wetlands were also a major source of error in these studies as they were either mapped as forested or disturbed forest. The objective of this study is to evaluate the use of inter-annual time series Landsat data to monitor disturbance in wetlands. We hypothesize that a time series of Landsat data will be able to capture the temporal variations in a wetland, which will allow us to differentiate natural temporal variability of wetland hydrology and vegetation from other temporary and more permanent wetland disturbances.

National Wetland Inventory Data

The U.S. Fish and Wildlife Service established the National Wetland Inventory (NWI) in 1974 to begin a nationwide effort to map wetlands. Manual photo-interpretation of mid-to-high altitude color infrared aerial photographs, usually taken during early spring (Hefner and Storrs 1994) coupled with field verification, topographic maps and soil information is used to map NWI wetlands (Dahl and Watmough 2007). The NWI uses hierarchical classification scheme of Cowardin et al. (1979) to describe wetland locations. Studies have shown varying levels of accuracies of NWI maps. In general, NWI maps have been reported to have low commission error and in many cases high omission error (Wright and Gallant 2007). Kudray and Gale (2000) reported commission error of less than 5 % in Massachusetts. Stolt and Baker (1995) found that all the palustrine wetlands delineated on NWI maps were correctly identified but the omission error were greater than 85 %. Even though many existing wetlands are not mapped in NWI, it can be used a baseline wetland distribution for regional change detection because of its low commission error, internal consistency, national scope and availability (Nielsen et al. 2008).

Data and Methods

Study Area

The study area incorporates counties in northern Virginia within a single Landsat scene path/row: 15/33 (Fig. 1). The most common wetland type is palustrine wetlands, which incorporates wetland types such as forested, scrub-shrub and emergent wetlands (Tiner and Finn 1986). Palustrine systems include all non-tidal wetlands dominated by trees, shrubs, persistent emergent, mosses or lichens (Cowardin et al. 1979). This region includes one of the fastest growing populations in Virginia and is under immense development pressure. The largest number of wetland permits in the commonwealth of Virginia was issued in Stafford County.

Landsat Time Series Development

A Landsat time series is a temporal sequence of Landsat images acquired at a nominal temporal interval for an area defined by a path/row tile of the World Reference System (Huang et al. 2010). A time series was developed using yearly Landsat Thematic Mapper (TM) and Enhanced Thematic Mapper (ETM) images (path/row: 15/33) taken between 1985 and 2009 (Table 1). Image acquired before 1985 were not used as they come from Landsat Multispectral Scanner and have different spatial resolution and radiometric resolution compared to TM and ETM. Leaf-on Landsat images acquired between June and September were used to avoid phenological inconsistencies. The temporal interval between successive images when using time series data is important for effective change detection. Ideally, it would be best to have an image each successive year so that the spectral trends are captured accurately. Due to extensive cloud cover, some years are absent from the time series stack. However, gaps in the image time series did not exceed two consecutive years. Longer gaps between the image dates will decrease the number of observations available to capture the spectral trends and will affect the ability to detect the disturbance event (de Beurs and Henebry 2005). Many studies utilizing Landsat time series (Kennedy et al. 2007; Huang et al. 2010) have shown that the biennial Landsat data can sufficiently capture the disturbance trend.

Precise geometric registration and radiometric and atmospheric correction are important in studies utilizing multi-temporal images to avoid spurious changes resulting from pixel mis-registration and differing atmospheric conditions. Atmospheric correction was conducted using automated algorithms with the Landsat Ecosystem Disturbance Adaptive Processing System (LEDAPS) (Masek et al. 2006, Huang et al. 2009). LEDAPS is based on 6SV radiative transfer model. The ancillary data used in the atmospheric correction process includes

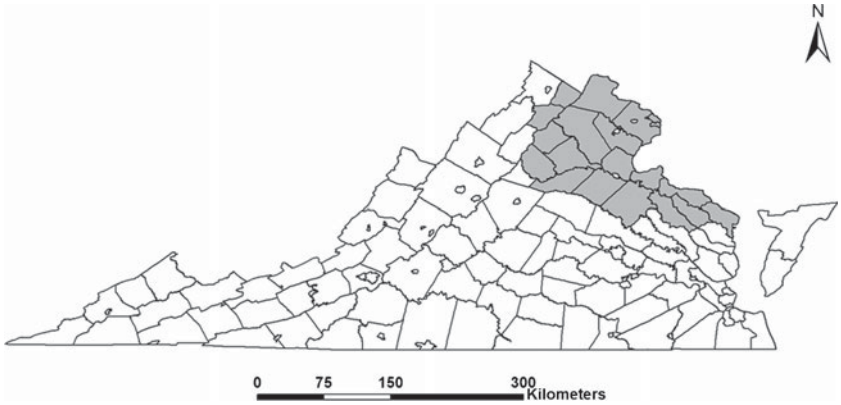

Fig. 1 Study area: State of Virginia showing study area

TOMS (Total Ozone Mapping Spectrometer) data, column water vapor from the NOAA National Centers for Environmental Prediction (NCEP) reanalysis data, digital topography and NCEP surface pressure data. The ancillary data are supplied to the 6S radiative transfer algorithm, which then inverts top of atmosphere reflectance to surface reflectance for each 30-m pixel (Masek et al. 2006). Landsat images used were processed at Level 1 terrain corrected (L1T) data, which have undergone systematic geometric correction (Roy et al. 2010). Digital ortho-photo quadrangle data (DOQ) were overlaid on the Landsat scene to further test their geometric accuracy.

Table 1 List of Landsat Thematic Mapper (TM) and Enhanced Thematic Mapper Plus (ETM+) image date, sensor types and assigned number in the time series

Assigned number in the time series	Image date	Sensor type
1	8/14/1985	TM
2	7/19/1987	TM
3	7/5/1988	TM
4	9/10/1989	TM
5	8/12/1990	TM
6	9/16/1991	TM
7	8/23/1994	TM
8	9/27/1995	TM
9	7/14/1997	TM
10	7/4/1999	TM
11	7/6/2000	TM
12	7/9/2001	TM
13	9/6/2002	ETM+
14	9/17/2003	TM
15	9/19/2004	TM
16	8/5/2005	TM
17	8/24/2006	ETM+
18	9/12/2007	TM
19	6/11/2008	TM
20	7/15/2009	TM

Aggregation of NWI Class

NWI maps for the study area were downloaded from US Fish and Wildlife Service website (U.S. Fish and Wildlife Service 2010). Table 2 shows the aerial photo dates of NWI maps in the study area. The majority of wetlands were delineated using aerial photos acquired prior to the year 2000 and they have not been updated with recent aerial photos. We limited the study to palustrine wetland types and eliminated some highly variable types to reduce spectral variability in the time series. Wetlands classified as open water were removed from the analysis as the reflectance from this land cover is highly variable depending on the water level and sediment content. We also eliminated the wetlands classified as Phragmites, dominated by *Phragmites australis* (Cav.) Trin. ex Steud., (Common Reed), as they covered only small portion of the study area and demonstrated high yearly variability in reflectance. This resulted in 533 unique NWI identifier codes. It was not possible to use each unique code as an independent class as many of the codes were only represented by few pixels. Therefore, it was necessary to merge the NWI codes into broader classes to have representative number of pixels for each wetland class. The spectral reflectance characteristics of

Table 2 Aerial photo dates used and corresponding percentage of NWI mapped in the study area

Aerial photo year	Percentage of NWI mapped
1980	3.27
1981	9.86
1982	3.27
1984	10.99
1988	6.61
1989	3.30
1990	3.31
1991	2.19
1994	41.71
2000	15.50

wetlands are mainly affected by vegetation structure, leaf characteristics, and soil moisture (Lang et al. 2008). The aggregation of NWI codes to broad classes was based on vegetation structure, vegetation phenology, wetland systems and their flooding regime. The final wetland classes were: *palustrine forested deciduous*, *palustrine forested evergreen*, *palustrine scrub-shrub deciduous*, *palustrine scrub-shrub evergreen*, *palustrine emergent persistent*, *mixed and palustrine forested dead*. The NWI maps with the final classes were rasterized to a 30 meter pixel.

Identification of Reference Wetland Samples

Reference wetland samples for each wetland category were identified using normalized difference vegetation index (NDVI) time series data. NDVI is a widely-used vegetation index that has been correlated to different vegetation parameters such as biomass, leaf area index, plant vigor, plant productivity. NDVI measures the contrast between surface reflectance in red and near infrared region. Reference wetland samples were required to be undisturbed throughout the monitoring period. Undisturbed wetland samples were identified randomly using images from Google Earth™ (earth.google.com). We used the NDVI temporal profile to assess the usability of selected wetlands location as reference samples. The underlying assumption is that an unchanged wetland will have an NDVI trajectory with small variation. Further, the selected pixels were manually examined in each image to ensure that they were not contaminated by clouds or shadows. 100 samples for each class were distributed throughout the scene to obtain a representative characterization of each class. Average NDVI values and standard deviations were calculated for each wetland class for each image used in the time series.

Z-Score Calculation

We adapted the Vegetation Change Tracker (VCT) algorithm developed by Huang et al. (2010) in our study to detect wetland disturbance. The model is a cross-correlation analysis, which uses the class boundaries to derive an expected class average spectral response. The Z-score is derived by subtracting the population mean from the individual value and then divided by the population standard deviation. The Z-score indicates how close a pixel's response is to the expected spectral response of its corresponding class value. The expected spectral response is derived from the reference or unchanged wetland samples. The Z-score is calculated as follows:

$$Zci = \frac{\mathrm{Xci} - \overline{\mathrm{Xci}}}{\mathrm{SDci}} \quad (1)$$

where

Z_{ci} is the Z statistics value of the pixel in wetland class c in year i

X_{ci} is the value of the pixel in wetland class c in year i

$\overline{Xci}$ is the average value of the unchanged wetland class c in year i, and

SD_{ci} is the standard deviation of the value of unchanged wetland class c in year i

The Z-score provides the standardized distance of a sample from the population mean. It measures the distance of a pixel belonging to a class from the center of that class in the spectral domain (Stueve et al. 2011). The likelihood of a pixel being changed depends on the Z-Score value. A lower Z-score value of the pixel indicates that no major disturbance event has occurred, while a higher Z-score of a pixel indicates that a major disturbance event has occurred. In our context, it can be interpreted as the odds of a pixel being a disturbed wetland. Pixels with low Z-score values are undisturbed wetlands and high Z-scores indicate a higher likelihood of disturbance. Standardization using Z-scores has the added advantage of further normalizing the image, which can substantially reduce the spatial and temporal variability of the spectral signatures caused by relatively homogenous atmospheric conditions, and instrument related issues (Huang et al. 2010). Different studies have demonstrated the use of Z-score based technique in wetland change detection. Houhoulis and Michener (2000) used a Z-score based technique using SPOT image to detect wetland conversion to agricultural uses. Koeln and Bissonnette (2000) used summed Z-scores determined independently for the red, near-infrared, and mid-infrared TM bands to identify hotspots of wetland change. Nielsen et al. (2008) developed a wetland change probability map for U.S mid-Atlantic region. They used deviation from median values instead of mean and used logistic regression to produce a pixel change likelihood index.

$$ZScore_{TC} = \frac{ZScore_B + ZScore_G + ZScore_W}{3} \quad (2)$$

where

ZScore_{TC} is the total Z-Score value of a pixel calculated using tasseled cap images

ZScore_B is the Z-Score value of calculated using brightness image

ZScore_G is the Z-Score value of calculated using greenness image

ZScore_W is the Z-Score value of calculated using wetness image

The Z-scores were calculated on a tasseled cap transformation (TCT) of the Landsat data. The TCT is an orthogonal transformation of Landsat bands that transforms the Landsat bands into brightness, greenness and wetness axis (Kauth and Thomas 1976). TCT is preferred over other data transformation methods such as principal component analyses as

the TCT components corresponds to the physical characteristics of vegetation and are ecologically interpretable (Parmenter et al. 2003). TCT has also been widely used for wetland classification and change detection. Hodgson et al. (1987) associated the wetness and greenness components of TCT to different wetland types. Ordoyne and Friedl (2008) showed that the wetness component is strongly correlated to water stage data across a range of surface vegetation types. Nielsen et al. (2008) and Baker et al. (2007) successfully utilized Landsat-based TCT to detect wetland changes. These components have been widely used for change analysis because changes in land cover are generally related to changes in brightness, greenness and wetness, while other sources of variability (sensor calibration, illumination angle, atmospheric effects) that might be unrelated to land cover change are reduced (Baker et al. 2007). Wetlands exhibit a variety of vegetative or hydrologic changes, which might not be detected using few spectral bands. TCT summarizes the spectral information of Landsat bands intro three components, so all the information can be utilized. Tasseled cap brightness, greenness and wetness components were calculated for each Landsat scene using coefficients (Table 3) developed by Crist (1985) for surface reflectance. An integrated Z-Score value was calculated using the tasseled cap brightness, greenness and wetness images as shown in equation 2.

Determining Change/No-change

Identification of change/no-change wetlands will depend on time series analysis of the Z score value. The Z-score trajectory for the monitoring period will vary depending on the wetland types and the type of disturbance occurring in the pixel. For an unchanged wetland, the Z-score value will remain low and stable throughout the period. In case of a disturbance, the Z-score value will increase in the year the disturbance occurred. The successive Z-score trajectory after the disturbance will depend on the type of disturbance. Discriminating a real change in the Z-score time series analysis will require a threshold selection. Selection of threshold is important for accurate change detection. A low threshold value will identify spurious changes, potentially identifying natural variability in Z-score value as real change which will lead to more area being identified as change location. On the contrary, a high threshold value will suppress significant change such that even the real change events will not be detected. A common method is to set change threshold in terms of the standard deviation about the mean (Morisette and Khorram 2000; Lunetta et al. 2006). If the Z-score values are normally distributed, the sum of squares of Z-score values will follow a Chi-square distribution with N degrees of freedom, where N is the number of classes. A null hypothesis testing procedure to decide about the changed or unchanged status can be implemented by choosing a confidence level $1-\alpha$ and the corresponding threshold associated with the probability that the squared Z-score value is lower than the threshold (Bontemps et al. 2008). Pixels where the Z-score value is greater than the threshold will then be considered as changed pixels. The accuracy and the sensitivity of threshold to different magnitude and types of changes will depend on the level of confidence $1-\alpha$ or the value of α. Higher values of α will result in a lower threshold value, which will lead to identification of more change area, but this will also include areas that have changed slightly. Lower values of α will result in higher threshold value and will only identify areas of significant change. We looked at the areas of known change locations and used different α value to test the ability to detect change points. The highest α (0.01)that could detect all the change points was selected. As the α was decreased the threshold value increased and known location of change were not being identified. The importance of selection of the threshold value is shown in Fig. 2. The figure shows an example where the wetland area has been changed to a suburban development. The disturbance occurs in the year 2000. When α value is set at 0.01, the change point is identified in the year 2000 (circled by solid line). However, lowering the α value at 0.001 (chi-square value of 10.83) will not identify this as change area. If the threshold value is set at 0.001, then the disturbance will only be identified in the year 2002 (circled by dotted line).

Flagging False Change

A unique advantage in change monitoring utilizing time series data is the ability to utilize temporal context to improve results (Pouliot et al. 2009). False change detection may result due to clouds, shadow or other sources of contamination. Huang et al. (2010) indicates that the likelihood of the pixel having unflagged data quality in consecutive

Table 3 Coefficients used for tasseled cap transformation of Landsat data based on Crist (1985)

Feature	Band 1	Band 2	Band 3	Band 4	Band 5	Band 7
Brightness	0.2043	0.4158	0.5524	0.5741	0.3124	0.2303
Greenness	−0.1603	−0.2819	−0.4934	0.7940	−0.0002	−0.1446
Wetness	0.0315	0.2021	0.3102	0.1594	−0.6806	−0.6109

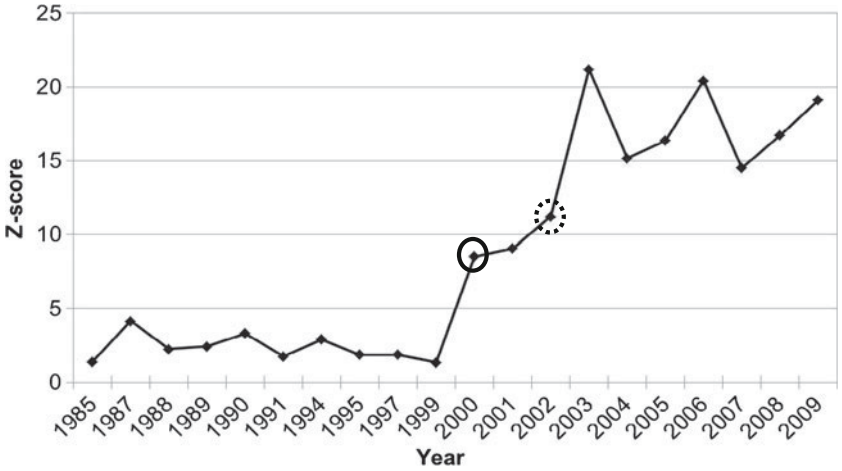

Fig. 2 Example of Z-Score profile of a changed location. The profile highlights the importance of threshold selection for change detection. The actual change for this example occurred in the year 2000 (circled in solid line). Increasing the threshold value (α =0.001) will not identify this point as changed. Change is only identified in the year 2002

years should be low. For a time series of annual observations, temporal test can be utilized to flag false changes. In the case of disturbance or when there is significant change in a wetland, the Z-score value will be significantly higher for at least a few consecutive years. But, if the increase in Z-score value is due to noise, the high value will not persist for consecutive years. Preliminary analysis indicated that two consecutive years is likely sufficient to indicate a real change. Other studies (Huang et al. 2010; Powell et al. 2010) have also shown that 2 year threshold is sufficient for capturing most of the change in the time series data. Therefore, the final decision rule required Z-scores greater than the threshold value for at least two consecutive years to classify a pixel as 'changed'. Use of a temporal test will also allow us to flag the natural variability in wetlands from real disturbances.

Validation

Validation of the change detection maps from the time series Landsat data is challenging as it is difficult to collect reference dataset to validate each annual time step. Most time series disturbance studies have reliably utilized visual interpretation of change events from the time series data for validation (Kennedy et al. 2007; Huang et al. 2010; Schroeder et al. 2011). In the study, we utilized available high resolution aerial images from National Agriculture Imagery Program (NAIP) and Virginia Base Mapping Program (VBMP) for interpretation of the validation points. NAIP images are acquired during the agricultural growing (leaf-on) seasons with a spatial resolution of 1 m. VBMP images are leaf-off images acquired with the resolution of 30 cm. The image dates available were 1994, 2002, 2008 and 2009.

We expected that the number of no-change pixels across the image should greatly exceed the detected change pixels. Therefore, to obtain a better understanding of map accuracy, we stratified the image into "change and no-change" pixels and assessed accuracy for both. Based on the stratification, 90 random samples were selected within the change class, and 90 from within the "no-change" class (Fig. 3). Most readers should interpret the "change" accuracy statistics to evaluate mapping accuracy. We included no-change statistics for completeness. The reference dataset was used to produce error matrix and the accuracy measures, which include overall accuracy, user's and producer's accuracy and kappa coefficient (Congalton and Green 1999). Both the overall accuracy and kappa coefficients are measures of agreement between the change map and the reference data. The overall accuracy is the proportion of correctly identified change events. Kappa coefficient takes into account chance agreement and quantifies to what extent the observed agreement between the proposed algorithm and reference data departs from the agreement that would be expected from a random classifier (Bontemps et al. 2008). The producer's accuracy measures the proportion of pixel belonging to a class that was correctly classified by the method and measures the error of omission. User's accuracy measures the proportion of the pixels classified as belonging to a class matches the reference data and measures the error of commission. The year of disturbance cannot be easily validated with independent samples. For each reference point, the year of disturbance assigned by the algorithm was recorded. The reference for year of disturbance for each sample was then manually obtained using Landsat time series. Since we have used annual time series data, the year of disturbance determined manually recorded should be reliable (Kennedy et al. 2007, Huang et al. 2010). In this context, the validation for year of disturbance is more of a 'quality control' to ensure that the automated procedure matches manual interpretation. In particular, this will help evaluate the suitability of Z-score thresholds and identify possible sources of error.

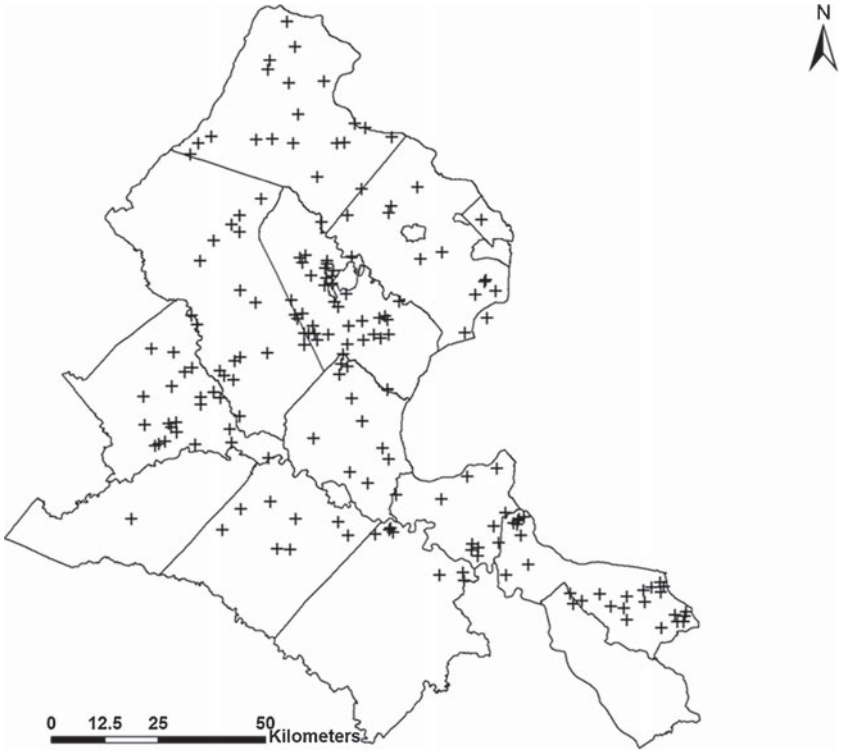

Fig. 3 Validation points used for accuracy assessment

Results

Z-score Profile of Reference Wetlands

The Z-score profiles for different reference wetland types are summarized in Fig. 4. The Z-score value ranges from 2 to 5. Compared to the forested wetlands the Z-score values of emergent, mixed and wetlands classified as dead in the NWI classification are more variable from year to year. The Z-score profiles of the reference wetland sample indirectly provide a justification to the threshold used to identify change. The profile indicates that the Z-Score value remains below 5 for the reference wetlands in all the years. Based on the Chi-square distribution, Chi-square value of 6.6 was used as threshold to detect change.

Accuracy Assessment

Table 4 provides the summary of the accuracy measures of the change detection analysis. The overall accuracy for the change detection analysis was 89 % with the kappa value of 0.79. The high user's accuracy (87.3 %) and producer's accuracy (92.2 %) for the unchanged wetlands indicate that the method can accurately detect wetlands that remain unchanged throughout the time series. The overall accuracy seems to be largely affected by the omission error (13.3 %)

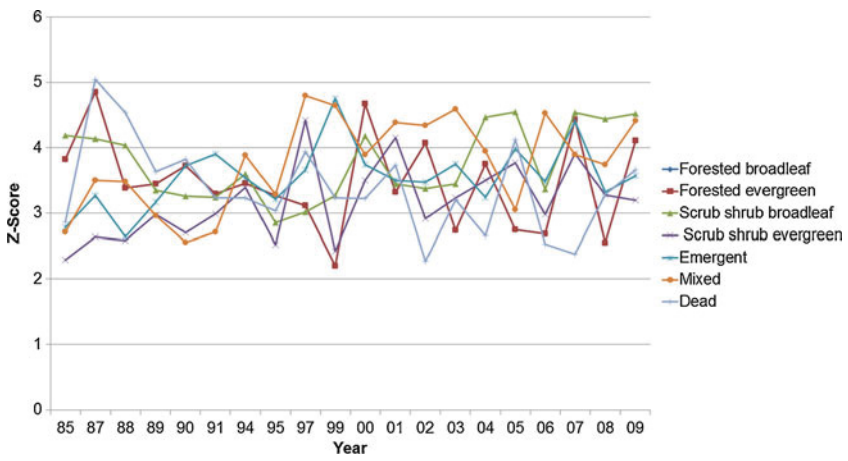

Fig. 4 Z-score profiles of different wetland types in the region produced using leaf on Landsat images. The X-axis represents different years (1985–2009) in the image time series

Table 4 Error matrix for the change detection analysis

	Reference data		
	Change	No change	User's accuracy
Change	78	7	91.7 %
No change	12	83	87.3 %
Producer's accuracy	86.6 %	92.2 %	
Omission error	13.3 %	Overall accuracy	89.4 %
Commission error	8.2 %	Cohen's Kappa	0.79
Percentage of change area	15.4 %		
Percentage of no-change area	84.6		

of the changed wetlands. The overall agreement between the disturbance year produced by the algorithm and visual interpretation of the Landsat time series and the trajectory itself was 74.4 %.

The result of the analysis (Table 5) showed that the wetland area has generally decreased in the study area. Approximately 15.4 % (6,065 ha) of the wetlands in the study area experienced some form of disturbance. The largest disturbance events were observed in the emergent persistent class (26.7 %). However, we have to keep in mind that majority of the false changes were also associated with this class. After the emergent class, largest disturbance event occurred in forested wetlands.

Disturbance events were dispersed throughout the study area (Fig. 5). However, majority of the disturbance events are occurring in more urban areas such as Fauqier and Prince William County. The year of disturbance as produced from the Landsat time series is shown in Fig. 6. The disturbance year showed that the majority of wetland disturbance occurred before 1999 and the rate of disturbance subsequently decreased in the time series. Fig. 7 represents Z-score trajectories of different disturbance events in the study area. The trajectories of different disturbance have distinctive temporal progression which will lead to characteristics temporal signature. The pattern of spectral value change is distinctive both before and after the disturbance event and therefore can be used as an indicator of the event. For example the Z-score trajectory associated with wetland loss (a) has a steady Z-score value till the year of disturbance and there is gradual increase in the Z-score value. On the other hand, in an area converted to a suburban development (b) Z-score value increases and then starts decreasing as various vegetation starts to grow. In comparison, when a forested wetland undergoes thinning (c) Z-score value increases and subsequently decreases. However, the trajectories after the disturbance are different. While the Z-score value in the suburban development decreases after the initial disturbance it is still high compared to the trajectory in thinning activity. Descriptive statistics for the Z-score trajectories for the examples shown in Fig. 7 are summarized in Table 6. The statistics includes mean and standard deviation of the Z-score values before and after the change. The mean and standard deviation of the Z-score values after the change events are indicative of types of disturbance. The mean and standard deviation for example (a), where wetland has been completely removed is higher compared to other examples. In example (b) although there is complete wetland loss, because there is vegetation growth after the development, the mean and standard deviation are low compared to (a). Similarly, the mean and standard deviation for the disturbance related to silviculture activities (c) are low. Example (d) where wetland has been converted to open water, the mean and standard deviation are low compared to complete wetland loss but high compared to suburban development and silviculture activities. The magnitude which is difference between the Z-score value before and after the change can provide another indication of the change events. The magnitude value is higher for complete wetland loss and conversion of wetland to open water compared to suburban development and silviculture activity.

Discussion

The National Wetland Inventory makes two distinctions in wetland change: wetland loss and conversion. Wetland loss

Table 5 Summary of wetland disturbance in the study area

Wetland classes	Total NWI area (hectare)	Change area (hectare)	% of the NWI class
Forested broadleaf	22585.86	2896.31	12.82
Forested evergreen	1211.01	275.37	22.74
Scrub-shrub broadleaf	1644.44	189.64	11.53
Scrub-shrub evergreen	139.61	10.35	7.41
Emergent persistent	5140.8	1351.95	26.3
Mixed	8375.42	1324.78	15.82
Dead	145.27	16.75	11.53
Total area	39242.41	6065.15	
Total change area=15.4 %			

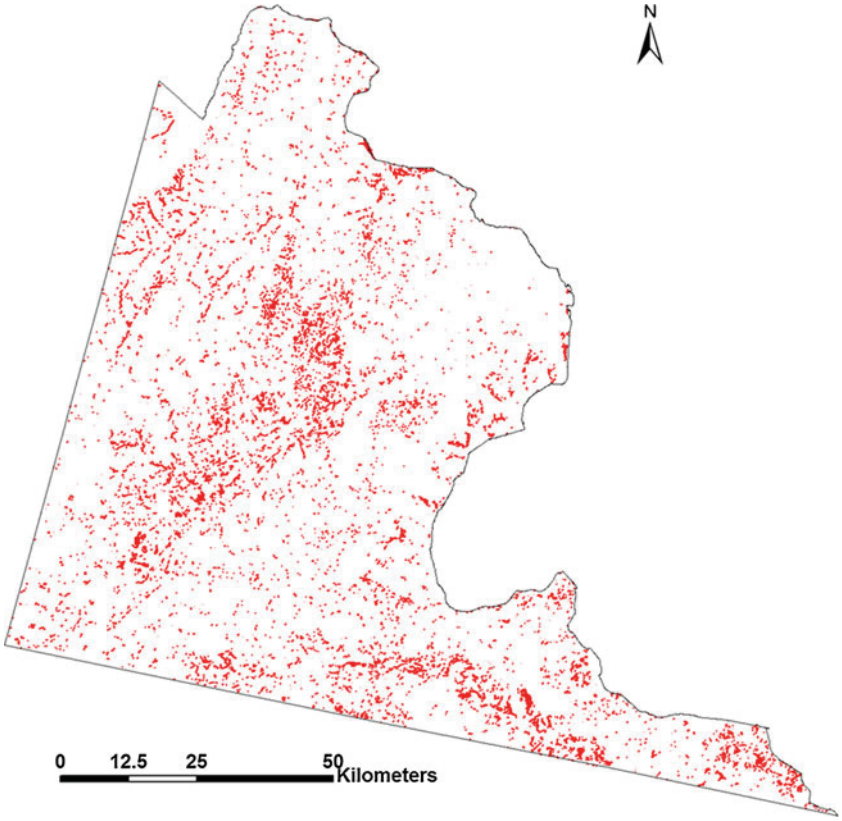

Fig. 5 Disturbance events occurring in the study area between 1985 and 2009 as captured by the Landsat time series

is complete conversion of a wetland to other land use types, where the wetland functionality is entirely lost. Whereas, wetland conversion is a change in state where the area still remains a wetland. Wetland conversion mainly results from activities such as farming, and silvicultural activities. Most of the wetland monitoring studies exclusively focus on

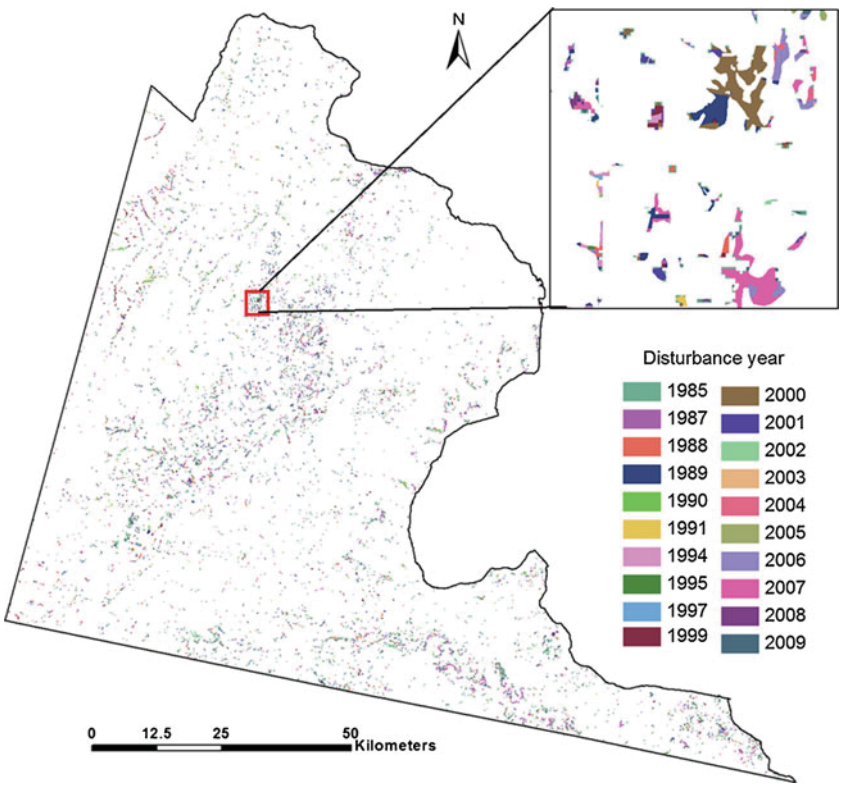

Fig. 6 Disturbance year map produced from Landsat time series

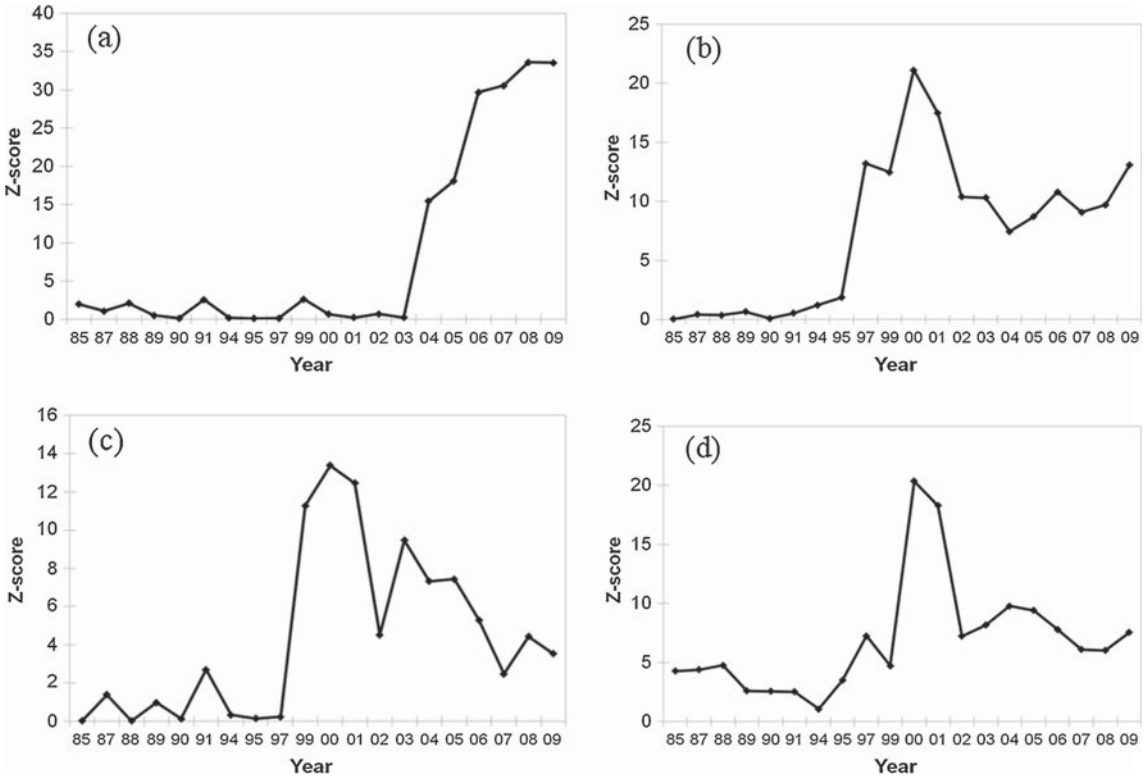

Fig. 7 Examples of Z-score trajectory of different disturbance events: (**a**) complete vegetation removal, (**b**) conversion to a suburban development, (**c**) thinning of a forested wetland, (**d**) conversion to open water

wetland loss. However, wetland conversions significantly affect the functioning of the wetlands. In order to obtain a better understanding of the status and trends in wetland, wetland monitoring activities should consider detailing the subtle changes in wetland together with obvious wetland loss.

In this study, we investigated the use of inter annual time series data to detect disturbances in National Wetland Inventory delineated wetlands in Northern Virginia. The goal of the study was to not only identify areas of complete wetland loss but also capture subtle and ephemeral disturbance events taking place in the wetlands. The use of continuous Landsat data of 20 years has enabled us to capture these changes, which will otherwise be missed if we had only used snapshot images from two time periods. The overall accuracy of the change detection procedure was 89 % and the agreement between the disturbance year produced by the algorithm and visual interpretation was 74 %. We also demonstrated that the use of time series Landsat data can successfully capture the trends. In absence of adequate field data, we did not classify our change map to identify different subtle and ephemeral disturbances in the study area. However, Fig. 7 (a) to (d) show that with further study and additional data, it is possible to use these time series data to classify subtle and ephemeral disturbances. Various studies have used different methods using Landsat time series data to classify these changes. Vogelmann et al. (2012) used linear regression model on a time series of spectral index to assess the long term gradual ecosystem changes. Schroeder et al. (2011) used a supervised classification approach on a 22 year Landsat time series data to map wildfire and clearcut disturbances in boreal forest.

Other studies have demonstrated the use of Z-score in identifying wetland change (Houhoulis and Michener 2000,

Table 6 Descriptive statistics for the change example. The statistics includes mean and standard deviation of the Z-score values before and after the change and change magnitude (difference between the Z-score value before and after the change)

	Before change		After change		Change magnitude
	Mean	Standard deviation	Mean	Standard deviation	
Example a	0.97	0.95	26.82	7.99	15.19
Example b	6.45	0.62	9.81	3.91	11.33
Example c	0.67	0.90	7.42	3.76	11.04
Example d	3.77	1.71	10.07	5.04	15.62

Koeln and Bissonnette 2000, Nielsen et al. 2008). Z-score is the expected spectral response of a class calculated based on the unchanged samples. One of the major factors affecting the accuracy of Z-score based techniques is the identification of unchanged reference wetland samples. The proposed method requires unchanged wetland sample for each year. We used the NDVI trajectory and available high resolution aerial photos to identify the unchanged wetland samples to calculate the Z-score. The variability in the Z-scores of unchanged reference (Fig. 4) wetland samples indicates the inherent variable nature of wetlands. The Z-score value for the wetland types considered in the study ranged from 2 to 5. Compared to the study of Huang et al. (2010) that only considered forested environment the Z-score value appears high in the wetland compared to uplands (Z-score value for the forest was less than 3). Again the yearly variability in the Z-scores is possibly associated with hydrology of wetlands, which in turn is affected by environmental factors. Schroeder et al. (2011) recommends using intra-annual images in the time series to minimize false change detection in wetland areas. The use of winter time series together with the growing season images might help address the variability in wetlands. However, the approach could not be tested in this study, due to lack of high quality winter images. Selection of appropriate threshold is important for the accuracy of change detection. The threshold used for determination of change was based on the chi-square distribution of Z-score values (chi-square value of 6.6). The sensitivity of the threshold used is difficult to assess when specific change types is not the focus of the study. Fig. 4 indicates that the Z-score value for the unchanged wetland sample remains below 5 for all the year. This indicates that the threshold used in this study for the determination of change is sensitive in differentiating actual change from natural variability. In addition, determination of threshold values based on statistical distribution is more accurate and reproducible than manually setting the threshold value (Warner 2005).

The major source of error in the change detection was the emergent wetland types. The temporary and seasonally flooded emergent wetland types are dry in some years and saturated in others. In some instances the emergent wetland type are farmed during the dry period. The year threshold we used did not mask these false changes resulting from natural variability. We can potentially increase the year threshold but then our ability to detect other subtle changes will be diminished. Despite these errors, the method appears successful in detecting various kinds of disturbance events. Visual identification of some of the disturbance events captured by the method included logging and thinning activities, farming, conversion of wetland to open water bodies and clearing for commercial and residential development. The disagreement between the disturbance year assigned by the method and visual interpretation was mostly because of the inability of the method to detect some disturbance events such as thinning activities that were not detected by the method and the threshold value and threshold year used to detect change. In some cases, disturbance will occur in multiple parts of the time series. Since we used the number of consecutive year threshold to identify change, even in case of real disturbances that do not meet the minimum year criteria they will not be detected as change. Disturbance year can be a useful product for wetland permitting agencies like Department of Environment Quality to monitor the compliance of wetland permit issued.

The total change area as summarized in Table 5 should be carefully interpreted. The change area identified by the method does not only represent wetland loss but also includes area which has experienced different disturbance events such as silviculture and agricultural activities. Therefore these areas should be used to identify potential hotspots of wetland change. The next stage in our study is to use the magnitude of Z-score during the disturbance event and the temporal spectral curve to label disturbance events. As shown in Fig. 7 and Table 6 spectral trajectories for different disturbance events vary. The relationship between various change events and parameters derived from the trajectory such as the mean and standard deviation of the Z-score after the disturbance, the magnitude of Z-score before and after the disturbance event, slope and direction of the trajectory after the disturbance can be evaluated to attribute the change process. This will help identify the major stressors affecting wetlands and can complement national wetland condition assessment underway through Environmental Protection Agency.

Conclusion

Capturing the nature of highly dynamic environment such as wetlands that exhibit high degree of natural temporal variability is a challenging task. The variability is due to seasonal fluctuations in water level due to changes in precipitation, temperature and other environmental conditions as well as human influences. In recent years, many studies have utilized inter-annual time series data to characterize various disturbances in different landscape. The goal of this study was to assess the utility of inter-annual Landsat time series data for wetland monitoring. A Z-score based technique was used to detect wetland change location in Landsat time series data. The Z-score trajectory of unchanged wetlands in the study area provided a description of the inter-annual variability in the spectral trends of different wetlands. This information allowed us to discriminate actual changes from the natural variability thus increasing the performance of the change detection method. The variability in the Z-score value can potentially be reduced by utilizing a winter time series data along with

growing season data. However, availability of Landsat data in winter will be a limiting factor. The resulting change map provides information on not only the current hotspots of wetland disturbance dynamics but also reconstructs the disturbance history. The information on the disturbance year along with the wetland permit database maintained by the state agencies can be used to track unpermitted wetland disturbances and produce wetland change rates in an annual basis. The change map showed the ability of the method to capture both abrupt as well as gradual changes occurring in the wetland. Different change events such as logging activities, farming suburban development were observed in the change map. With adequate field data on these change events, the Z-score trajectory can be utilized to provide information on various disturbance events occurring in the study area. With the recent free availability of past and future Landsat data, this method could be an important process for updating the existing NWI maps and identifying major stressor to wetlands.

Acknowledgements The authors would like to acknowledge the help of Kevin McGuckin and Brian Diggs from Conservation Management Institute at Virginia Tech for their help in interpreting the aerial photos.

References

Baker C, Lawrence R, Montagne C, Patten D (2007) Change detection of wetland ecosystems using Landsat imagery and change vector analysis. Wetlands 27:610–619

Bontemps S, Bogaert P, Titeux N, Defourny P (2008) An object-based change detection method accounting for temporal dependences in time series with medium to coarse spatial resolution. Remote Sensing of Environment 112:3181–3191

Congalton RG, Green K (1999) Assessing the accuracy of remotely sensed data. CRC Press, Boca Raton, FL

Coppin P, Jonckheere I, Nackaerts K, Muys B, Lambin E (2004) Digital change detection methods in ecosystem monitoring: A review. International Journal of Remote Sensing 25:1565–1596

Cowardin LM, Carter V, Golet FC, Laroe ET (1979) Classification of wetlands and deepwater habitats of the United States. U.S. Fish and Wildlife Service, Washington DC

Crist EP (1985) A TM tasseled cap equivalent transformation for reflectance factor data. Remote Sensing of Environment 17:301–306

Dahl TE, Watmough MD (2007) Current approaches to wetland status and trends monitoring in prairie Canada and the continental United States of America. Canadian Journal of Remote Sensing 33:S17–S27

Dahl TE (2006) Status and trends of wetlands in the conterminous United States, 1998–2004. U.S. Fish and Wildlife Service, Washington, DC

de Beurs KM, Henebry GM (2005) A statistical framework for the analysis of long image time series. International Journal of Remote Sensing 26:1551–1573

Harvey KR, Hill GJE (2001) Vegetation mapping of a tropical freshwater swamp in the Northern Territory, Australia: A comparison of aerial photography, Landsat TM and SPOT satellite imagery. International Journal of Remote Sensing 22:2911–2925

Hefner JM, Storrs CG (1994) Classification and inventory of wetlands in the southern Appalachian region. Water, Air, and Soil Pollution 77:209–216

Hodgson ME, Jensen JR, Mackey HE, Coulter MC (1987) Remote sensing of wetland habitat: A wood stork example. Photogrammetric Engineering and Remote Sensing 53:1075–1080

Houhoulis PF, Michener WK (2000) Detecting wetland change: a rule-based approach using NWI and SPOT-XS data. Photogrammetric Engineering and Remote Sensing 66:205–11

Huang C, Goward SN, Masek JG, Thomas N, Zhu Z, Vogelmann JE (2010) An automated approach for reconstructing recent forest disturbance history using dense Landsat time series stacks. Remote Sensing of Environment 114:183–198

Huang C, Goward SN, Masek JG, Gao F, Vermote EF, Thomas N, Schleeweis K, Kennedy RE, Zhu Z, Eidenshink JC, Townshend JRG (2009) Development of time series stacks of Landsat images for reconstructing forest disturbance history. International Journal of Digital Earth 2:195–218

Kauth RJ, Thomas GS (1976) The tasseled cap - a graphic description of the spectral temporal development of agricultural crops as seen in Landsat. Proceedings on the Symposium on Machine Processing of Remotely Sensed Data, West Lafayette, Indiana, pp 41–51

Kennedy RE, Townsend PA, Gross JE, Cohen WB, Bolstad P, Wang YQ, Adams P (2009) Remote sensing change detection tools for natural resource managers: Understanding concepts and trade-offs in the design of landscape monitoring projects. Remote Sensing of Environment 113:1382–1396

Kennedy RE, Cohen WB, Schroeder TA (2007) Trajectory-based change detection for automated characterization of forest disturbance dynamics. Remote Sensing of Environment 110:370–386

Koeln G, Bissonnette J (2000). Cross-correlation analysis: mapping landcover change with a historic land cover database and a recent, single-date multispectral image. Proceedings 2000 ASPRS Annual Convention, Washington, DC Available at the website: http://www.glc.org/wetlands/docs/CCA_Paper.doc

Kudray GM, Gale MR (2000) Evaluation of National Wetlands Inventory maps in a heavily forested region in the upper Great Lakes. Wetlands 20:581–587

Lang MW, Kasischke ES, Prince SD, Pittman KW (2008) Assessment of C-band synthetic aperture radar data for mapping coastal plain forested wetlands in the mid-Atlantic region USA. Remote Sensing of Environment 112:4120–4130

Lunetta RL, Knight FK, Ediriwickrema J, Lyon JG, Worthy LD (2006) Land-cover change detection using multi-temporal MODIS NDVI data. Remote Sensing of Environment 105:142–154

Mackey HE (1990) Monitoring seasonal and annual wetland changes in a freshwater marsh with SPOT HRV Data, vol. 4. Proceedings of American Society for Photogrammetry and Remote Sensing, Denver, CO, pp 283–292

Masek JG, Vermote EF, Saleous N, Wolfe R, Hall EF, Huemmrich KF, Gao F, Kutler J, Lim T (2006) A Landsat surface reflectance data set for North America, 1990–2000. Geoscience and Remote Sensing Letters 3:68–72

Morisette JT, Khorram S (2000) Accuracy assessment curves for satellite-based change detection. Photogrammetric Engineering and Remote Sensing 66:875–880

Murphy PNC, Ogilvie J, Connor K, Arp PA (2007) Mapping wetlands: A comparison of two different approaches for New Brunswick, Canada. Wetlands 27:845–54

Nielsen EM, Prince SD, Koeln GT (2008) Wetland change mapping for the U.S. Mid-Atlantic Region using an outlier detection technique. Remote Sensing of Environment 112:3993–3995

National Oceanic and Atmospheric Administration-Coastal Services Center (2012) Land Cover Analysis: NOAA Coastal Change Analysis Program. http://www.csc.noaa.gov/crs/lca/ccap.html. Accessed 5 June 2012.

Ordoyne C, Friedl M (2008) Using MODIS data to characterize seasonal inundation patterns in the Florida Everglades. Remote Sensing of Environment 112:4107–4119

Parmenter AW, Hansen A, Kennedy R, Cohen W, Langner U, Lawrence R, Maxwell B, Gallant A, Aspinall A (2003) Land use and land cover change in the Greater Yellowstone Ecosystem: 1975–1995. Ecological Applications 13:687–701

Pavri F, Aber JS (2004) Characterizing wetland landscapes: A spatio-temporal analysis of remotely sensed data at Cheyenne Bottoms, Kansas. Physical Geography 25:86–104

Pouliot D, Latifovic D, Fernandes R, Olthof I (2009) Evaluation of annual forest disturbance monitoring using a static decision tree approach and 250 m MODIS data. Remote Sensing of Environment 113:1749–1759

Powell SL, Cohen WB, Healey SP, Kennedy RE, Moisen GG, Pierce KB, Ohmann JL (2010) Quantification of live aboveground forest biomass dynamics with Landsat time-series and field inventory data: A comparison of empirical modeling approaches. Remote Sensing of Environment 114:1053–1068

Ramsey EW, Laine SC (1997) Comparison of Landsat Thematic Mapper and high resolution aerial photography to identify change in complex coastal wetlands. Journal of Coastal Research 13:281–92

Ramsey EW, Nelson GA, Sapkota SK (2001) Coastal change analysis program implemented in Louisiana. Journal of Coastal Research 17:53–71

Ramsey EW, Rangoonwala A, Middleton B, Lu Z (2009) Satellite optical and radar image data of forested wetland impact on and short-term recovery from Hurricane Katrina in the lower Pearl River flood plain of Louisiana, USA. Wetlands 29:66–79

Ramsey EW, Spruce J, Rangoonwala A, Suzuoki Y, Smoot J, Gasser J, Bannister T (2011) Monitoring wetland forest recovery along the lower Pearl river with daily MODIS satellite data. Photogrammetric Engineering and Remote Sensing 77:1133–1143

Rebelo LM, Finlayson M, Nagabhatla N (2009) Remote sensing and GIS for wetland inventory, mapping and change analysis. Journal of Environment Management 90:2234–2242

Roy DP, Ju J, Kline K, Scaramuzza PL, Kovalskyy V, Hansen M, Loveland TR, Vermote E, Zhang C (2010) Web-enabled Landsat Data (WELD): Landsat ETM+composited mosaics of the conterminous United States. Remote Sensing of Environment 114:35–49

Schroeder T, Wulder MA, Healey SP, Moisen GG (2011) Mapping wildfire and clearcut harvest disturbances in boreal forest with Landsat time series data. Remote Sensing of Environment 115:1421–143

Stolt MH, Baker JC (1995) Evaluation of national wetland inventory maps to inventory wetlands in the southern Blue Ridge of Virginia. Wetlands 15:346–353

Stueve KM, Housman IW, Zimmerman PL, Nelson MD, Webb JB, Perry CH, Chastain RA, Gormanson DD, Huang C, Healey SP, Cohen WB (2011) Snow-covered Landsat time series stacks improve automated disturbance mapping accuracy in forested landscapes. Remote Sensing of Environment 115:3203–3219

Syphard AD, Garcia MW (2001) Human and beaver induced wetland changes in the Chickahominy River watershed from 1953 to 1994. Wetlands 21:342–53

Tiner RW, Finn JT (1986) Status and Recent Trends of Wetlands in Five Mid-Atlantic States: Delaware, Maryland, Pennsylvania, Virginia, and West Virginia. U.S. Fish and Wildlife Service, Region 5, National Wetlands Inventory Project, Newton Comer, MA and U.S. Environmental Protection Agency, Region III, Philadelphia, PA

Tuxen K, Schile L, Kelly M, Siegel S (2008) Vegetation colonization in a restoring tidal marsh: A remote sensing approach. Restoration Ecology 16:313–323

U.S. Fish and Wildlife Service (2010) U.S. Fish and Wildlife Service National Wetlands Inventory. Available via http://www.fws.gov/wetlands/Data/DataDownload.html. Accessed August 15 2010

Vogelmann JE, Xian G, Homer C, Tolk B (2012) Monitoring gradual ecosystem change using Landsat time series analyses: Case Studies in selected forest and rangeland ecosystems. Remote Sensing of Environment, Available online 9 February 2012

Warner T (2005) Hyperspherical direction cosine change vector analysis. International Journal of Remote Sensing 26:1201–15

Wright C, Gallant A (2007) Improved wetland remote sensing in Yellowstone National Park using classification trees to combine TM imagery and ancillary environmental data. Remote Sensing of Environment 107:582–605

CHAPTER 3

Discriminating Forested Wetlands and Uplands Using Temporal Metrics Derived from Landsat Time Series

Prepared for submission to Remote Sensing of Environment

Abstract:

Successful conservation and management of wetlands requires up to date and accurate information on their properties and location. Forested wetlands are difficult to map because of their canopy cover which prevents viewing of the soil saturation and topography beneath the canopy. Forested wetlands are extremely underrepresented in current wetland maps such as the National Wetland Inventory (NWI) in the United States, so improved detection is needed. A common approach in mapping wetlands is to compare a series of aerial photo or satellite images between seasons or across years. Time series data provide information on key aspects of hydrology and vegetation functions, such as seasonality, productivity and temporal variability that enhance discrimination between different land cover types. In this paper, we present a technique to characterize differences in spectro-temporal profile of forested uplands and wetlands using time series of Landsat data (1999-2012). The results show that the temporal metrics derived from Landsat can accurately discriminate between forested upland and wetland (accuracy of 88.5%). The accuracy of temporal metrics derived from Normalized Difference Moisture Index (NDMI) was higher than the accuracy achieved by Normalized Difference Vegetation Index (NDVI) and Tasseled Cap Wetness index (TCW). Now that corrected Landsat data are available free of cost, the technique presented here can be easily implemented and tested in other areas.

Keywords: Landsat, Wetlands, Multi-temporal, Curve-fitting, Random forest, Lowess

1. Introduction

Wetlands are one of the most unique and productive ecosystems on earth, providing numerous ecological and economical values such as habitat for wildlife, resources for human consumption, flood control, and ground water recharge (Mitsch and Gosselink, 2000). Despite the undisputed economic and ecological importance of wetlands they are under enormous threat due to human exploitation and climate change (van der Valk, 2006). In addition, there is lot of uncertainty associated with the extent and distribution of wetlands which further increases the threats to the well-being of these vulnerable ecosystems. Accurate and up-to-date information on the distribution and extent of wetland ecosystems both regionally and globally is required for the successful protection and management of wetlands.

Wetlands occur in diverse landscapes and in a wide range of climates. Hydrology plays a key role in wetlands which distinguishes them from other terrestrial and aquatic systems. Wetlands are characterized by periodic to continuous inundation or saturation with water during the growing season and soils that are periodically deficient in oxygen (hydric soils), and vegetation that is adapted to periods of anaerobic or anoxic soil conditions (hydrophytic vegetation). Along with soil type and land-use, the duration, depth, and frequency of inundation, water sources and properties determine the distribution and characteristics of wetland vegetation. The effect and variability of hydrology between wetlands exerts a major controlling force in the establishment and development of vegetation and produces vegetation communities with more distinct spatial and temporal pattern than vegetation in upland areas (Todd et al., 2010).

Earth observation data has been widely used for mapping and monitoring wetland distribution. Multispectral satellite imagery, especially that collected by Landsat Thematic Mapper (TM) and Enhanced Thematic Mapper (ETM+), has been widely used for wetland inventory and mapping. Harvey and Hill (2001) compared wetland classification using aerial photos (1 m), SPOT XS (20 m) and Landsat (30 m) and found that Landsat provided a more accurate classification than SPOT XS and comparable accuracy to that of aerial photographs. Superior performance of Landsat compared to SPOT was attributed to better spectral resolution and inclusion of middle infrared bands not available in SPOT. Sader et al. (1995) used unsupervised classification of Landsat data and classified forested wetlands with an overall accuracy of 72%. However, the user's accuracy for the forested wetland was very low (58%) indicating poor ability of this method to map forested wetlands. Despite extensive use of remote sensing data, wetlands are inherently difficult to map because the spectral reflectance properties of wetland vegetation are often similar to vegetation in the upland areas (Adam et al., 2010 and Ozesmi and Bauer, 2002). Forested wetlands, which represent 50% of the wetlands in United States, are one the most difficult wetland types to map. Forested wetlands mainly occur along a drier water regime and the canopies in the forested wetlands prevent viewing of the soil saturation in the ground (Ozesmi and Bauer, 2002) making them difficult to detect with remote sensing data.

The temporal resolution of images used has been found to be important for discriminating wetland from upland vegetation. Many wetland species have overlapping reflectance at peak biomass (Schmidt and Skidmore, 2003) and aggregation to broad wetland classes are necessary to achieve better accuracies (Wright and Gallant, 2007). Use of multi-season images helped in discriminating between wetland types by detecting hydrological and phenological changes

characteristic of those types (Baker et al., 2006 and Wolter et al., 2005). The basic approach is the use of leaf-off and leaf-on images from a single growing season. Leaf-on images are used for discrimination among vegetation communities while leaf-off images are used to detect wetland hydrology. The accuracy of wetland maps produced from multi-season images has shown to be superior compared to a single date image. Mackey (1990) noted that satellite imagery collected during different seasons enhanced the ability to discriminate between wetland vegetation types, and that multi-temporal data can help evaluate phenological, hydrological, and compositional changes across seasons and between years. Using images from two dates, Lunetta and Balogh (2000) improved the accuracy of wetland maps from 69% to 88% compared to a single date image. However, the accuracy of wetland and upland forest was low and majority of upland forests were confused with wetland forests. Pantaleoni et al. (2009) used March and October ASTER images during a single growing season to discriminate between uplands, woody wetlands, emergent wetlands and open water, however the accuracy of forested wetland was low. This study also recommended that the use of inter-annual images would better characterize the phenological differences between wetland and upland vegetation communities for improved wetland classification because of climatic variation between years. Townsend and Walsh (2001) used Landsat TM data from March to August in a single year and produced a detailed classification of vegetation communities with an overall accuracy of 92%. However the accuracy of wetland forested communities in their study was only 75%.

Most of the studies utilizing multi-temporal data use relatively few dates and study within a single growing season. In recent years, multi-year seasonal time-series data have been used for improved land-cover classification. These studies have utilized longer time series (greater than 10 years) representing seasonal and inter-annual variability between land cover classes for

improved discrimination (Bradley and Mustard, 2008 and Zoffoli et al., 2008). Time series remote sensing data provide information that are directly linked to key aspects of vegetation functions, such as seasonality, productivity and inter-annual variability and therefore have tremendous potential for characterizing, classifying and mapping vegetation (Wessels et al., 2010). Inter-annual variability derived from time series data can be a useful metric when land cover types show amplified response to differences in environment condition. When several years of data are combined, characteristic temporal patterns can be observed which can be used to classify land cover (Liang, 2001 and Moody & Johnson, 2001). Data collected by sensors such as Advanced Very High Resolution Radiometer (AVHRR) and the Moderate Resolution Imaging Spectroradiometer (MODIS) provide daily observation. Numerous studies have utilized the rich temporal information provided by these sensors to study vegetation dynamics at global and regional level. However, the coarser spatial resolution (MODIS-250 meter; AVHRR-1 km) especially limit their application in studying wetlands as they often occur as small, fragmented polygons as small as a few meters across, or as narrow linear features (Fig. 1).

Recently, Landsat data have become available free of cost. At the spatial resolution of 30 meters and images dating back to 1972, the opening of Landsat archive provides an opportunity to study vegetation dynamics at higher spatial and temporal resolution. The Landsat archive can be used to assess the temporal pattern of different vegetation communities to improve discrimination which would otherwise not be possible using few images taken at different dates. Few studies have utilized time series Landsat data to assess vegetation dynamics. Most of these studies have focused on characterizing long-term average and inter-annual variability in vegetation phenology (Fisher et al., 2006, Elmore et al., 2012 and Melass et al., 2013). In these studies, time series Landsat images are arranged by Julian dates discarding the year of

acquisition to create a temporal profile indicative of average phenology curve. Walker et al. (2012) are among few researchers who utilized data fusion techniques which downscale MODIS data to spatial resolution of Landsat to characterize phenology at annual scale. However, information derived from such fused techniques is complicated by land cover heterogeneity below the spatial resolution of MODIS and uncertainty introduced by data fusion algorithm (Melaas et al., 2013).

Despite numerous attempts, there is a need for developing a better and more accurate approach for discriminating forested uplands from wetlands. The objective of the study is to investigate if the temporal pattern derived from time series of Landsat data can accurately discriminate between wetland and upland forest. Our hypothesis is that during the period of the growing season when trees do not have full canopy cover, a wetland forest and upland forest will exhibit different temporal trend owing to the hydrology which can be characterized using time series data from Landsat.

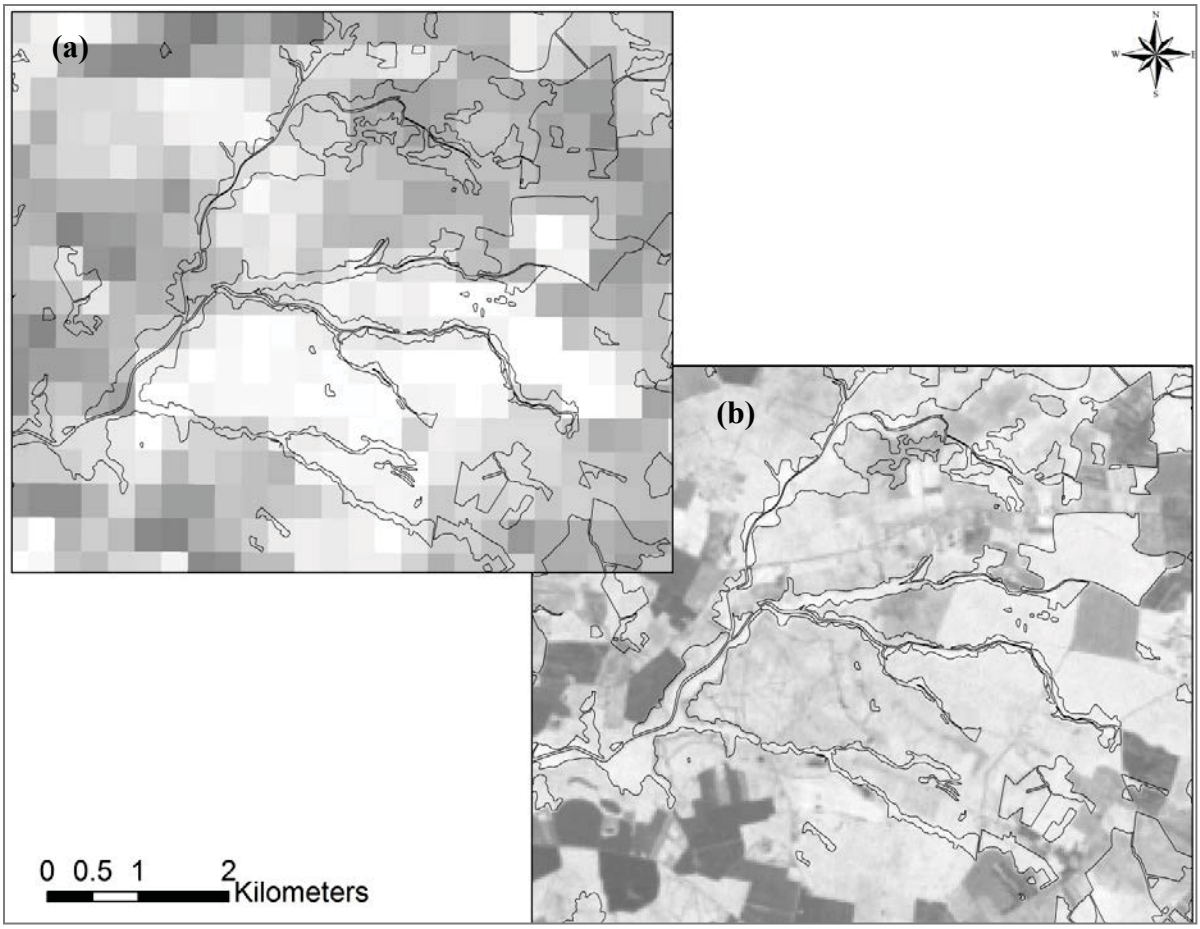

Fig. 1. Comparison of MODIS (a) and Landsat (b) spatial scale overlaid with the wetland layer. National Wetland Inventory wetlands in the study area occur in small, narrow patches and are fragmented. The resolution of MODIS pixels in (a) is too coarse to capture the spatial detail required.

2. Methods

2.1 Study area

The study focuses on the non-tidal forested wetland and forested uplands in the state of Delaware (Fig. 2.). The area is characterized by temperate humid continental climate with annual average rainfall of 114 cm (http://climate.udel.edu/delawares-climate). Almost all of Delaware's landscape falls on the Coastal Plain. Around 38% of the state is represented by hydric soils owing to the relatively flat topography of the area. The water table is at or near the surface in most wetlands from winter to mid-spring or early summer, resulting in ponding or flooding of the wetland surface. The water table begins to drop in May or June and reaches its low point in

September or October (Lang et al., 2013). About 25% of Delaware is covered by wetlands of various types, dominated by palustrine forests (characterized by woody vegetation taller than 6 m). Palustrine forests cover 64% of the state's wetlands, with deciduous wetlands that are temporarily-flooded being predominant (Tiner et al., 2011). In terms of the hydrogeomorphic classification, the majority of the wetlands are classified as flats which are located in the headwaters and the interfluves between streams, have poor vertical drainage and are fed by precipitation and groundwater (Jacobs et al., 2009). The most recent wetland status and trend report indicated that between 1992 and 2007, 1,578 hectares of vegetated wetlands were lost primarily to agriculture and development. In addition to the loss of wetland extent, the report also emphasizes that the ecosystem functioning of the remaining wetlands is impaired due to adjacent development and fragmentation.

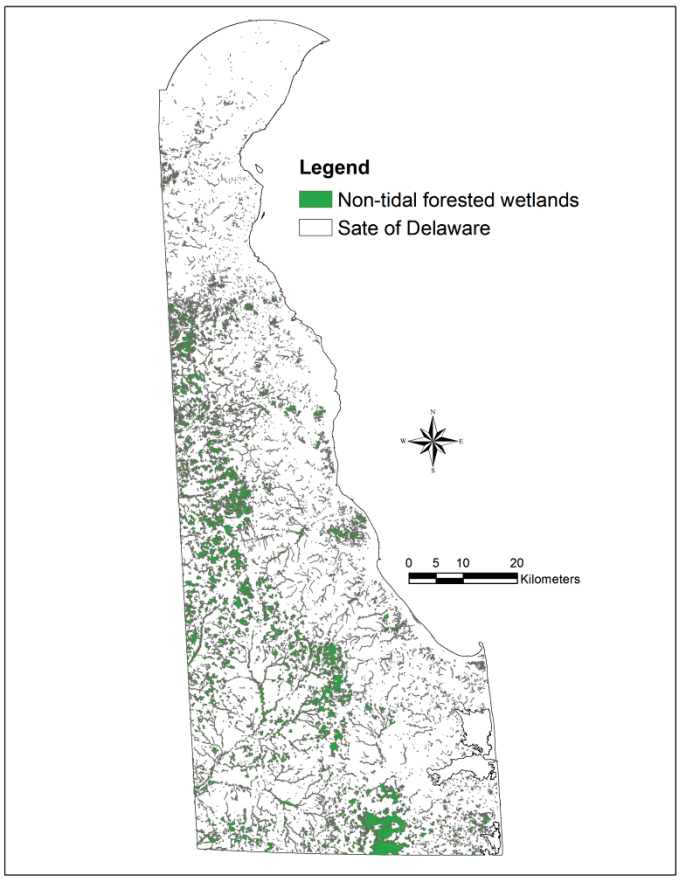

Fig. 2. The state of Delaware showing distribution of non-tidal forested wetlands derived from National Wetland Inventory data (http://www.fws.gov/wetlands/Data/Mapper.html).

2.2 Field data

The wetland data used in this study was collected by Delaware Department of Natural Resources and Environmental Control using the Delaware Comprehensive Assessment Procedure (DECAP) (Jacobs et al., 2009). The comprehensive assessment method is used for determining the condition of a wetland site relative to reference condition. The data were collected between 1999 and 2012. The DECAP uses a hydrogeomorphic approach for classification of wetlands, where wetlands are classified as flats, riverine, slope or depressions. The majority of the wetlands in the Delaware data were classified either as flats or riverine

wetlands. Flats occur on interfluves, in the headwaters of watersheds, or large floodplain terraces, where the dominant water source is precipitation. Riverine wetlands occur in floodplains and riparian corridors in association with stream channels and the dominant source of water is overbank flow from channel or subsurface hydraulic connections. DECAP uses existing wetlands maps and a probabilistic sampling design technique to select sampling locations. Detailed description of field data collection can be found in Jacobs et al. (2009) and Jacobs et al. (2010) and is briefly described here. In each sampling location, an assessment area (AA) is established by centering a 40m radius circle. In each AA, information on hydrologic condition, vegetation communities, vegetation disturbance, soil, topography and surrounding land use is collected. All the collected variables are scored to produce a qualitative rating of wetland condition.

The field data was combined with the Delaware wetlands layer that was revised using 2007 aerial imagery. Field data that was classified as palustrine forest in the Delaware wetlands layer was extracted. We further separated the data as palustrine broadleaf forest and mixed forest and scrub-shrub. The field data did not contain enough samples for evergreen forested wetland. We therefore focused the study on deciduous palustrine wetland forest and mixed vegetation wetland types (mixed types contained forest and scrub-shrub vegetation types). For further analysis, we also differentiated flats and riverine wetlands from the broadleaf forest and mixed wetland types. The upland forest sample was generated from the 2007 Delaware land cover and land use map (http://dataexchange.gis.delaware.gov). The 2007 land-cover map was developed based on aerial photos acquired in the summer of 2007 (http://dataexchange.gis.delaware.gov/dataexchange/metadata.aspx). From the 2007 land-cover map, we separated the deciduous forest pixels. We randomly distributed 100 sampling points

within this area and only used points falling within the non-hydric soil layer derived from USDA-NRCS Soil Survey Geographic Database (http://websoilsurvey.sc.egov.usda.gov/App/HomePage.htm) for the three counties in Delaware.

2.3 Landsat data and indices calculation

We used all Landsat Thematic Mapper (TM) and Enhanced Thematic Mapper Plus (ETM+) data available from 1995 to 2011 (274 scenes) covering state of Delaware (Path:Row 14:33). The cloud cover was visually assessed in each image. Images with minimum cloud cover in the study areas were included. The images were converted to surface reflectance using the Landsat Ecosystem Distribution Adaptive Processing System (LEDPAS). LEDAPS uses the MODIS/ 6S radiative transfer algorithm to invert the top of atmosphere reflectance to surface reflectance for each 30-m pixel (Masek et al., 2006). The LEDAPS generated cloud mask was used to mask out the clouds in the images.

Previous studies have used and assessed performance of different Landsat bands and band combinations (indices) for wetland mapping. The Federal Geographic Data Committee (1992) identified Landsat TM bands 4 and 5 as most effective for wetland delineation. Ozesmi and Bauer (2002) indicate that Landsat band 5 is the most important band for wetland identification because of its ability to discriminate vegetation from soil moisture. Bwangoy et al. (2010), in using combination of optical and radar data for mapping wetland in the Congo River basin found that Landsat band 5 was the most important variable for wetland identification after elevation. Normalized Difference Vegetation index (NDVI: band4-band3/band4+band3) is a commonly used index for wetland delineation and wetland vegetation mapping (Aslam et al., 2008, Gilmore et al., 2008 and Townsend and Walsh 2001). NDVI provides as indicator of relative abundance and activities of green vegetation and is sensitive to biophysical

characteristics such as leaf area index, net primary productivity and vegetation phenology (Griffiths, 2002). Another index Normalized Difference Moisture Index (NDMI) is also widely used in mapping wetlands (Li and Chen, 2005, Davranche et al., 2010 and Luyan et al., 2011). NDMI combines the near infrared and mid-infrared bands (band4-band5/band4+band5) and has been shown to be sensitive to soil moisture (Fensholt and Sandholt, 2003). de Alwis et al.(2007) used time series of Landsat images and demonstrated that the NDWI can be effectively used to classify saturated areas in the landscape. The Tasseled cap transformation (TC) is an orthogonal transformation of Landsat bands that transforms the Landsat bands into brightness, greenness and wetness axes (Kauth and Thomas 1976). TC is preferred over other data transformation methods such as principal component analyses as the TC components corresponds to the physical characteristics of vegetation and are ecologically interpretable (Parmenter et al., 2003). Dymond et al. (2002) showed that the tasseled cap transformation enhances the phenological differences between different forest types leading to improved discrimination of different types of deciduous forest. Hodgson et al. (1987) associated the wetness and greenness components of TC to different wetland types. Ordoyne and Friedl (2008) compared the effectiveness of Tasseled Cap wetness, TC brightness, TC greenness, and NDWI. TC wetness was found to be highly correlated with seasonal inundation patterns across a range of surface vegetation types. For this study we compared performance of NDVI, NDWI and Tasseled Cap Wetness (TCW).

2.4 Smoothing and curve fitting

We used a locally weighted regression smoothing (Lowess) technique to filter and fit a smoothed curve in the time series of vegetation index. The Lowess technique has been widely used in studies employing remote sensing data such as: smoothing long term vegetation index data to analyze the trend (Pouliot et al., 2009); curve fitting in time series data to derive

phenological parameters (Lancaster et al., 1996, Briber et al., 2013, Jenerette et al., 2013 and Morris et al., 2013) and to estimate pasture quality using time series NDVI (Dymond et al., 2006). Lowess is a non-parametric technique designed to identify the trend in the data without prior specification of the model (Cleveland, 1979). It uses a local regression technique within a moving window, where points within the moving window are inversely weighted such that the observation closest to the point of interest will have more weight (Jacoby, 2000 and Knudsen et al., 2007). The degree of smoothing depends on the span of the window which determines the proportion of observation used in each local regression. A smaller span parameter will likely overfit the data (the fitted curve will be exactly interpolated as original data), while a larger parameter will discount the trend in the data. Despite our effort to remove clouds and shadows from the images, some small clouds and shadows remained in the images. These outliers can distort the smoothed values. In order to make time series reliable, we used a robust lowess (rlowess) technique in which the fitted curves are not affected by the outliers in the time series. This is achieved through iterative reweighting in which the weights for each iteration are adjusted based on the previous fit (Mathworks, 2013). In robust lowess, after the initial fit a different set of weights are determined based on the size of the residuals. Large residuals result in smaller weights and small residuals result in large weights in the subsequent fit, resulting in a fit that is less influenced by outliers (Cleveland, 1979). One of the critical issues in smoothing is the selection of the smoothing parameter or the window size. The optimal smoothing parameter was determined both by visual inspection and cross-validation. The span parameter with the lowest cross validation error was visually checked for the best fit.

2.5 Extraction of temporal metrics

One of the most common uses of time series vegetation index data is extraction of phenological metrics (e.g., start of the growing season, end of the growing season, length of the growing season),which is achieved using remote sensing data with greater temporal resolution such as MODIS. In recent years, few studies have utilized time series vegetation data from Landsat to extract phenological markers mainly start and the end of growing season (Fisher et al., 2006, Fisher et al., 2007, Elmore et al., 2012 and Melaas et al., 2013). Since our goal in this study is to investigate if the temporal pattern of vegetation indices can discriminate between wetland and upland deciduous forest, using only the standard phenological metrics such as start and end of the growing season may not reveal subtle differences between upland and wetland forests. Therefore, we calculated other different temporal metrics from the fitted curve. Table 1 lists the temporal metrics extracted in this study. We assume that these metrics sufficiently capture the different temporal trend between wetland and upland forests. We extracted these temporal metrics using observations from March to November in order to minimize the effect of snow on vegetation index values.

Table 1. List and description of temporal metrics derived from Landsat time series data.

Temporal metric	**Description**
Spring	Julian day at first inflection point
Fall	Julian day at second inflection point
Growing Days	Length of growing season (fall - spring)
AOCin	Area under the curve between inflection points
AOCin1	Area under the curve before spring
AOCin2	Area under the curve after fall
STDIN1	Bootstrap median width of 95% confidence interval until first inflection point
STDIN2	Bootstrap median width of 95% confidence interval after second inflection point
AUCFWHM	Area under the curve related to FWHM
AUCRFW	Area under the curve of left side of FWHM
AUCLFW	Area under the curve of right side of FWHM
TAUC	Total area under the curve

Max	Median value of greater than 75th percentile
MaxD	Julian day corresponding to maximum
Min05R	Minimum of median of 5% from the right side of the curve
Min05L	Minimum of median of 5% from the left side of the curve
KU	Kurtosis
SK	Skewness

A common method to derive phenological markers from time series data is to calculate inflection points in the time series curve (White et al., 1997, Sakamoto et al., 2005 and Baltzer et al., 2007). The first inflection point (Spring) is where there is maximum change in the rising limb of the curve and the second inflection point (Fall) is where there is maximum change in the falling limb of the curve. The first and the second inflection point calculated in this way generally refer to start and the end of the season (de Beurs et al., 2010). The difference between these two inflection points (Growing Days) is indicative of growing season length. The total area under the curve between the inflection points (AUCin) was calculated as the integral of vegetation indices values between the two inflection point and when calculated with NDVI is indicative of vegetation productivity (Hird and McDermid, 2009). We also calculated the area under the curve before the first inflection point (AOCin1) and second inflection point (AOCin2). The full width half maximum (FWHM) of the time series vegetation index value has also been used in deriving phenological parameters (Coops et al., 2011 and El Vilaly et al., 2013). Similar to the area under the curve calculation using inflection point, the area under the curve at FWHM (AUCFWHM), area under the curve of the left side of FWHM (AUCLFW) and right side (AUCRFW) was calculated. The maximum value of the time series (Max) was calculated as median of the values greater than 75^{th} percentile and the day corresponding to the maximum value (MaxD) was also extracted. Visual analysis of the time series data indicated that the minimum value in the beginning and end of the time series were different for wetland and upland forests. To quantify this we calculated the median of the 5 percentile values for the left and right side of the time series curve (Min05L and Min05R). We calculated the median value instead of mean so that they were not affected by outliers. The left and right side of the

time series curve was divided based on the maximum value of the fitted curve. The kurtosis (KU) and skewness (SK) were calculated to assess the symmetry in the time series curve.

2.6 Random forest classification

We used random forest algorithm to investigate the ability of the derived temporal metrics to discriminate between wetland and upland forests. Random forest is a non- parametric classification tree technique that randomly and iteratively samples the data and variables to generate large groups of classification trees (Breiman, 2001). The algorithm implements a bootstrapping procedure (generating random sample from training data with replacement) to generate random subset of training data (approximately 63%), which is used to fit a classification tree with small number of randomly selected variables (Cutler et al., 2007). The portion of training data not selected for generation of the classification tree (often termed as "out-of-bag" sample) is classified using the fitted tree and is used to calculate bootstrap error estimates and accuracy for each tree. After all the trees are grown, overall error and accuracy is calculated by averaging error rates across all trees in the forest. Since out-of-bag observations are not used in fitting the trees, out-of-bag error estimates provide an unbiased estimate of classification accuracy (Cutler et al., 2007). Random forest classification is robust against overfitting and correlated variables and can produce higher accuracies than traditional classification tree (Falkowski et al., 2009). Classification accuracy was assessed with the bootstrap error estimates and error matrices calculated by random forest. Overall accuracy, producer's and user's accuracy were calculated and examined to assess the effectiveness of classification. The overall accuracy is the proportion of correctly identified change events. The producer's accuracy measures the proportion of pixel belonging to a class that was correctly classified by the method and measures the error of omission. User's accuracy measures the proportion of the pixels classified as

belonging to a class matches the reference data and measures the error of commission. Random forest also calculates the importance of each predictor variable upon model accuracy. The out-of-bag values for each variable in a bootstrap sample are randomly permuted. The importance is then measured as the difference between the prediction accuracy before and after the permutation and averaged over all the trees (Tooke et al., 2013). The magnitude of the decrease in prediction accuracy indicates the importance of a predictor variable.

We trained and validated random forest classification models based on: (1) temporal metrics derived from the NDVI time series, (2) temporal metrics derived from NDMI time series, and, (3) temporal metrics derived from TCW time series. We also developed similar models for classification of wetland forest into riverine and flats.

We aimed to investigate which index provides better discrimination between forested wetlands and uplands. To achieve this, random forest models were built from temporal metrics derived from each index separately. The classification accuracy of each model was compared to assess their performance in discriminating wetlands from upland forests.

3. Results

3.1 Time series profile of wetland and upland forests.

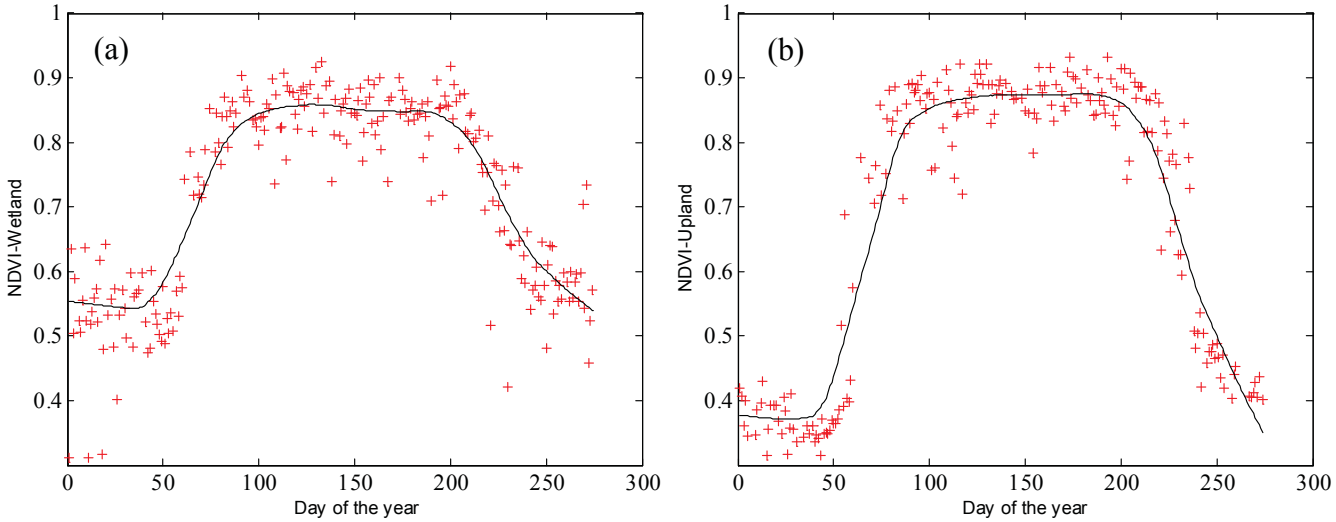

Fig. 3. An example of temporal profile of wetland (a) and upland (b) from NDVI time series, with the fitted curve from rlowess (solid line)

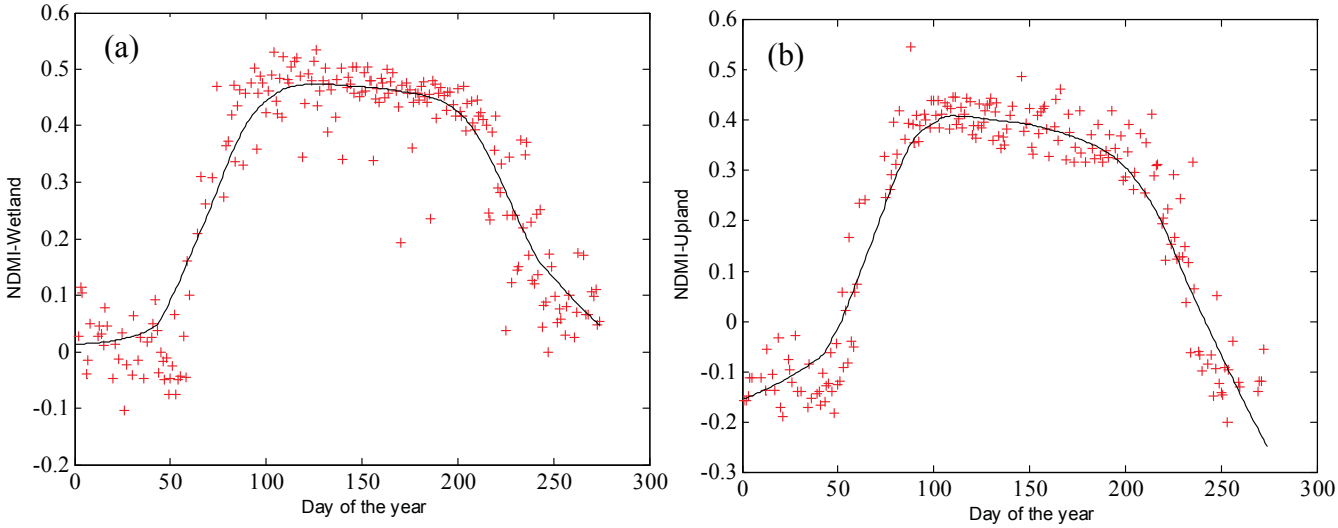

Fig. 4. An example of temporal profile of wetland (a) and upland (b) from NDMI time series, with the fitted curve from rlowess (solid line)

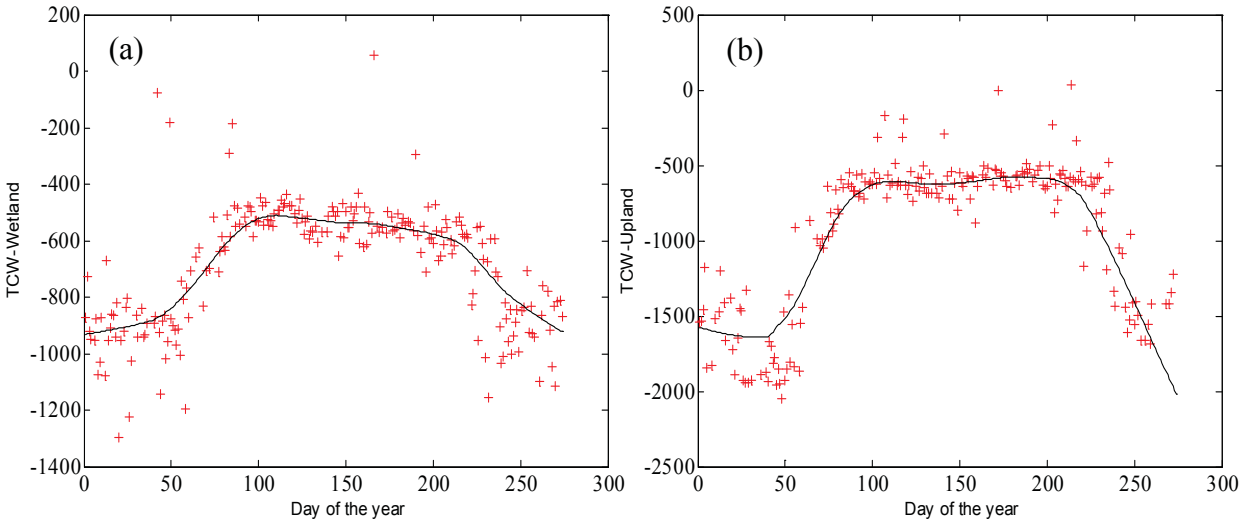

Fig. 5. An example of temporal profile of wetland (a) and upland (b) from TCW time series, with the fitted curve from rlowess (solid line)

Fig. 3, 4 and 5 show examples of the temporal profile of wetland and upland areas created by the three compared vegetation indices. Although visual inspection might not show clear differences between wetlands and uplands, some differences are evident in the time series. The minimum value during early spring (beginning of the curve) is different between wetlands and uplands in all three indices. For example, during summer and early fall when the leaf are out (flattened portion of the curve, where most of the observations are located) there is no difference between the wetlands and uplands. The range of vegetation indices values in this section of the curve is similar in both wetlands and uplands. The width of the curve also appears to be different between wetlands and uplands. It can be seen from the figures that the fitted curve follows the trend in the time series data and are also not affected by outliers. An example of the 95% bootstrap confidence interval of the rlowess fit is shown in Fig 6. The 95% confidence bound of the fitted curve is narrow and follows the contour of the fitted curve. Also, the confidence bound is much narrower for uplands compared to wetlands. In the early spring, the confidence bound is wider for wetlands than uplands.

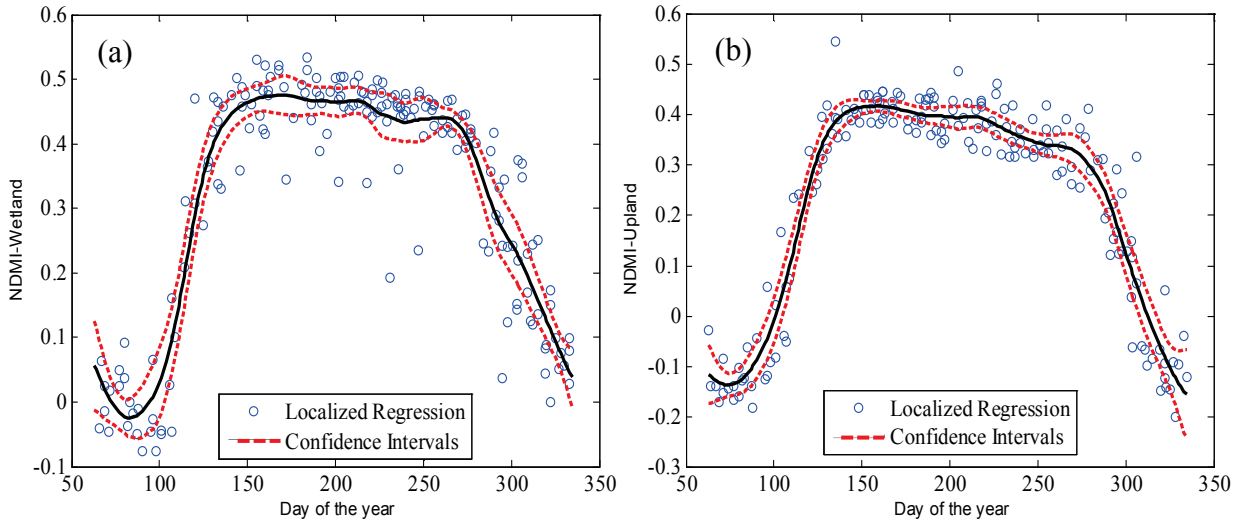

Fig. 6. An example of rlowess fit (black line) with 95% confidence interval boundary (red dashed lines)

3.2 Random forest classification

The temporal metrics derived from time series data were used in random forest classification. We first ran random forest classification with three classes (upland forest, wetland forest and mixed wetlands). Secondly, we ran random forest classification for only two vegetation type classes (upland forest and wetland forest). Finally, a random forest model was built for hydrogeomorphic classification of wetlands into flats and riverine classes. Accuracies were compared for random forest model built from temporal metrics derived from NDVI, NDMI and TCW time series.

Table 2. Accuracy statistics for three class classification (upland forest, wetland forest and mixed wetland)

Classes	Producer's accuracy (%)	User's accuracy (%)	Overall accuracy (%)
NDMI temporal metrics			
Upland forest	88	86.2	82.2
Wetland forest	61.1	68.7	
Mixed wetlands	77.5	70.3	
NDVI temporal metrics			
Upland forest	78	84.7	76.2
Wetland forest	64.8	62.5	
Mixed wetlands	75.5	72.5	
TCW temporal metrics			
Upland forest	80	81.6	73.2
Wetland forest	55.5	55.5	
Mixed wetlands	67.3	66	

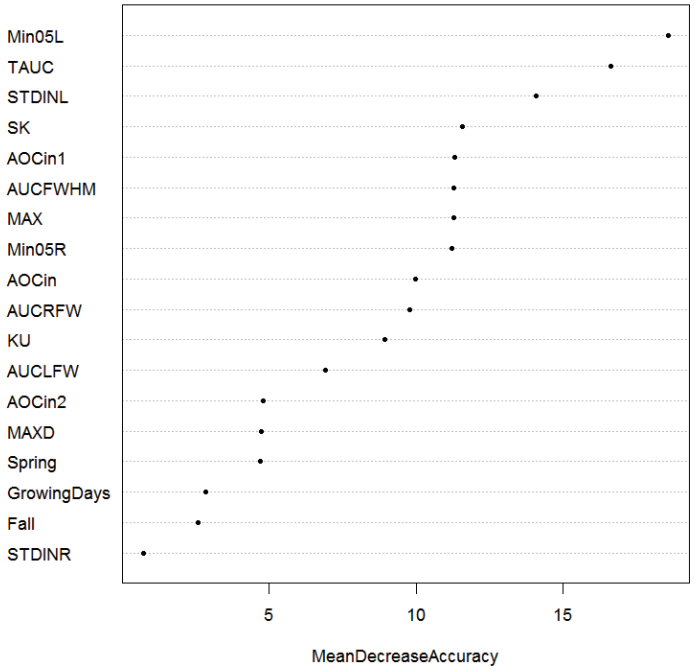

Fig. 7. Variable importance plot for a three-class random forest model developed with NDMI temporal metric. Units are percent reduction in classification accuracy which would results when a given variable is removed from the classification model. See Table 1 for variable definition.

When classifying three vegetation type classes, the model derived from NDMI temporal metrics produced highest classification accuracy (82.2%) followed by classification using NDVI temporal metrics (76.2%). The error matrix (Table 2) shows that the upland forest area was more often classified accurately (producer's accuracy of 88% in NDMI model) than wetland areas. Wetland areas were confused with uplands 14% of the time in NDMI model. The major classification confusion was between wetland forest and mixed wetland types. In the variable importance plot (Fig.7) the three most important variables were total area under the curve (TAUC), median of 5th percentile values of the left side of the curve (MIN05L) and bootstrap median width of 95% confidence interval until first inflection point (STDINL). When these three variables are removed from the model, the classification accuracy decreases by more than 15%.

Table 3. Accuracy statistics for two class classification (wetland forest and upland forest)

Classes	Producer's accuracy (%)	User's accuracy (%)	Overall accuracy (%)
NDMI temporal metrics			
Upland forest	86	89.5	88.5
Wetland forest	90.7	87.5	
NDVI temporal metrics			
Upland forest	80	86.9	84.6
Wetland forest	88.9	82.8	
TCW temporal metrics			
Upland forest	80	83.3	82.7
Wetland forest	85.1	82.1	

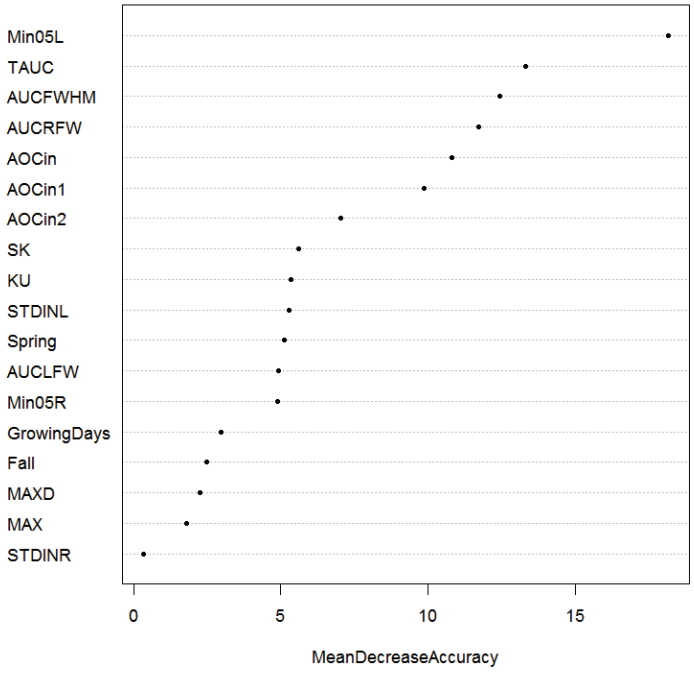

Fig. 8. Variable importance plot for two class random forest model developed with NDMI temporal metrics. Units are percent reduction in classification accuracy which would result when a given variable is removed from classification model. See Table 1 for variable definition.

When we only considered two vegetation type classes (upland forest and wetland forest), the classification accuracy significantly improved (Table 3). The best classification accuracy was again obtained with NDMI model. The overall classification accuracy achieved was 88.5% followed by classification using metrics derived from NDVI time series, with overall

classification accuracy of 84.6%. In the NDMI model, upland areas were confused with wetland areas only 10% of the time (commission error) and wetland areas were confused with upland areas only 13% of the time. The temporal metrics derived from TCW time series resulted in lowest accuracy (82.7%). The variable importance figure (Fig.8) shows that the most important variable in the NDMI model were minimum of the 5th percentile in the left hand side of the curve (Min05L), area under the curve of the full width half maximum (AUCFWHM), area under the curve of the right side of full width half maximum (AUCRFW) and total area under the curve (TAUC). Removal of these four variables decreases the classification accuracy by more than 10%. We created a scatter plot of two most important variables as identified by random forest. As seen in the scatter plot (Fig. 9), just using these two variables there is very good separation between wetlands and uplands.

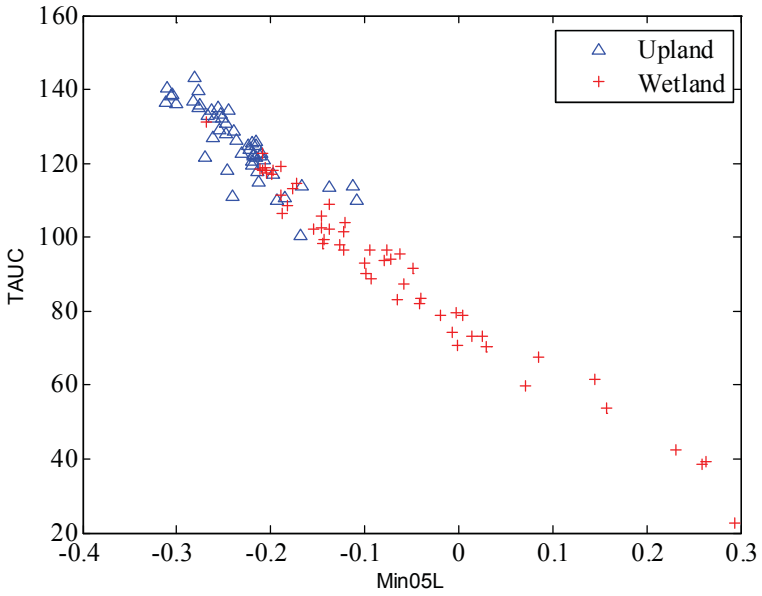

Fig. 9. Scatter plot of two most important variable identified by random forest in discriminating between wetlands (plus sign) and uplands (triangle sign). TAUC is total area under the curve and Min05L is 5th percentile of the left hand side of the curve.

Table 4. Classification accuracy statistics for classification of flat and riverine wetland types

Classes	Producer's accuracy (%)	User's accuracy (%)	Overall accuracy (%)
NDMI temporal metrics			
Flat	92	77.9	77.3
Riverine	48	75	
NDVI temporal metrics			
Flat	92	77.9	77.3
Riverine	48	75	
TCW temporal metrics			
Flat	84	64.6	58.6
Riverine	8	2	

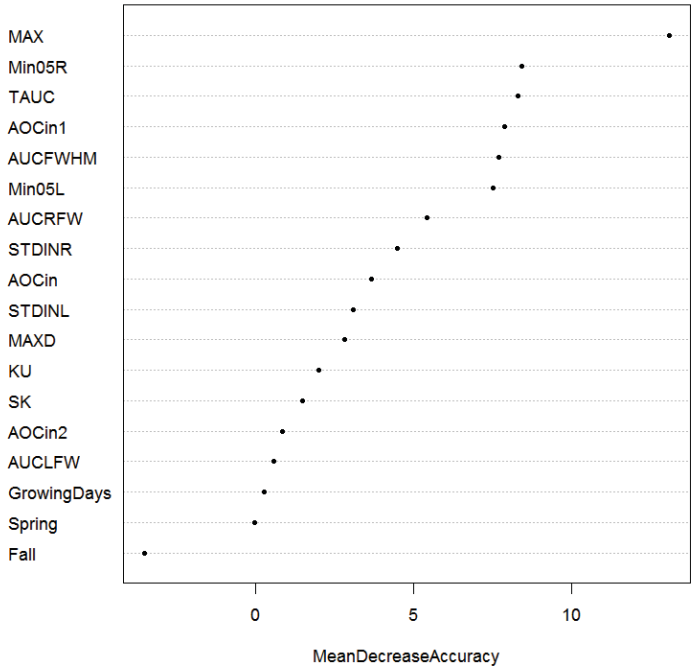

Fig. 10. Variable importance plot for classification of flat vs. riverine wetland types developed with NDVI temporal metrics. Units are percent reduction in classification accuracy which would results when a given variable is removed from classification model. See Table 1 for variable definition.

For the discrimination between flat and riverine wetlands, the both the NDMI and NDVI model resulted in the overall accuracy of 77.3%. The accuracy of TCW model was only 58.6% Producer's accuracy shows that the flats are classified more accurately than riverine wetlands. Flat wetland types are classified correctly 92% of the time, whereas riverine wetlands are only classified correctly 48% of the time. The variable importance plot (Fig.10.)The maximum NDVI

value (MAX), the day corresponding to maximum value (MAXD) and the area under the curve of FWHM (AUCFWHM) were important variables.

4. Discussion

The vast majority of forested wetlands are often broadly classified as deciduous forest, which is due to limitation of the traditional methodologies to discriminate between upland forest and wetland forest. In this study we have demonstrated that the temporal metrics derived from time series of remote sensing data provide information to detect subtle differences between these two classes, leading to accurate discrimination. This is in contrast to the study of Knight et al. (2006), where they did not find any difference between the temporal profile of deciduous forest and woody wetlands using time series MODIS data. We had the advantage of higher spatial resolution from Landsat, which captured the fine scale variability exhibited due to wetland hydrology.

The best accuracy achieved in this study for discrimination between forested uplands and wetlands was 92%. The accuracies of the classification achieved in this study are similar to or higher than those attained in other studies classifying forested uplands from wetlands using remotely sensed data. For example, Lang et al., (2008) using radar data, mapped woody wetland and upland areas and found that the areas that were flooded for 25% of the time were mapped with accuracy ranging 63–96% and areas flooded for 5% were mapped with accuracy ranging from 44–89%. Similarly, Corcoran et al. (2013) used combination of Landsat, topographic, radar and soils data to map upland and wetland areas in Minnesota and achieved an accuracy of 85%. The use of optical imagery in wetland mapping is limited because of its inability to directly observe inundation beneath forest canopies, especially in leaf on condition (e.g., Toyra and Pietroniro, 2005 and Lang et al., 2008). However, in this study we have demonstrated that

temporal pattern that can be extracted from time series of Landsat data alone can accurately discriminate between forested upland and wetland areas.

The accuracy of the three class vegetation type model (forested uplands, forested wetland and mixed wetland) was slightly lower (82.2%) compared to the accuracy of two class model (forested uplands and forested wetland), which was 88.5 %. The mixed wetland class contained areas of mixed vegetation that included scrub-shrub wetlands, deciduous forest and coniferous forest. The overlap in plant types might have resulted in confusion between the forested wetland and mixed wetland class, and caused the slight reduction in accuracy in three class model. However, with the accuracy of 82%, the method used in this study was still successful in discriminating the three classes with reasonably high accuracy.

In terms of different vegetation indices used in this study, NDMI temporal metrics achieved higher accuracy than NDVI and TCW temporal metrics. This is in contrast to other studies that have shown better performance of TCW in classifying wetlands (Baker et al., 2006, Orodyne and Friedl, 2008. TCW index is the contrast of visible and near infrared bands with the middle infrared bands. The longer wavelength middle infrared bands (bands 5 and 7 in Landsat) are sensitive to soil moisture. The contrast provided by TCW aims to enhance the soil moisture status. To our surprise, classification based upon tasseled cap wetness provided the worst accuracy in this study compared to the classification based upon the temporal profile created by NDVI and NDMI. Temporal profile of TCW were widely irregular for all classes (widely varying shape ranging from flattened curve to symmetric curve) as opposed to comparatively regular and symmetric temporal profiles of NDMI. The best classification model was provided by NDMI temporal metrics. Time series NDMI has been successfully used by other studies (eg. de Alwis et al., 2007) to map saturated areas in the landscape. NDMI values vary proportionally

with surface water content during leaf off period and the leaf water content during leaf-on period (de Alwis et al., 2007). Comparing the temporal profile of three vegetation index visually (Fig.3 to Fig. 5) we can see that the differences in NDMI temporal profile between forested uplands and wetlands is greater than in NDVI and TCW temporal profile. The difference in the temporal profile is highest in the early spring. The differences in the temporal profile in the summer and early fall between these two classes diminishes, because at this time tree are fully foliated and if any soil saturation or flooding is present it is obscured by the canopies.

The random forest model used in this study allowed us to assess the variable importance of each temporal metrics for classification. The most important variables identified in all the model was the median of the 5th percentile value of the left side of the curve (Min05L), which is during early growing season. This indicates that the time series data can sufficiently capture the difference in soil saturation/flooding between wetland and upland areas during growing season. The wetlands in this area are inundated or saturated for a short period of time in early spring (in or around March) when evapotranspiration has been relatively low for the longest period of time (Lang et al., 2013). In both the combined model and NDMI model (which provided the best accuracy after the combined model) for two class classification, the other important variables were total area under the curve (TAUC) and area under full width half maximum (TAUCFWHM). These two variables might be indicative of seasonal pattern of forested uplands and wetlands and the variable importance plot indicates that these variables are different in these two classes. The scatter plot of the two important variable (Fig. 9) shows that the forested upland and wetland class are linearly separable in the feature space. Combined with a machine learning algorithm such as random forest and other variables derived from the time series, the method provided a better separation between the wetland and upland class. The accuracy of model to

discriminate between flats and riverine wetland was lower (best accuracy of 80%) compared to forested upland and wetland classification. The riverine class had very high error of omission (52%). One of the reasons for poor classification of riverine wetlands might be because they occur as narrow, linear features along riparian corridors in association with stream channels, which might induce greater heterogeneity in their spectral signature. The wetland components used to make hydrogeomorphic classification (e.g., geomorphic setting, water sources and transport and hydrodynamics- direction and strength of flow) are not discernible from spectral information. However, newer remote sensing techniques such as Light Detection and Ranging (lidar) terrain analysis that provides accurate information on topography can potentially be utilized together with optical data to develop classification based on both hydrogeomorphic and biotic factors such as vegetation and soil saturation.

Finally, accuracy of the technique used in this study depends on the accuracy of the time series data. Errors are introduced in the time series data due to clouds, shadow, location error and atmospheric interferences. We used a cloud mask to remove clouds and cloud shadows. Further the filtering approach using robust lowess was able to remove the effect of outliers from the fitted vegetation index curve.

Due to insufficient number of field samples for coniferous and scrub shrub wetland vegetation types, we limited our study only to deciduous upland and wetland forest. Future research should also investigate the ability of this method in discriminating coniferous wetlands forest and scrub shrub from their upland counterparts. The NWI classification does not provide much information on the hydroperiod of the wetlands. The method can be combined with data on long term hydrology monitoring to investigate if the temporal patterns differ in wetlands with different level of flooding and saturation.

5. Conclusion

We investigated a new method for discriminating between forested uplands and forested wetlands using temporal metrics derived from time-series Landsat data. The method consists of (i) arranging Landsat data based on the day of acquisition to develop a characteristic temporal signature; (ii) filtering and fitting a curve in the time-series data; (iii) extracting temporal metrics from the time series data; and (iv) using random forest model for classification and identification of important variables. We hypothesized that a classification approach using suite of temporal metrics that characterize the differences in vegetation and soil saturation pattern between forested uplands and forested wetlands will enable us to discriminate between these two classes with greater accuracy. The classification accuracy presented here achieved the accuracy of 92% for a two vegetation type class model and 85% for three vegetation type class model thus demonstrating that Landsat time series data alone can provide accurate discrimination of forested uplands and wetlands. Given that the highly processed Landsat data is now available free of cost, the techniques presented in this study can be readily implemented in other similar areas.

Acknowledgment

The authors would like to thank Ms. Alison Rogerson (Delaware Department of Natural Resources and Environmental Control) for providing the field data collected for comprehensive assessment of wetlands in Delaware.

References

Adam, E., Mutanga, O., & Rugege, D. (2010). Multispectral and hyperspectral remote sensing for identification and mapping of wetland vegetation: a review. Wetlands Ecology and Management, 18, 281-296

Baker, C., Lawrence, R., Montagne, C., & Patten, D. (2006). Mapping wetlands and riparian areas using Landsat ETM+ imagery and decision-tree-based models. Wetlands, 26, 465-474

Balzter, H., Gerard, F., George, C., Weedon, G., Grey, W., Combal, B., Bartholomé, E., Bartalev, S., & Los, S. (2007). Coupling of vegetation growing season anomalies and fire activity with hemispheric and regional-scale climate patterns in central and east Siberia. Journal of Climate, 20, 3713-3729

Beurs, K., & Henebry, G. (2010). Spatio-temporal statistical methods for modelling land surface phenology. In I.L. Hudson, & M.R. Keatley (Eds.), Phenological Research (pp. 177-208): Springer Netherlands

Bradley, B.A., & Mustard, J.F. (2005). Identifying land cover variability distinct from land cover change: Cheatgrass in the Great Basin. Remote Sensing of Environment, 94, 204-213

Breiman, L. (2001). Random Forests. Machine Learning, 45, 5-32

Briber, B., Hutyra, L., Dunn, A., Raciti, S., & Munger, J. (2013). Variations in Atmospheric CO2 Mixing Ratios across a Boston, MA Urban to Rural Gradient. Land, 2, 304-327

Bwangoy, J.-R.B., Hansen, M.C., Roy, D.P., Grandi, G.D., & Justice, C.O. (2010). Wetland mapping in the Congo Basin using optical and radar remotely sensed data and derived topographical indices. Remote Sensing of Environment, 114, 73-86

Cleveland, W.S. (1979). Robust Locally Weighted Regression and Smoothing Scatterplots. Journal of the American Statistical Association, 74, 829-836

Coops, N.C., Hilker, T., Bater, C.W., Wulder, M.A., Nielsen, S.E., McDermid, G., & Stenhouse, G. (2011). Linking ground-based to satellite-derived phenological metrics in support of habitat assessment. Remote Sensing Letters, 3, 191-200

Corcoran, J., Knight, J., & Gallant, A. (2013). Influence of multi-source and multi-temporal remotely sensed and ancillary data on the accuracy of random forest classification of wetlands in northern Minnesota. Remote Sensing, 5, 3212-3238

Cutler, D.R., Edwards, T.C., Beard, K.H., Cutler, A., Hess, K.T., Gibson, J., & Lawler, J.J. (2007). Random forests for classification in ecology. Ecology, 88, 2783-2792

Davranche, A., Lefebvre, G., & Poulin, B. (2010). Wetland monitoring using classification trees and SPOT-5 seasonal time series. Remote Sensing of Environment, 114, 552-562

DeAlwis, D.A., Easton, Z.M., Dahlke, H.E., Philpot, W.D., & Steenhuis, T.S. (2007). Unsupervised classification of saturated areas using a time series of remotely sensed images. Hydrolic Earth System Science, 4, 1663-1696

Dymond, C.C., Mladenoff, D.J., & Radeloff, V.C. (2002). Phenological differences in Tasseled Cap indices improve deciduous forest classification. Remote Sensing of Environment, 80, 460-472

Dymond, J.R., Shepherd, J.D., Clark, H., & Litherland, A. (2006). Use of VEGETATION satellite imagery to map pasture quality for input to a methane budget of New Zealand. International Journal of Remote Sensing, 27, 1261-1268

Elmore, A.J., Guinn, S.M., Minsley, B.J., & Richardson, A.D. (2012). Landscape controls on the timing of spring, autumn, and growing season length in mid-Atlantic forests. Global Change Biology, 18, 656-674

El Vilaly, M.A. (2013). Drought monitoring with remote sensing based land surface phenology: applications and validation. PhD Thesis, University of Arizona http://arizona.openrepository.com/arizona/bitstream/10150/301553/1/azu_etd_12880_sip1_m.pdf

Falkowski, M.J., Evans, J.S., Martinuzzi, S., Gessler, P.E., & Hudak, A.T. (2009). Characterizing forest succession with lidar data: An evaluation for the Inland Northwest, USA. Remote Sensing of Environment, 113, 946-956

Federal Geographic Data Committee (1992). Application of satellite data for mapping and monitoring wetlands — Facts finding report: Technical report 1 Washington, D.C: Wetlands Subcommittee, Federal Geographic Data Committee

Fensholt, R., & Sandholt, I. (2003). Derivation of a shortwave infrared water stress index from MODIS near- and shortwave infrared data in a semiarid environment. Remote Sensing of Environment, 87, 111-121

Fisher, J.I., & Mustard, J.F. (2007). Cross-scalar satellite phenology from ground, Landsat, and MODIS data. Remote Sensing of Environment, 109, 261-273

Fisher, J.I., Mustard, J.F., & Vadeboncoeur, M.A. (2006). Green leaf phenology at Landsat resolution: Scaling from the field to the satellite. Remote Sensing of Environment, 100, 265-279

Gilmore, M.S., Wilson, E.H., Barrett, N., Civco, D.L., Prisloe, S., Hurd, J.D., & Chadwick, C. (2008). Integrating multi-temporal spectral and structural information to map wetland vegetation in a lower Connecticut River tidal marsh. Remote Sensing of Environment, 112, 4048-4060

Griffith, J. (2002). Geographic techniques and recent applications of remote sensing to landscape-water quality studies. Water, Air, and Soil Pollution, 138, 181-197

Harvey, K.R., & Hill, G.J.E. (2001). Vegetation mapping of a tropical freshwater swamp in the Northern Territory, Australia: A comparison of aerial photography, Landsat TM and SPOT satellite imagery. International Journal of Remote Sensing, 22, 2911-2925

Hird, J.N., & McDermid, G.J. (2009). Noise reduction of NDVI time series: An empirical comparison of selected techniques. Remote Sensing of Environment, 113, 248-258

Hodgson, M. E., Jensen, J. R., Mackey, H. E., & Coulter, M. C. (1987). Remote sensing of wetland habitat: A wood stork example, Photogrammetric Engineering and Remote Sensing, 53, 1075-1080

Jacobs, A.D., D.F. Whigham, D.Fillis, E.Rehm, & Howard, A. (2009). Delaware comprehensive assessment procedure Version 5.2. Delaware Department of Natural Resources and Environmental Control, Dover, DE

Jacoby, W.G. (2000). Loess: a nonparametric, graphical tool for depicting relationships between variables. Electoral Studies, 19, 577-613

Jenerette, G.D., Miller, G., Buyantuev, A., Pataki, D.E., Gillespie, T.W., & Pincetl, S. (2013). Urban vegetation and income segregation in drylands: a synthesis of seven metropolitan regions in the southwestern United States. Environmental Research Letters, 8, 044001

Kauth, R. J., & Thomas, G. S. (1976). The Tasseled Cap — a graphic description of the spectral-temporal development of agricultural crops as seen by Landsat. Proceedings of the Symposium on Machine Porcessing of Remotely Sensed Data (pp. 4B41–44B51). West Lafayette, Indiana: Purdue University

Knight, J.F., Lunetta, R.S., Ediriwickrema, J., & Khorram, S. (2006). Regional scale land cover characterization using MODIS-NDVI 250 m multi-temporal imagery: A phenology-based approach. GIScience & Remote Sensing, 43, 1-23

Knudsen, E., Lindén, A., Ergon, T., Jonzén, N., Vik, J.O., Knape, J., Røer, J.E., & Stenseth, N.C. (2007). Characterizing bird migration phenology using data from standardized monitoring at bird observatories. Climate Research, 35, 59-77

Lancaster, J., Mouat, D., Kuehl, R., Whitford, W., & Rapport, D. (1996). Time series satellite data to identify vegetation response to stress as an indicator of ecosystem health. Proceedings, Shrubland Ecosystem Dynamics in a Changing Environment, 23-25 May 1995, Las Crucas, New Mexcio, General Technical Report INT-GTR-338, U.S. Department of Agriculture, Forest Service, Intermountain Research Station, Ogden, Utah, pp. 255-261

Lang, M., McCarty, G., Oesterling, R., & Yeo, I.-Y. (2013). Topographic Metrics for Improved Mapping of Forested Wetlands. Wetlands, 33, 141-155

Lang, M.W., Kasischke, E.S., Prince, S.D., & Pittman, K.W. (2008). Assessment of C-band synthetic aperture radar data for mapping and monitoring Coastal Plain forested wetlands in the Mid-Atlantic Region, U.S.A. Remote Sensing of Environment, 112, 4120-4130

Li, J., & Chen, W. (2005). A rule-based method for mapping Canada's wetlands using optical, radar and DEM data. International Journal of Remote Sensing, 26, 5051-5069

Liang, S. (2001). Land-cover classification methods for multi-year AVHRR data. International Journal of Remote Sensing, 22, 1479-1493

Lunetta, R., & Balogh, M. (1999). Application of multi-temporal Landsat 5 TM imagery for wetland identification. Photogrammetric Engineering and Remote Sensing, 65, 1303-1310

Luyan, J., Kang, J., Xiurui, G., Hairong, T., Kai, Y., & Yongchao, Z. (2011). Improving Wetland Mapping by Using Multi-Source Data Sets. In, Image and Data Fusion (ISIDF), 2011 International Symposium on (pp. 1-4)

Mackey, H.E.J. (1989). Monitoring seasonal and annual wetland changes in a freshwater marsh with SPOT HRV data.

Masek, J.G., Vermote, E.F., Saleous, N.E., Wolfe, R., Hall, F.G., Huemmrich, K.F., Feng, G., Kutler, J., & Teng-Kui, L. (2006). A Landsat surface reflectance dataset for North America, 1990-2000. Geoscience and Remote Sensing Letters, IEEE, 3, 68-72

Melaas, E.K., Friedl, M.A., & Zhu, Z. (2013). Detecting interannual variation in deciduous broadleaf forest phenology using Landsat TM/ETM+ data. Remote Sensing of Environment, 132, 176-185

Mitsch, W.J., & Gosselink, J.G. (2007). Wetlands. Hoboken, N.J.: Wiley

Moody, A., & Johnson, D.M. (2001). Land-Surface Phenologies from AVHRR Using the Discrete Fourier Transform. Remote Sensing of Environment, 75, 305-323

Morris, D., Boyd, D., Crowe, J., Johnson, C., & Smith, K. (2013). Exploring the Potential for Automatic Extraction of Vegetation Phenological Metrics from Traffic Webcams. Remote Sensing, 5, 2200-2218

Ordoyne, C., & Friedl, M.A. (2008). Using MODIS data to characterize seasonal inundation patterns in the Florida Everglades. Remote Sensing of Environment, 112, 4107-4119

Ozesmi, S.L., & Bauer, M.E. (2002). Satellite remote sensing of wetlands. Wetlands Ecology and Management, 10, 381-402

Pantaleoni, E., Wynne, R.H., Galbraith, J.M., & Campbell, J.B. (2009). Mapping wetlands using ASTER data: a comparison between classification trees and logistic regression. International Journal of Remote Sensing, 30, 3423-3440

Parmenter, A.W., Hansen, A., Kennedy, R.E., Cohen, W., Langner, U., Lawrence, R., Maxwell, B., Gallant, A., & Aspinall, R. (2003). Land use and land cover change in the greater yellowstone ecosystem: 1975–1995. Ecological Applications, 13, 687-703

Pouliot, D., Latifovic, R., & Olthof, I. (2008). Trends in vegetation NDVI from 1 km AVHRR data over Canada for the period 1985–2006. International Journal of Remote Sensing, 30, 149-168

Sader, S.A., Ahl, D., & Liou, W.-S. (1995). Accuracy of landsat-TM and GIS rule-based methods for forest wetland classification in Maine. Remote Sensing of Environment, 53, 133-144

Sakamoto, T., Yokozawa, M., Toritani, H., Shibayama, M., Ishitsuka, N., & Ohno, H. (2005). A crop phenology detection method using time-series MODIS data. Remote Sensing of Environment, 96, 366-374

Schmidt, K.S., & Skidmore, A.K. (2003). Spectral discrimination of vegetation types in a Coastal wetland. Remote Sensing of Environment, 85, 92-108

Tiner, R.W., Biddle, M.A., Jacobs, A.D., Rogerson, A.B., & McGuckin, K.G. (2011). Delaware Wetlands: Status and Changes from 1992 to 2007. Cooperative National Wetlands Inventory Publication. U.S. Fish and Wildlife Service, Northeast Region, Hadley, MA and the Delaware Department of Natural Resources and Environmental Control, Dover, DE. 35 pp

Todd, M.J., Muneepeerakul, R., Pumo, D., Azaele, S., Miralles-Wilhelm, F., Rinaldo, A., & Rodriguez-Iturbe, I. (2010). Hydrological drivers of wetland vegetation community distribution within Everglades National Park, Florida. Advances in Water Resources, 33, 1279-1289

Tooke, T.R., Coops, N.C., & Webster, J. (2013). Predicting Building Ages from LiDAR data with Random Forests for Building Energy Modelling. Energy and Buildings

Townsend, P., & Walsh, S. (2001). Remote sensing of forested wetlands: application of multitemporal and multispectral satellite imagery to determine plant community composition and structure in southeastern USA. Plant Ecology, 157, 129-149

Töyrä, J., & Pietroniro, A. (2005). Towards operational monitoring of a northern wetland using geomatics-based techniques. Remote Sensing of Environment, 97, 174-191

Valk, A.v.d. (2006). The biology of freshwater wetlands. Oxford; New York: Oxford University Press

Walker, J.J., de Beurs, K.M., Wynne, R.H., & Gao, F. (2012). Evaluation of Landsat and MODIS data fusion products for analysis of dryland forest phenology. Remote Sensing of Environment, 117, 381-393

Wessels, K., Steenkamp, K., von Maltitz, G., & Archibald, S. (2011). Remotely sensed vegetation phenology for describing and predicting the biomes of South Africa. Applied Vegetation Science, 14, 49-66

White, M.A., Thornton, P.E., & Running, S.W. (1997). A continental phenology model for monitoring vegetation responses to interannual climatic variability. Global Biogeochemical Cycles, 11, 217-234

Wolter, P.T., Johnston, C.A., & Niemi, G.J. (2005). Mapping submergent aquatic vegetation in the US Great Lakes using Quickbird satellite data. International Journal of Remote Sensing, 26, 5255-5274

Wright, C., & Gallant, A. (2007). Improved wetland remote sensing in Yellowstone National Park using classification trees to combine TM imagery and ancillary environmental data. Remote Sensing of Environment, 107, 582-605

Zoffoli, M., Kandus, P., Madanes, N., & Calvo, D. (2008). Seasonal and interannual analysis of wetlands in South America using NOAA-AVHRR NDVI time series: the case of the Parana Delta Region. Landscape Ecology, 23, 833-848

CHAPTER 4

Utility of Lidar Derived Topographic Metrics for Improved Wetland Mapping

Prepared for submission to ISPRS Journal of Photogrammetry and Remote Sensing

Abstract:

Accurate and updated wetland maps are important for wetland conservation and management. Optical remote sensing data has been widely used for mapping and monitoring wetlands. Topography plays a key role in the formation and functioning of wetlands, but use of topographic information in wetland mapping has been constrained by limited availability of high resolution topographic data such as that provided by Light Detection and Ranging (lidar) data. In this study, we assessed the utility of topographic variables generated from a lidar-derived DEM to discriminate wetland from upland in in Virginia. We assessed multiple terrain variables, including slope, curvature, plan curvature, profile curvature, the topographic position index (TPI), and the topographic wetness index (TWI) derived using four different flow routing algorithms. We also assessed the most important variables that can accurately discriminate wetland from upland using the Random Forest classification technique. The best classification discriminated wetland from upland pixels with an accuracy of 72%. The TWI calculated from the distributed flow routing algorithm, slope and TPI were found to be important predictors. The study shows that the topographic variables generated from high resolution DEM can improve the accuracy of wetland mapping. Lidar data has great potential to aid wetland mapping especially in areas where availability of optimal optical remote sensing data may be limited due to cloud cover. In addition, the combined use of optical data such as Landsat and lidar may be a superior approach for operation wetland mapping.

Keywords: Wetness Index, Random Forest, Terrain Analysis, Digital Elevation Model

1. Introduction

Wetlands are among the most unique and productive ecosystems on earth, providing habitat for numerous rare and endangered plants and animals. Wetlands play an important role in biogeochemical cycling and flood control and provide numerous ecological and economical values and services (Mitch and Gosselink, 2000). Historically regarded as wastelands, large areas of wetlands have been filled for urban use or drained for agriculture. The biologic, aesthetic, and economic values of wetlands are now known to be disproportionately large compared to the often small percentage of the landscape they occupy (Lang et al., 2008). This growing recognition of importance of wetlands has led to national and international efforts for wetland conservation and protection.

Successful conservation of wetlands requires up-to-date and accurate maps that show the type, location, size and extent of wetlands. The most common methods of wetland mapping uses optical imagery derived from multi-spectral sensors or aerial photography. The US Fish and Wildlife Service's National Wetland Inventory (NWI) program initiated the first nationwide survey of wetlands in the conterminous US. NWI wetland maps are produced using mid-to-high altitude aerial photographs, usually taken during early spring. Aerial photographs at scales from 1:40,000 to 1:80,000 (or 1:133,000 for earlier maps) are used. Manual photo-interpretation techniques coupled with field verification, topographic maps and soil information are used for identification and classification of wetlands (Dahl and Watmough, 2007). Studies have shown varying levels of accuracies of NWI maps. In general they have been reported to have low commission error and in many cases high omission error (Wright and Gallant, 2007). Stolt and

Baker (1995) reported omission error rates greater than 85% in the Blue Ridge Physiographic region of Central Virginia, while Werner (2003) reported that 42% of field surveyed Palustrine wetlands were not mapped by NWI. Forested wetlands, small wetlands, and narrow wetlands are often the source of omission as they are more difficult to locate accurately. Optical remote sensing data from moderate resolution sensors such as Landsat and SPOT have been widely used for mapping wetlands (Wright and Gallant, 2007, Harvey and Hill, 2001 and Baker et al., 2006). However, the dynamic nature of wetlands, especially their alternating dry and wet nature pose problems for accurate wetland mapping using optical data acquired in one time period. In addition, use of optical data depends on availability optimal data, which is often hindered by clouds and atmospheric condition. In many cases, vegetation communities of the drier wetlands are not dramatically different from adjacent uplands, making wetland identification difficult. Imaging radar data which operates in the microwave region of the electromagnetic spectrum have also been widely used in wetland mapping. The longer wavelength of microwave data can penetrate vegetation canopies and is sensitive to variation in soil moisture and inundation making them ideal for wetland detection (Li and Chen, 2005 and Corcoran et al., 2011). Although, studies have demonstrated great potential for using radar data for mapping wetlands many limitations prevent the use of radar data alone for mapping wetlands. The interpretation of radar data is not as intuitive as optical imagery. In addition, some landscapes where there is very little tree canopy may not benefit from using SAR data (Corcoran et al., 2011). Wetland detection using radar data depends on soil saturation or flooding (the double bounce effect in radar data is enhanced due to flooding, which helps discriminate wetlands from uplands). However, wetland hydrology is highly variable. They maybe wet one season and dry another season. Images

acquired during abnormal weather condition (such as drought or excessive rainfall) will affect the utility of radar data for wetland detection.

Topography provides an alternative for mapping wetlands and spatial patterns of wetness. Topography controls water flow by directing water from higher elevation to lower elevation and by forcing water to converge or diverge due to the shape of the surface (Creed and Sass, 2011). Most wetlands occur in low or depressional areas; "landscape sinks" where ground and/or surface water collects (Zedler and Kercher, 2005). Information on vegetation communities and observable moisture that are often used for wetland mapping may change over time whereas terrain morphology remains relatively static. Therefore use of terrain morphology for wetland mapping provide an objective wetland mapping in comparison to approaches that map vegetation and moisture condition at the time of data acquisition (Hogg and Holland, 2007). This is especially true for areas where the terrain is not modified by human activities.

Digital terrain analysis has been widely used to describe hydrologic processes in the landscape (Wilson and Gallant, 2000). Digital terrain analysis uses a Digital Elevation Model (DEM), which provides a digital representation the Earth's surface topology over an area. A DEM is usually derived from stereoscopic interpretation of aerial photographs or satellite imagery (Wilson and Gallant, 2000 and Liu, 2008). Although topographic information is commonly available for the United States, the vertical and spatial resolution of these data is often not sufficient for wetland identification, especially in areas of subtle topographic change (Lang et al., 2013). In recent years, advances in lidar systems have significantly improved the generation of high quality DEM. Lidar sensors are active sensors, where high energy laser pulses transmitted in short intervals are directed toward the ground and the time of pulse return is measured. Since the velocity of light is constant (i.e., 3 x 108 m s-1), the elapsed time between

transmitting and receiving the pulse can be used to determine the distance between the sensor and object or the ground, a process known as pulse ranging (Wehr and Lohr, 1999). Using this concept, x, y, and z measures can be obtained, with horizontal accuracies of 50 cm and vertical accuracies of 10 cm (Baltsavias, 1999, Wehr and Lohr, 1999 and Thomas, 2006).

In recent years use of lidar data in wetland mapping has increased. Fine-scale elevation data provided by lidar is particularly helpful in flat, wetland-rich areas where complex interspersion of uplands and lowlands may cause mapping confusion and inaccuracy (Maxa and Bolstad, 2009). This combination occurs in nearly level or gently rolling Triassic Basins and coastal plains, where most of the wetlands in the eastern US are found. Creed et al. (2003) investigated optimal DEM spatial resolution for locating closed canopy wetlands. Lidar was found to be better than field based delineation at discriminating wetlands. Hogg and Holland (2008) compared the use of DEM derived from lidar, 1:20,000 point elevation data source and 1:50,000 National Topographic Series-based DEMs to detect wetlands. Wetland classification results with lidar were significantly high compared to the other two methods; 35% of the wetland area mapped by lidar was not detected by other methods. Richardson et al. (2009) used a DEM derived from lidar to classify wetlands and delineate wetland boundaries using various topographic indices and edge detection procedures. Leonard et al. (2012) demonstrated that lidar-derived DEMs can successfully capture slight geomorphic changes and can predict wetland boundaries in low relief ecosystems. Lang et al. (2013) used topographic information from lidar DEMs to map wetland location and inundation periodicity with high accuracy in forested wetlands.

In terrain analysis, a DEM is used to derive primary and secondary topographic attributes. Primary topographic attributes include slope, aspect, and curvature. Secondary topographic

attributes such as topographic wetness index (TWI) are calculated from two or more primary attributes and provide an opportunity to describe patterns as a function of processes (Wilson and Gallant, 2000). Topographic wetness index is calculated following Beven & Kirkby (1979) as:

$$\text{TWI} = ln\left(\frac{\alpha}{tan\beta}\right) \quad (1)$$

Where: α is the upslope catchment area in m^2, and β is the local slope in percentage.

The TWI defines the hydrologic characteristics of a point in the landscape as a relationship between two spatial parameters: upslope catchment area and the slope. TWI reflects the tendency of water to accumulate at a point in the landscape (accumulated drainage), countered by the tendency of the site to transmit this water (i.e., slope) (Murphy et al., 2007). The TWI has been widely used to derive information about the spatial distribution of soil moisture (Moore et al., 1991, Hornberger and Boyer, 1995, Iverson et al., 1997, Boerner et al., 2000, Gessler et al., 2000, and Case et al., 2005). Although TWI has been widely used to predict zones of soil saturation, only a few studies have explored the use of TWI to map wetlands (Rohde and Seibert, 1999, Curie et al., 2007, Hogg and Holland, 2007, Murphy et al., 2009 and Richardson et al., 2009). Conceptually, the computation of TWI is straightforward as it only requires two input parameters: slope and upslope contributing area. Slope is measured using a standard procedure. However, methods to calculate upslope area vary considerably with different flow routing algorithms (Lang et al., 2013). The flow routing algorithm to calculate upslope area varies based on how the flow is distributed from the center cell to downslope neighbors. They have been categorized into two types: single-direction and multiple-direction. A single-direction algorithm transfers all flow from the center cell to one downslope neighbor, while multiple-direction algorithm partitions flow to multiple downslope neighbors (Erskine et al., 2006). The choice of

flow routing algorithm significantly affects the prediction of spatial pattern of saturation. Various studies have compared the use of different flow routing methods for modeling patterns of soil saturation (Wilson et al., 2008, Kopecký and Čížková, 2010 and Besnard et al., 2013), but there is no consensus on the best one model that suits certain landscapes or applications. Few studies have compared the performance of algorithms in areas of low topographic relief where wetlands are most common (Lang et al., 2013).

Hydrologic conditioning is often applied to ensure continuous water flow while modeling hydrologic pathways. The main purpose of the hydrologic conditioning is to remove topographic depressions which are caused due to errors in the DEM while retaining the true depressions (Li et al., 2011). However, the standard procedure is to remove every topographic depression, which in fact assumes that all topographic depressions in the DEM are artifacts (Wilson and Gallant, 2000, Lindsay and Creed, 2006 and Wechsler, 2007). The process of removing depressions, often referred to as depression filling in the literature, modifies the DEM and affects the parameters derived from the DEM. However, all the depressions in the DEM are not artifacts and some of these may be real features. True depressions represent low-lying areas in the landscape or blocked drainageways where water accumulates. Rodhe and Seibert (1999) treated depressions in the DEM as real topographic features as a part of the process to identify mires. Artifact depressions in the DEM result due to data error, error due to interpolation techniques while creating the DEM and limited vertical and horizontal resolution of the DEM (Lindsay and Creed, 2006). However, DEMs produced from lidar data with their fine scale and high precision are capable of capturing the landscape features accurately. Spurious depression identification due to errors can be removed through coarsening and smoothing (Li et al., 2011)

The objective of this study is to evaluate the predictive power of different terrain indices derived from high resolution lidar DEM for mapping wetlands. We examined the relevance of different terrain variables for predicting presence of wetlands in our study area using field validation. We also compared the strength of TWI derived from four different flow routing algorithms in detecting wetlands. In addition, we assessed if the DEMs derived from lidar data provide information on depression features that would improve the identification of wetlands in agricultural fields, forested wetlands, or other areas that have large omission errors in the NWI data.

2. Methods

2.1 Study area

The study area is located in northern Virginia (Fig. 1). It incorporates Prince William County and Faquier County in the Piedmont Physiographic Province southwest of the District of Columbia in the Northern Virginia metropolitan area. The area has a temperate climate with an average annual precipitation of about 105.5 cm, with highest precipitation occurring in May and June (Troyer, 2013). The maximum elevation within the study site is approximately 200 m. The bedrock is maroon siltstone and shale in a Triassic basin, and the relief is gently rolling. The predominant land cover types are agriculture and pasture.

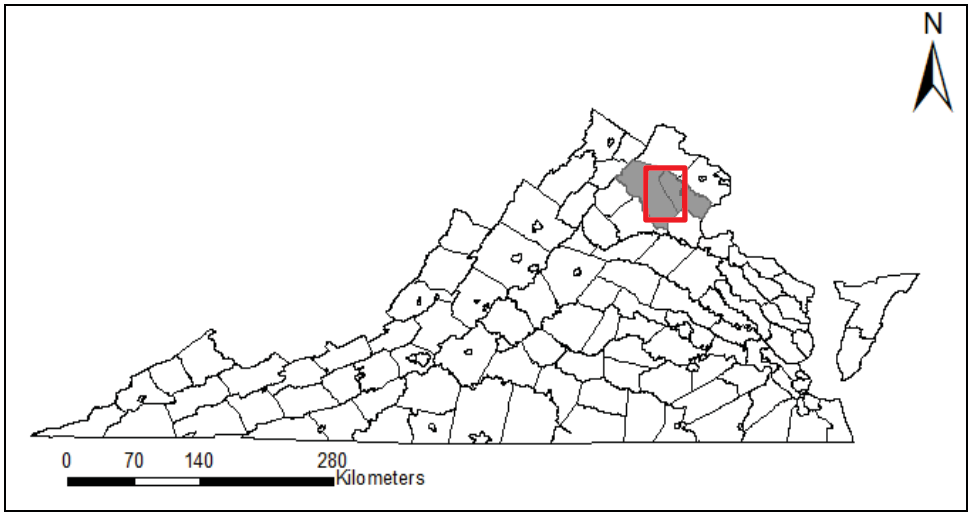

Fig. 1. Map of the study area showing location within the Commonwealth of Virginia. The grey shaded area represents Prince William and Faquier County and the red box represents the approximate location of our study area.

2.2 Lidar data and preprocessing

Lidar data used in this study were acquired using the Leica Systems ALS50 II on December of 2008 by Science Applications International Corporation at a height of 1981 m using scan angle of 44 degrees and scan frequency of 41.3 Hz. First and last returns were collected for each pulse. A digital elevation model was calculated by identifying the ground returns and interpolating a surface between these points with a resolution of 1 m. Based on 45 control points, the average error between bare earth and control points was 0.004 m with a root mean square error of 0.107 m. The 1 m DEM was resampled to 3 m DEM and a smoothing filter using a 3x3 kernel. The use of smoothing filter helps eliminate spurious data points and removes any systematic errors from the DEM (Nichol and Hang, 2008).

2.3 Computation of terrain variables

We used the lidar DEM to calculate the following terrain variables: (1) Curvature, (2) Plan Curvature, (3) Profile Curvature, (4) Slope, (5) Topographic Position Index, (6) TWI_{D8}, (7)

$TWI_{D\infty}$, (8) TWI_{MFD}, and (9) TWI_{SAGA}. Variables 1-4 were computed based on Zevenbergen and Thorne (1987). The topographic position index (TPI) measures the difference between elevation at the central point and the average elevation around it within the predetermined radius (Wilson and Gallant, 2000 and Weiss, 2001). Positive TPI values indicate the point is located higher than its average surrounding and negative value indicates that the point is lower than its surrounding. TPI has been used to classify landscape into morphological classes based on topography (Tagil and Jenness, 2008 and McGarigal et al., 2009); prediction of soil properties (Francés and Lubczynski, 2011) and wetland mapping (Liu et al., 2011). The value of TPI depends on the user defined radius. We calculated the TPI with a radius of 45, 60, 90 and 120 m. A two sample T-test was used to assess which neighborhood size provided a significant difference in mean index value between the wetland and upland classes. A larger significant difference in mean value was considered to be indicative of greater ability to differentiate between wetlands and uplands. Variables 6-7 were calculated according to Equation 1 based on different flow routing algorithm. TWI_{D8} was calculated based on O'Callaghan and Mark (1984), which is a single flow direction algorithm and directs flow from each grid cell to one of the eight nearest neighbors based on slope gradient. $TWI_{D\infty}$ is a calculated based on deterministic infinity algorithm which allows flow into one or two neighbors depending on flow direction determined by the steepest descent. If the angle falls on a cardinal or diagonal direction, the flow from each cell drains to one neighboring cell. If the flow direction falls between the direct angle to adjacent neighbors, the flow is proportioned between the two neighboring cells according to how close the flow direction angle is to the direct angle for those cells (Wilson et al., 2007). TWI_{MFD} was calculated using multiple flow direction algorithm (Quinn et al., 1991) which allows flow to all neighboring downslope cell determined by the slope between the target cells and source cell. Cells with the

steeper slope receive larger amounts of the flow. The final variable TWI_{SAGA} is a modified TWI calculated based on Bohner and Selige (2006). The traditional TWI calculation is problematic in lowland environments because it does not adequately account for extensive lateral dispersion of water that occurs in such landscapes (Richardson et al., 2012). The TWI_{SAGA} is formulated to account for this dispersion through an iterative process that distributes calculated contributing area values between pixels as a function of local slope. It uses the same formula as the traditional TWI (Equation 1) but is based on a modified specific catchment area calculation (Bohner and Selige, 2006).

2.4 Field data collection

TWI_{SAGA} map was created for the study area, and was classified into five groups using unsupervised classification. Twenty-five points were randomly generated in each group for field verification. The sites were classified as either wetland or upland during a field visit. Wetlands were identified using the US Army Corps of Engineers (USA COE) Wetland Delineation Manual (U.S. Army Corps of Engineers, 2012). Information on presence of hydric soil, wetland hydrology and wetland vegetation was collected at each site. The site was classified as a wetland only if it met all three criteria.

2.5 Random forest classification

We employed the random forest algorithm to classify wetland and upland based on the terrain variables. Random forest is a non-parametric classification tree technique that randomly and iteratively samples the data and variables to generate a large group of classification trees (Breiman 2001). The algorithm implements a bootstrapping (generating random sample from training data with replacement) procedure to generate random subset of training data (approximately 63%), which is used to fit a classification tree with small number of randomly

selected variables (Cutler et al., 2007). The portion of training data not selected for generation of the classification tree (often termed as the "out-of-bag" sample) is classified using the fitted tree and is to calculate bootstrap error estimates and the accuracy for each tree. After all the trees are grown, overall error and accuracy is calculated by averaging error rates across all trees. As out-of-bag observations are not used in fitting the trees, out-of-bag error estimates are analogous to cross-validated estimate of error and accuracy (Cutler et al., 2007). Random forest classification is robust against overfitting and correlated variables and can produce higher accuracies than traditional classification tree (Falkowski et al., 2009). Classification accuracy was assessed with the bootstrap error estimates and error matrices calculated by random forest. Overall accuracy, producer's and user's accuracy were calculated and examined to assess the effectiveness of classification. The overall accuracy is the proportion of correctly identified change events. The producer's accuracy measures the proportion of pixels belonging to a class that was correctly classified by the method and measures the error of omission. User's accuracy measures the proportion of the pixels classified as belonging to a class matching the reference data and measures the error of commission. Random forest also calculates the importance of each predictor variable upon model accuracy. The variable importance can be calculated using the Gini index, a measure of node impurity, or the degree to which a variable produces terminal nodes in the forest of classification trees (Mitchell et al., 2013). Random Forests^{TM} (Salford Systems, CA, USA) was used to perform the classification.

2.6 Depression identification

In order to identify depressions in the study area, the depression filling method of Planchon and Darboux (2002) was used to produce a depression-free DEM from the smoothed 3 m DEM. This algorithm first covers the DEM entirely in water, and then iteratively drains the excess

water from each cell. The DEM is scanned from eight alternating to determine the downslope path. The algorithm then searches for an upstream tree by following dependence links, from where the excess water is removed from this network. Finally, the water in the depression is drained to the highest pour point on the flow path to an outlet resulting in flat depression. The depression-free DEM was subtracted from the original DEM. The difference grid provides information on the potential depressions in the DEM.

3. Results

3.1 Wetness indices from different flow routing algorithm

Visual inspection of the wetness index map illustrated the difference between the four flow routing methods (Figure 2). The hydric soil layer for the study area was overlaid on each wetness map. The wetness index map produced by the TWI_{D8} and $TWI_{D\infty}$ showed a channelized flow where the distribution of the saturated zone occurred in a linear pattern. In contrary, saturated areas in TWI_{MFD} and TWI_{SAGA} appeared as smoother, broader zones. The hydric layer also indicated that the transition between the hydric area and the surrounding area was more pronounced in the wetness map from TWI_{MFD} and TWI_{SAGA} than from TWI_{D8} and $TWI_{D\infty}$. Statistical analysis using t-test showed that all four wetness maps contained significant difference between the mean values of the wetland and upland area (Table 1).

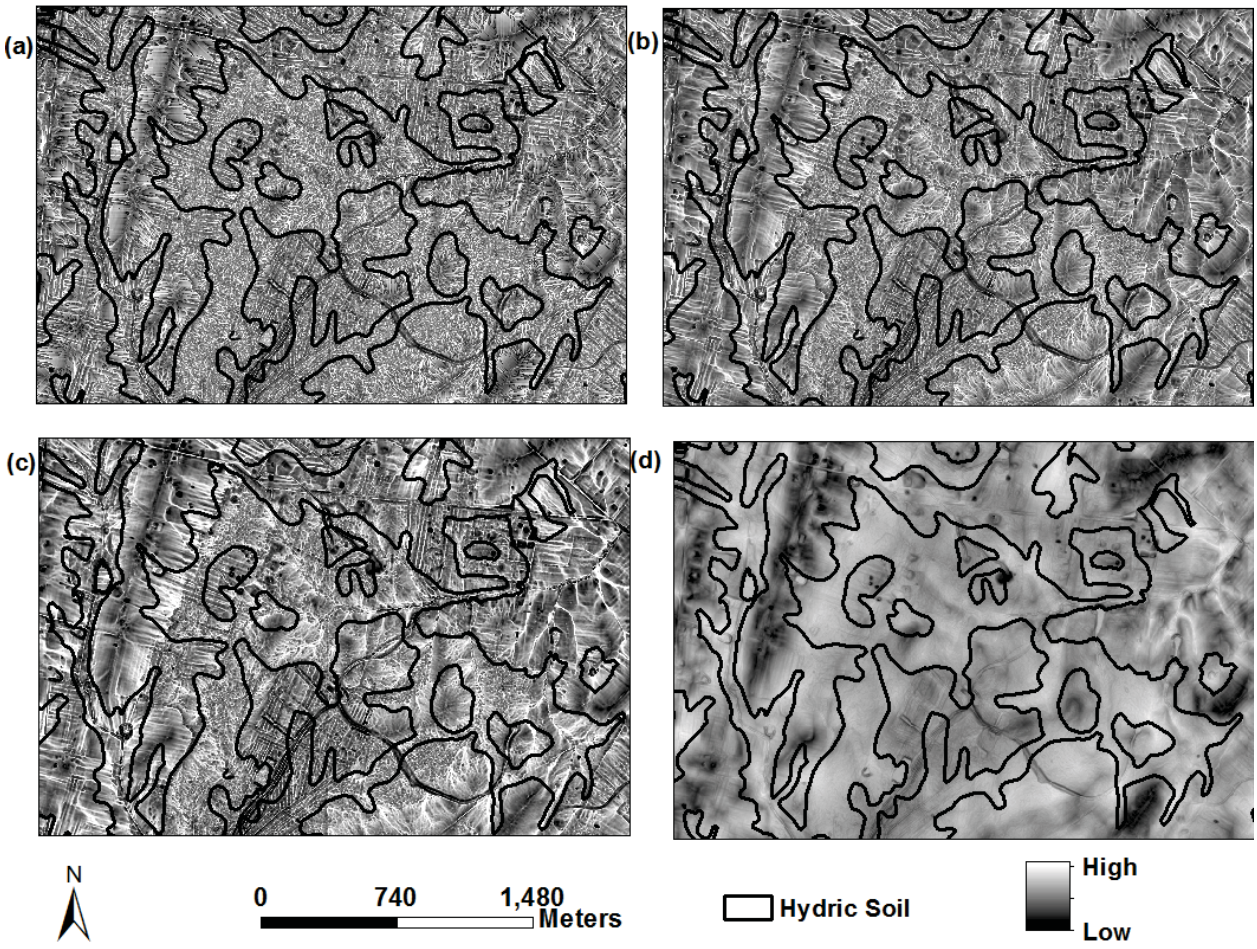

Fig. 2. Wetness index calculated from different flow routing methods D8 (a), D∞ (b), MFD (c), and SAGA (d)

Visual inspection of the wetness index map illustrated the difference between the four flow routing methods (Fig. 2). The hydric soil layer for the study area was overlaid on each wetness map. The wetness index map produced by the TWI_{D8} and $TWI_{D\infty}$ showed a channelized flow where the distribution of the saturated zone occurred in a linear pattern. In contrary, saturated areas in TWI_{MFD} and TWI_{SAGA} appeared as smoother, broader zones. The hydric layer also indicated that the transition between the hydric area and the surrounding area was more pronounced in the wetness map from TWI_{MFD} and TWI_{SAGA} than from TWI_{D8} and $TWI_{D\infty}$. Although both the TWI_{MFD} and TWI_{SAGA} are calculated using distributed flow routing method,

TWI_{SAGA} appears smoother than TWI_{MFD}. This is because TWI_{SAGA} is based on modified specific catchment area, which disperses the flow across all pixels within a localized flat area and the predicted wetness index is higher compared to the standard method. Statistical analysis using t-test showed that all four wetness maps contained significant difference between the mean values of the wetland and upland area (Table 1).

Table 1. Difference in mean index value of TWI generated using different flow routing method between wetlands and uplands.

Wetness Index	t-value
D8	2.12*
D∞	2.38**
MFD	2.85**
SAGA wetness	4.95***

,,*** indicates that the difference in the mean value was significant at the p level of 0.05, 0.01 and 0.001 respectively*

3.2 Wetland classification accuracy

The overall accuracy, producer's and user's accuracy were calculated and examined to assess the accuracy of classification. Tables 2 to 5 summarize the random forest classification accuracy. The classification accuracy ranged from 67% to 72%, which is comparable to wetland classification using other remote sensing data (Lin and Chen, 2005, Baker et al., 2006, Pantaleoni et al., 2009 and Corcoran et al., 2011).. The error matrix in Table 2 for random forest classification with terrain variables, together with TWI_{SAGA} index provided the highest classification accuracy of 72%. The lowest classification accuracy was obtained with classification of terrain variables together with wetness index calculated by TWI_{D8}. While using wetness index map from SAGA, the largest improvement was in the producer's accuracy (omission error) for both wetland and upland class.

Table 2 Wetland Classification accuracy with TWI_{SAGA}

Class	Wetland	Upland	Total	Producer's accuracy (%)
Wetland	46	15	61	75.4
Upland	45	109	154	70.8
Total	91	124	215	
User's accuracy (%)	50.5	87.9		
Overall accuracy (%)	72.09			

Table 3 Wetland Classification accuracy with TWI_{MFD}

Class	Wetland	Upland	Total	Producer's accuracy
Wetland	45	16	61	73.77
Upland	48	106	154	68.33
Total	93	122	215	
User's accuracy	48.38	86.88		
Overall accuracy	70.23			

Table 4 Wetland Classification accuracy with $TWI_{D\infty}$

Class	Wetland	Upland	Total	Producer's accuracy
Wetland	42	19	61	68.8
Upland	47	107	154	69.5
Total	83	126	215	
User's accuracy	50.6	84.9		
Overall accuracy	69.3			

Table 5 Wetland Classification accuracy with TWI_{D8}

Class	Wetland	Upland	Total	Producer's accuracy
Wetland	40	21	61	65.57
Upland	49	105	154	68.18
Total	89	126	215	
User's accuracy	44.94	83.33		
Overall accuracy	67.44			

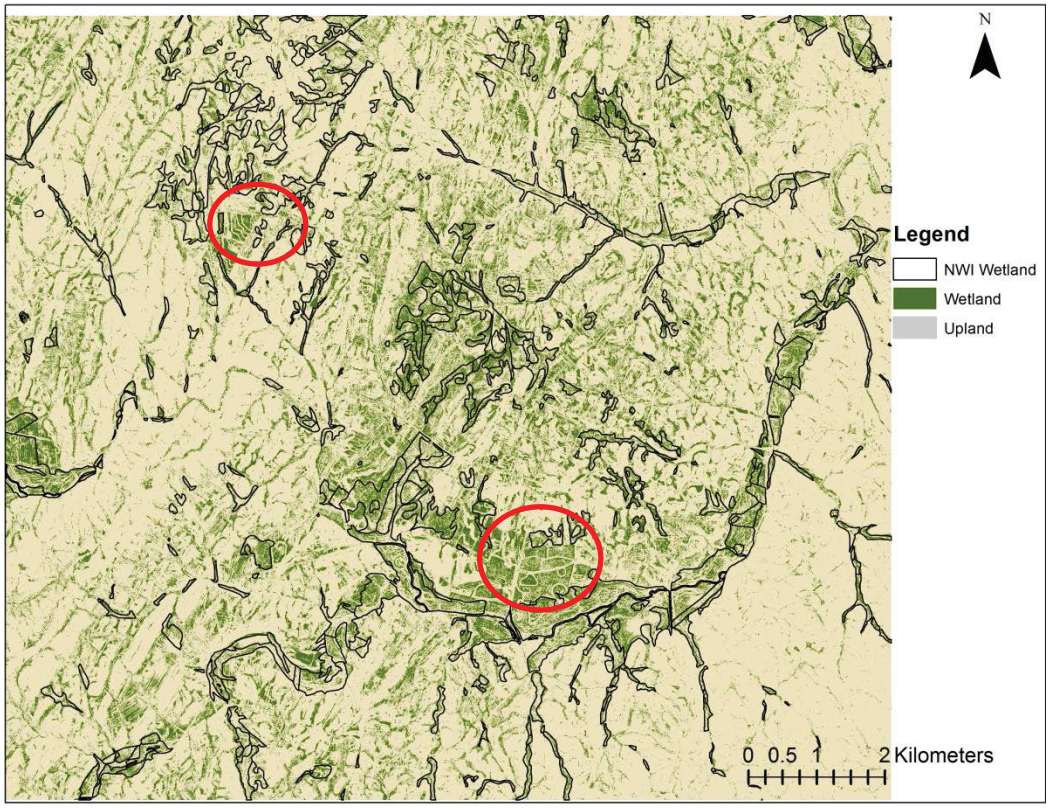

Fig. 3. Classification output of the most accurate random forest model overlaid with NWI wetlands. This model included wetness index calculated from distributed flow routing method and other terrain variables. The red circle indicates the general location of wetland mitigation site in the study area.

The classification output map of the most accurate and the least accurate shows the difference in performance of these two models in detecting wetlands in the study area. Classification that used the wetness index from single direction flow routing algorithm (Fig. 4) clearly underestimates the wetland in the area. In the classification map with the distributed flow (Fig. 3), the wetland area is greater. The NWI wetland areas are more accurately identified in this classification. It is also interesting to note that the wetland mitigation sites constructed in this area (marked in red circle) are clearly delineated, while these areas are not clear in the least accurate classification (Fig. 4).

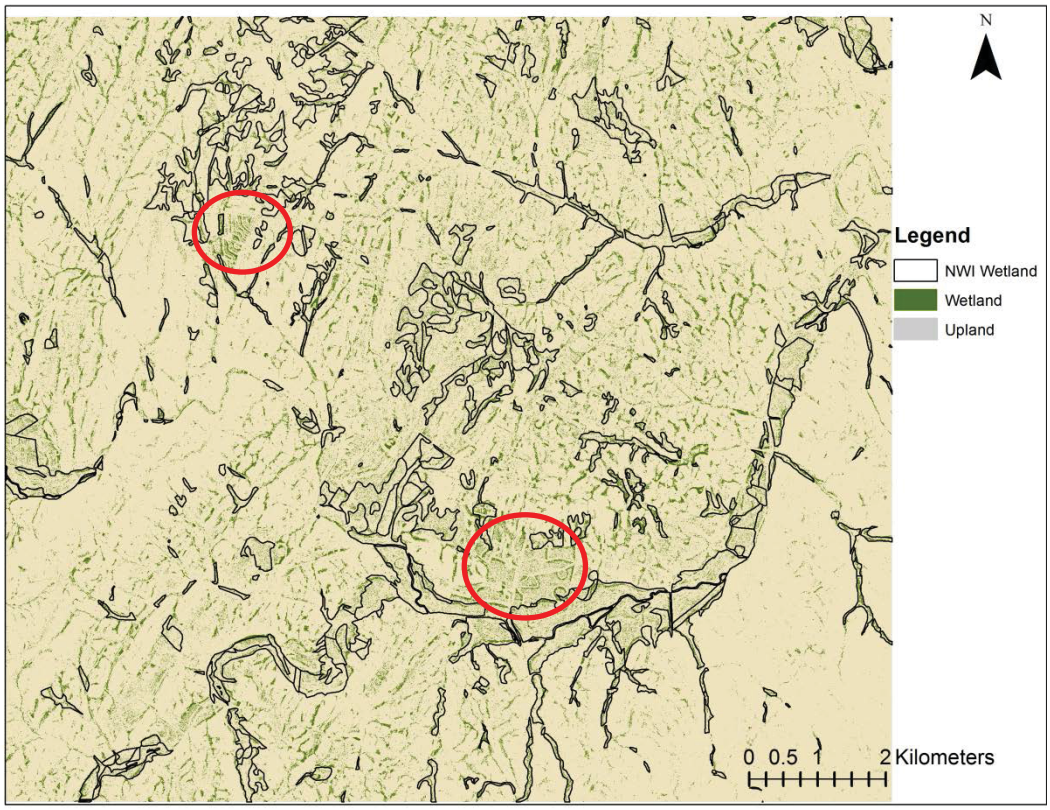

Fig. 4. Classification output of the least accurate random forest model, overlaid with NWI wetlands. This model included wetness index calculated from single direction flow routing method and other terrain variables. The red circle indicates the general location of wetland mitigation site in the study area.

Table 6 Summary table of variable importance for random forest classification

Classification with TWI_{SAGA}		**Classification with TWI_{MFD}**	
Variable	Score	Variable	Score
TWI_{SAGA}	100	TWI_{MFD}	100
Slope	89.41	Slope	77.12
TPI60	58.46	TPI60	19.49
Curvature	19.75	Curvature	19.28
Plan Curvature	18.52	Plan Curvature	17.94
Profile Curvature	15.51	Profile Curvature	15.51
Classification with D∞		**Classification with D8**	
Variable	Score	Variable	Score
Slope	100	Slope	100
TPI60	67.26	TPI60	77.12
$TWI_{D\infty}$	33.43	Curvature	19.49
Curvature	21.06	TWI_{D8}	19.28
Plan Curvature	20.02	Plan Curvature	17.94
Profile Curvature	14.40	Profile Curvature	15.51

Table 6 summarizes the importance of each terrain variable in the classification. The random forest algorithm ranks the most important variables in the classification. The topographic wetness index calculated using multiple flow direction (TWI_{SAGA} and TWI_{MFD}) was selected as the most important variable in the classification and it produced the highest overall accuracy. Slope and TPI60 were also ranked as important variables in this classification. However, in the classification using TWI_{D8} and $TWI_{D\infty}$, the most important variables were slope and TPI60. In the classification using $TWI_{D\infty}$, the wetness index was not ranked as an important variable.

3.3 Accuracy of depression identification

Table 7 Comparison of sinks with the NWI wetland and hydric/non-hydric soils

Depressions	**Yes**	**No**
NWI wetlands	31	84
Hydric soil	58	57
Non-Hydric soil	11	104

In order to avoid spurious sink (depressional) areas, we excluded sinks that were smaller than 10 pixel clusters. This resulted in total of 115 areas that were identified as sinks (Fig. 5). Out of the 115 sinks, 39 that were accessible were field-validated and classified as upland or wetlands. Out of 39 sinks, 20 classified as wetlands based on Cowardin et al. (1979). We also compared the identified sinks with the current NWI layer for the study area. Out of 115 sinks, only 31 were classified as wetlands on the NWI map (Table 7). Fifty-eight of the 115 sinks were mapped as hydric soils. The sinks are distributed throughout the landscape and include areas that are already classified as wetlands and also newer areas of constructed wetlands (mitigation banks) (Fig. 5).

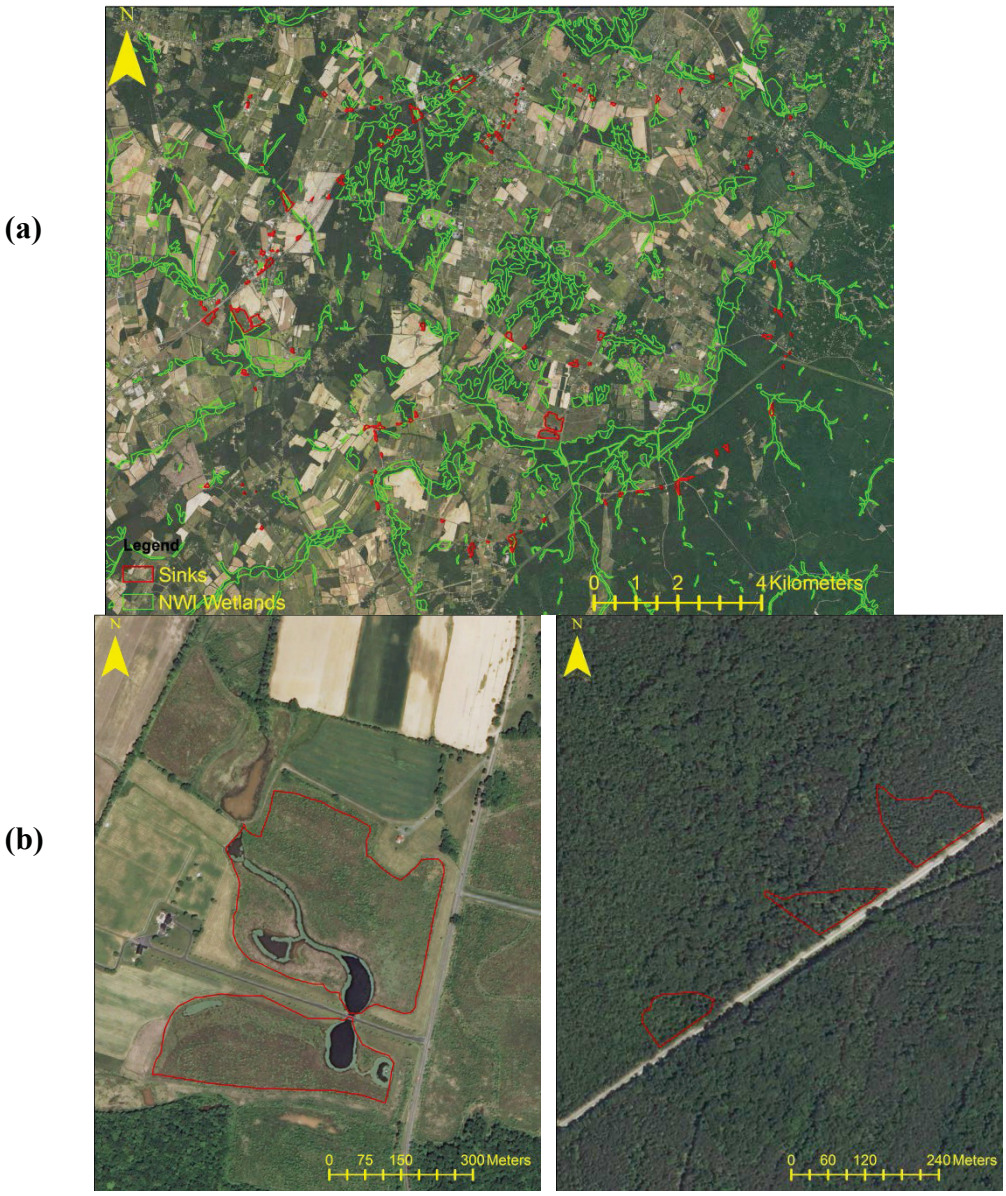

Fig. 5. Sinks identified in red polygons using depression filling technique (a) and examples of identified sinks (b). On the left is a new wetland site created for wetland mitigation, which is not mapped as wetlands in NWI and on the right are sinks identified in a forested area impounded by the road, which are mapped as wetlands in NWI.

4. Discussion

Data from optical sensors such as Landsat and microwave have been widely used for mapping wetlands. Topographic attributes were only used as ancillary data in these classification approaches. The use of topographic information for wetland identification was limited mainly

due to the low spatial resolution of available digital elevation products. However, with the availability of high resolution topographic information from lidar, the use of terrain attributes in mapping wetland is gaining wide attention.

In this study, we assessed the utility of primary and secondary terrain variables generated from high resolution lidar data for discriminating wetlands from uplands. The best classification results had an accuracy of 72%. The classification accuracy is similar to other studies which have utilized optical or radar data or combination of optical, radar, topographic and soils data. Our results indicate that that topographic information from lidar data alone can be used to accurately discriminate wetlands from uplands. The majority of the error in the classification resulted from upland areas being classified as wetlands as indicated by user's accuracy in the error matrix table. Many wetlands in the study area have been drained and/or cleared and changed into agriculture or pasture. The large commission error for wetlands achieved by this study indicates that most of these drained, converted areas were classified as wetland. Including farmed wetlands as wetlands even though they are currently without wetland vegetation is beneficial when the objective of making the map is to identify all possible wetland locations. This will also increase the overall accuracy of wetland mapping.

A number of flow routing algorithm have been proposed for calculation of topographic wetness index. The result of this study supports the use of more distributed flow routing algorithms for wetland delineation. The use of multiple flow direction has been shown to better characterize gradual ecologic transitions than single flow direction, based on soil moisture gradients, especially in areas of low topographic relief where slopes are more gradual and flow is less channelized (Lang et al., 2013). In this study, wetness index calculated with distributed flow (TWI_{SAGA} and TWI_{MFD}) yielded the highest accuracy. As expected, the accuracy of classification

with wetness index calculated from single direction flow routing algorithm (TWI_{D8}) provided the lowest accuracy. SAGA wetness index uses the same formula as the traditional topographic wetness index but it accounts for extensive lateral dispersion of water in flat terrain (Richardson et al., 2012). The classification with SAGA wetness and MFD wetness improved the producer's accuracies of wetland in both the classification.

Studies have shown that the spatial pattern of potential soil saturation based on wetness index values, which emphasizes the lateral flow, are better predictors of water accumulation during wet condition than in dry condition (Lang et al., 2013, McNamara et al., 2005 and Grayson et al., 1997). Considering the limitation of the wetness index in dry conditions, it is recommended using multiple topographic metrics that account for both the lateral and vertical flow (Grayson et al., 1997). The random forest classification provided a means to assess the relative importance of each terrain variable to discriminate wetlands from uplands. The variable importance factor for each classification presents the most effective data set for wetland/upland discrimination. For the best classification, the SAGA wetness index, slope and TPI60 were the most important variables. The same pattern was observed in the classification using wetness index calculated using MFD. However, in the classification with D∞, slope and TPI60 were more important variables during classification then the wetness index itself. Slope, TPI60 and curvature were more important than the wetness index in the classification using D8 flow routing method. This indicates that primary topographic attributes such as slope, curvature and topographic position index provide better representation of wetlands than wetness index calculated using single flow direction. The variable importance factor further shows that the wetness index calculated using a distributed flow routing algorithm is better at predicting wetland presence than those using a single flow direction. Slope has been widely used variable

for wetland detection. The TPI measures the difference between elevation at a point and the average elevation around it within a predetermined radius. These indices model local elevation changes highlighting curvature and have been found to be useful variable in wetland delineation (Lang et al., 2013 and Leonard et al., 2012). TPI is scale dependent and varies based on neighborhood size used for calculation. The appropriate neighborhood size will vary with the landscape and target topographic feature. We calculated the TPI with different neighborhood sizes and used the t-test to determine the TPI that provided the best discrimination between wetlands and uplands.

The result of depression identification suggests that a relatively simple depression filling technique can be used for improved identification of wetlands in woody areas and agricultural fields. The validation sampling for assessing the accuracy was small mainly due to restricted accessibility of the depressional areas. But it shows that majority of the areas identified as sinks were wetlands and were missed in the NWI maps. This might be due to the minimum mapping unit of the NWI, as majority of identified depressions were small. In addition, majority of these areas might have developed after NWI mapping. Human activities mainly construction of roads has modified the landscapes and created areas where water can accumulate. Although only 20 of these areas were validated as wetlands, the majority of the areas failed to be classified as wetlands because they failed to meet all the three criteria (hydrology, soil and vegetation) to be classified as wetlands. However, they had either one or two indicators present, typically missing only vegetation, indicating that if the current farming or pasturing land use is stopped they will regain wetland vegetation. It makes sense that areas that have hydric soils and wetland hydrology will support wetland vegetation. Further studies with large number of validation sample and different landscapes are needed to assess the sensitivity of this method in detecting wetlands. It

was also observed the human modification of landscape such as roads and small diversion and ditches have modified the flow of water creating wetlands where they did not exist before.

Topographic indices depend on the quality and resolution of the DEM from which they were derived. Lidar can produce a DEM with very fine spatial resolution. However, the fine resolution DEM is not always appropriate for mapping wetlands. The resolution of input DEM should reflect topographic variations which affect the spatial pattern of soil saturation leading to wetland formation. The resampling and smoothing technique was used in this study to reduce the DEM errors and topographic features that lead to unrealistic flow patterns. As shown by this study and others, lidar data can be used to map wetland distribution accurately. While the adoption of lidar data for forest inventory purposes is being closely examined by many interested parties, the use of lidar for wetland studies is really in its infancy. In addition to wetland inventorying and mapping, the ability of lidar data to accurately detect topographic features can provide information on wetland disturbance and restoration activities. For example, in Fig. 6 linear man-made drainage features evident in the aerial photo are also visible in lidar DEM. The DEM can potentially be processed to automatically identify these man-made features which can then be used to assess the wetland condition.

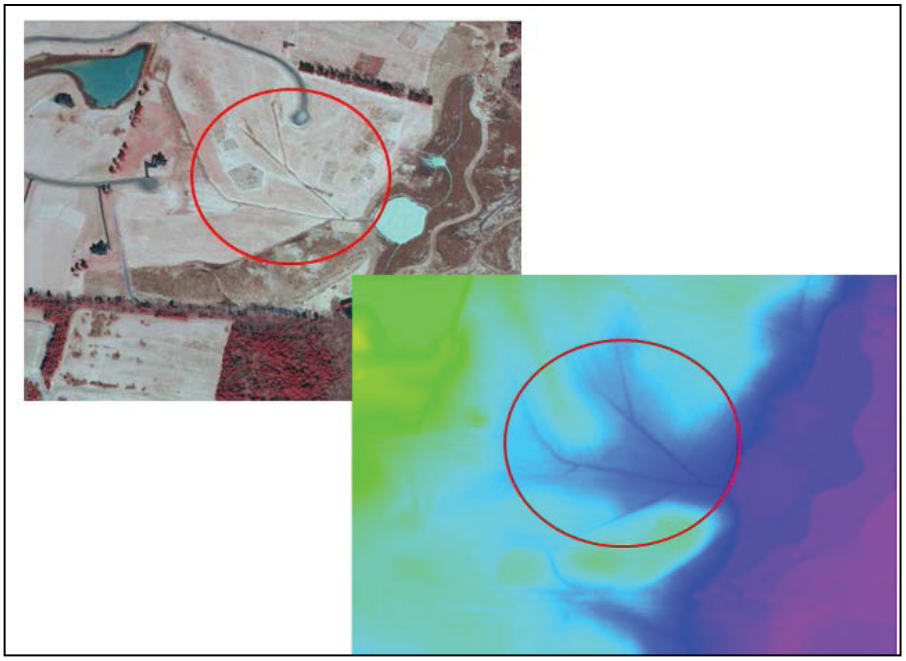

Fig. 6. Liner man-made drainage features aerial photo (top) and lidar DEM (bottom).

The use of lidar data in operational wetland mapping processes by federal agencies such as US Fish and Wildlife Service that makes NWI maps and state agencies that maps wetlands will eventually depend on the availability of lidar data. Use of topographic information derived will require a highly accurate DEM for which the lidar data has to be acquired during leaf off- period, with the goal of removing as much of 'confounding vegetation' as possible prior to the development analysis of the DEM. Removal of vegetation is a somewhat divergent goal between wetland studies and most vegetation/forestry studies. In practical terms, this means that it is generally not optimal to use the same lidar acquisition for forestry and wetlands applications (unless wetland vegetation is the primary interest). In addition, the accuracy of the DEM is affected by herbaceous vegetation, dense understory and presence of water. Future studies should focus on the parameters for optimal lidar data collection, timing and processes to reduce error in DEM in different landscapes and wetland types.

5. Conclusion

The predictive power of topographic variables derived from a high resolution lidar DEM using random forest classification was explored in this study. In summary, the topographic variables from a high resolution lidar data can produce accurate wetland maps, which are comparable to present wetland classification techniques using optical and microwave data in agricultural area and forests. The use of topography alone for wetland mapping is justified as movement of water in landscape is governed by the local topography. The use of multiple topographic variables allows us to account for both the lateral and vertical flows in a landscape and can be accurately derived using high resolution and accurate DEM derived from lidar. In combination with optical data, lidar data can significantly improve mapping of wetlands, especially forested wetlands in flat, low lying areas, which are difficult to map using optical data alone. The study also showed that the TWI calculated from more distributed flow routing methods and terrain variables that represent local topography are better suited for mapping wetlands. During our field validation we also observed that the wetness indices predicted a wet area in incised channels and meandering floodplains. Though these areas receive overbank flooding, they are not flooded long enough to develop hydric soil or hydrophytic vegetation and thus did not meet the criteria for wetland classification. Future research should focus on identifying best topographic indices in different landscape condition and wetland types. In addition to mapping the current wetland extent, the classification can also provide information on areas that apparently were wetlands before conversion to the current land use, and could easily be restored to wetlands by restoring the hydrology or vegetation. With the increasing availability of high resolution and accurate lidar based DEM, lidar data should be used in the operational wetland mapping activities. Use of lidar data for wetland mapping will be highly valuable in

areas where the availability of optical data will be limited due to cloud over and flat, low lying areas such as coastal plains, where small changes in topography leads to wetland formation.

References

Baker, C., Lawrence, R., Montagne, C., & Patten, D. (2006). Mapping wetlands and riparian areas using Landsat ETM+ imagery and decision-tree-based models. Wetlands, 26, 465-474

Baltsavias, E.P. (1999). Airborne laser scanning: basic relations and formulas. ISPRS Journal of Photogrammetry and Remote Sensing, 54, 199-214

Besnard, A.G., La Jeunesse, I., Pays, O., & Secondi, J. (2013). Topographic wetness index predicts the occurrence of bird species in floodplains. Diversity and Distributions, 19, 955-963

Beven, K.J., & Kirkby, M.J. (1979). A physically based, variable contributing area model of basin hydrology. Hydrological Sciences Bulletin, 24, 43-69

Boerner, R.J., Morris, S., Sutherland, E., & Hutchinson, T. (2000). Spatial variability in soil nitrogen dynamics after prescribed burning in Ohio mixed-oak forests. Landscape Ecology, 15, 425-439

Böhner, J., & Selige, T. (2006). Spatial prediction of soil attributes using terrain analysis and climate regionalisation. In J. Böhner, K. R. McCloy, & J. Strobl (Eds.),SAGA—analyses and modelling applications. Göttinger Geographische Abhandlungen, 115 (pp. 13–28 and 118–120). Göttingen, Germany: Verlag Goltze.

Breiman, L. (2001). Random Forests. Machine Learning, 45, 5-32

Case, B.S., Meng, F.-R., & Arp, P.A. (2005). Digital elevation modeling of soil type and drainage within small forested catchments. Canadian Journal of Soil Science, 85, 127-137

Corcoran, J., Knight, J., Brisco, B., Kaya, S., Cull, A., & Murnaghan, K. (2011). The integration of optical, topographic, and radar data for wetland mapping in northern Minnesota. Canadian Journal of Remote Sensing, 37, 564-582

Cowardin, L.M., Carter, V., Golet, F.C., & LaRoe, E.T. (1979) Classification of wetlands and deepwater habitats of the United States. U.S. Fish and Wildlife Service, Washington, DC. Report FWS/OBS-79/31

Creed, I., & Sass, G. (2011). Digital terrain analysis approaches for tracking hydrological and biogeochemical pathways and processes in forested landscapes. In D.F. Levia, D. Carlyle-Moses, & T. Tanaka (Eds.), Forest Hydrology and Biogeochemistry (pp. 69-100): Springer Netherlands

Creed, I.F., Sanford, S.E., Beall, F.D., Molot, L.A., & Dillon, P.J. (2003). Cryptic wetlands: integrating hidden wetlands in regression models of the export of dissolved organic carbon from forested landscapes. Hydrological Processes, 17, 3629-3648

Curie, F., Gaillard, S., Ducharne, A., & Bendjoudi, H. (2007). Geomorphological methods to characterise wetlands at the scale of the Seine watershed. Science of the Total Environment, 375, 59-68

Cutler, D.R., Edwards, T.C., Beard, K.H., Cutler, A., Hess, K.T., Gibson, J., & Lawler, J.J. (2007). Random Forests for Classification in Ecology. Ecology, 88, 2783-2792

Dahl, T.E., & Watmough, M.D. (2007). Current approaches to wetland status and trends monitoring in prairie Canada and the continental United States of America. Canadian Journal of Remote Sensing, 33, S17-S27

De Reu, J., Bourgeois, J., Bats, M., Zwertvaegher, A., Gelorini, V., De Smedt, P., Chu, W., Antrop, M., De Maeyer, P., Finke, P., Van Meirvenne, M., Verniers, J., & Crombé, P. (2013). Application of the topographic position index to heterogeneous landscapes. Geomorphology, 186, 39-49

Erskine, R.H., Green, T.R., Ramirez, J.A., & MacDonald, L.H. (2006). Comparison of grid-based algorithms for computing upslope contributing area. Water Resources Research, 42, W09416

Falkowski, M.J., Evans, J.S., Martinuzzi, S., Gessler, P.E., & Hudak, A.T. (2009). Characterizing forest succession with lidar data: An evaluation for the Inland Northwest, USA. Remote Sensing of Environment, 113, 946-956

Francés, A.P., & Lubczynski, M.W. (2011). Topsoil thickness prediction at the catchment scale by integration of invasive sampling, surface geophysics, remote sensing and statistical modeling. Journal of Hydrology, 405, 31-47

Gessler, P.E., Chadwick, O.A., Chamran, F., Althouse, L., & Holmes, K. (2000). Modeling Soil–Landscape and Ecosystem Properties Using Terrain Attributes. Soil Sci. Soc. Am. J., 64, 2046-2056

Grayson, R.B., Western, A.W., Chiew, F.H.S., & Blöschl, G. (1997). Preferred states in spatial soil moisture patterns: Local and nonlocal controls. Water Resources Research, 33, 2897-2908

Harvey, K.R., & Hill, G.J.E. (2001). Vegetation mapping of a tropical freshwater swamp in the Northern Territory, Australia: A comparison of aerial photography, Landsat TM and SPOT satellite imagery. International Journal of Remote Sensing, 22, 2911-2925

Hogg, A.R., & Holland, J. (2008). An evaluation of DEMs derived from LiDAR and photogrammetry for wetland mapping. The Forestry Chronicle, 84, 840-849

Hogg, A.R., & Todd, K.W. (2007). Automated discrimination of upland and wetland using terrain derivatives. Canadian Journal of Remote Sensing, 33, S68-S83

Hornberger, G.M., & Boyer, E.W. (1995). Recent advances in watershed modeling. Reviews of Geophysics, 33, 949-957

Iverson, L., Dale, M., Scott, C., & Prasad, A. (1997). A GIS-derived integrated moisture index to predict forest composition and productivity of Ohio forests (U.S.A.). Landscape Ecology, 12, 331-348

Kopecký, M., & Čížková, Š. (2010). Using topographic wetness index in vegetation ecology: does the algorithm matter? Applied Vegetation Science, 13, 450-459

Lang, M., McCarty, G., Oesterling, R., & Yeo, I.-Y. (2013). Topographic metrics for improved mapping of forested wetlands. Wetlands, 33, 141-155

Lang, M.W., Kasischke, E.S., Prince, S.D., & Pittman, K.W. (2008). Assessment of C-band synthetic aperture radar data for mapping and monitoring Coastal Plain forested wetlands in the Mid-Atlantic Region, U.S.A. Remote Sensing of Environment, 112, 4120-4130

Leonard, P.B., Baldwin, R.F., Homyack, J.A., & Wigley, T.B. (2012). Remote detection of small wetlands in the Atlantic coastal plain of North America: Local relief models, ground validation, and high-throughput computing. Forest Ecology and Management, 284, 107-115

Li, J., & Chen, W. (2005). A rule-based method for mapping Canada's wetlands using optical, radar and DEM data. International Journal of Remote Sensing, 26, 5051-5069

Li, S., MacMillan, R.A., Lobb, D.A., McConkey, B.G., Moulin, A., & Fraser, W.R. (2011). Lidar DEM error analyses and topographic depression identification in a hummocky landscape in the prairie region of Canada. Geomorphology, 129, 263-275

Liu, H., Bu, R., Liu, J., Leng, W., Hu, Y., Yang, L., & Liu, H. (2011). Predicting the wetland distributions under climate warming in the Great Xing'an Mountains, northeastern China. Ecological Research, 26, 605-613

Maxa, M., & Bolstad, P. (2009). Mapping northern wetlands with high resolution satellite images and LiDAR. Wetlands, 29, 248-260

McGarigal, K., Tagil, S., & Cushman, S. (2009). Surface metrics: an alternative to patch metrics for the quantification of landscape structure. Landscape Ecology, 24, 433-450

McNamara, J.P., Chandler, D., Seyfried, M., & Achet, S. (2005). Soil moisture states, lateral flow, and streamflow generation in a semi-arid, snowmelt-driven catchment. Hydrological Processes, 19, 4023-4038

Mitchell, J., Shrestha, R., Moore-Ellison, C., & Glenn, N. (2013). Single and multi-date Landsat classifications of basalt to support soil survey efforts. Remote Sensing, 5, 4857-4876

Mitsch, W.J., & Gosselink, J.G. (Eds.) (2007). Wetlands. Hoboken, N.J.: Wiley

Moore, I.D., Grayson, R.B., & Ladson, A.R. (1991). Digital terrain modeling: A review of hydrological, geomorphological, and biological applications. Hydrological Processes, 5, 3-30

Murphy, P.C., Ogilvie, J., Connor, K., & Arp, P. (2007). Mapping wetlands: A comparison of two different approaches for New Brunswick, Canada. Wetlands, 27, 846-854

O'Callaghan, J.F., & Mark, D.M. (1984). The extraction of drainage networks from digital elevation data. Computer Vision, Graphics, and Image Processing, 28, 323-344

Pantaleoni, E., Wynne, R.H., Galbraith, J.M., & Campbell, J.B. (2009). Mapping wetlands using ASTER data: a comparison between classification trees and logistic regression. International Journal of Remote Sensing, 30, 3423-3440

Planchon, O., & Darboux, F. (2002). A fast, simple and versatile algorithm to fill the depressions of digital elevation models. CATENA, 46, 159-176

Quinn, P., Beven, K., Chevallier, P., & Planchon, O. (1991). The prediction of hillslope flow paths for distributed hydrological modeling using digital terrain models. Hydrological Processes, 5, 59-79

Richardson, M.C., Fortin, M.J., & Branfireun, B.A. (2009). Hydrogeomorphic edge detection and delineation of landscape functional units from lidar digital elevation models. Water Resources Research, 45, W10441

Rodhe, A., & Seibert, J. (1999). Wetland occurrence in relation to topography: a test of topographic indices as moisture indicators. Agricultural and Forest Meteorology, 98–99, 325-340

Stolt, M.H., & Baker, J.C. (1995). Evaluation of national wetland inventory maps to inventory wetlands in the southern Blue Ridge of Virginia. Wetlands, 15, 346–353

Tagil, S., & Jenness, J. (2008). GIS-based automated landform classification and topographic, landcover and geologic attributes of landforms around the Yazoren Polje, Turkey. Journal of Applied Sciences, 8, pp. 910–921

Thomas, V., Treitz, P., McCaughey, J.H., & Morrison, I. (2006). Mapping stand-level forest biophysical variables for a mixedwood boreal forest using lidar: An examination of scanning density. Canadian Journal of Forest Research, 36, 34-47

Troyer, N.L.(2013). Monitoring hydrology in created wetland systems with clayey soils. MSc. Thesis. Department of Crop and Soil Environmental Sciences, Virginia Polytechnic Institute and State University. http://vtechworks.lib.vt.edu/bitstream/handle/10919/23806/Troyer_NL_T_2013.pdf?sequence=1

Wechsler, S.P. (2007). Uncertainties associated with digital elevation models for hydrologic applications: a review. Hydrology and Earth System Science, 11, 1481-1500

Wehr, A., & Lohr, U. (1999). Airborne laser scanning—an introduction and overview. ISPRS Journal of Photogrammetry and Remote Sensing, 54, 68-82

Weiss, A.D. (2001). Topographic position and landforms analysis. Poster Presentation, ESRI Users Conference, San Diego, CA

Werner, H. (2005). Assessment of National Wetland Inventory maps for Sequoia and Kings Canyon National Parks, 2000–2001. Sequoia and Kings Canyon National Parks, Three Rivers , CA : unpublished report.

Wilson, J.P., Aggett, G., Yongxin, D., & Lam, C.S. (2008). Water in the Landscape: A Review of Contemporary Flow Routing Algorithms. In Q. Zhou, B. Lees, & G.-a. Tang (Eds.), Advances in Digital Terrain Analysis (pp. 213-236): Springer Berlin Heidelberg

Wilson, J. P., & Gallant, J. C. (Eds.). (2000). Terrain Analysis: Principles and Applications. New York: Wiley.

Wright, C., & Gallant, A. (2007). Improved wetland remote sensing in Yellowstone National Park using classification trees to combine TM imagery and ancillary environmental data. Remote Sensing of Environment, 107, 582-605

Xiaoye Liu (2008). Airborne LiDAR for DEM generation: some critical issues. Progress in Physical Geography, 32, 31-49

Zedler, J.B., & Kercher, S. (2005). Wetland resources: Status, trends, ecosystem services, and restorability. Annual Review of Environment and Resources (pp. 39-74)

Zevenbergen, L.W., & Thorne, C.R. (1987). Quantitative analysis of land surface topography. Earth Surface Processes and Landforms, 12, 47-56

CHAPTER 5

Conclusions

Wetlands are an important component of the ecological infrastructure and provide numerous ecosystem services to human communities. These ecosystems are also greatly threatened due to human activities mainly conversion to commercial and agricultural use. To successfully manage and conserve wetlands, efficient tools and techniques are required to detect where wetlands are, the wetland type, and how they are changing. Landsat data for mapping and monitoring wetland is widely prevalent. However, multi-temporal analysis that extends beyond the use of two images in mapping and monitoring wetlands is very limited. Newer remote sensing technology such as lidar that can provide highly detailed and accurate topographic information is becoming more readily available. In this dissertation, we have developed techniques presented as three independent studies using multi-temporal Landsat data in forests and lidar in cropland and pastureland for improved mapping and monitoring of wetlands.

In the first study, we presented a trajectory based change detection technique using annual Landsat images to detect changes in wetlands. Wetlands exhibit high degree of natural temporal variability due to seasonal fluctuations in water level due to changes in precipitation, temperature and other environmental conditions as well as human influences. Our multi-temporal approach characterized the inter-annual variability in the spectral trends of different wetlands, which allowed us to discriminate actual change from the natural variability thus increasing the performance of the change detection method. The overall change detection accuracy achieved in this study was 89%, with a kappa value of 0.79. The resulting change map provides information on not only the current hotspots of wetland disturbance dynamics but also reconstructs the disturbance history and vegetation recovery. The information on the disturbance year along with

the wetland permit database maintained by the state agencies can be used to track unpermitted wetland disturbances and produce wetland change rates in an annual basis.

The majority of studies using trajectory-based disturbance analysis have focused on identifying disturbances in forested uplands. This is the first study, to our knowledge, that has used trajectory-based technique for wetland disturbance analysis. This approach has potential to be integrated with wetland monitoring activities of state environmental agencies to monitor compliance of wetland permits issued (year of disturbance, acreage of disturbance) and identify major stressors affecting wetland health. The disturbances can also be classified into temporal and permanent and a tracking of the areal losses can be tabulated. One of the major limitations of this method is identification of reference wetlands. We used an image based reference wetland identification technique. However, a field validated reference wetlands would be ideal for using this method across different geographic region.

In the second study, we extended the use of multi-temporal Landsat images in discrimination of forested wetlands and uplands. Forested wetlands are one of the most difficult wetlands to detect using remote sensing data, as the canopy prevents detection of soil saturation. In addition, the species present in forested wetland and neighboring uplands are often the same, making spectral discrimination difficult. Despite the presence of same species in wetlands and uplands, vegetation communities in wetlands exhibit different pattern (in terms of productivity, stress) due to soil saturation/flooding during growing season. These trends will not be visible using single image or multiple images within a single year. In this study, both intra and inter annual Landsat data dating back to 1995 were analyzed to extract temporal patterns of forested wetlands and uplands. The temporal metrics derived from the time series data discriminated between forested upland and wetland with an accuracy of 88.5%. Our results also showed that

the temporal metrics representing early growing season were most effective in classifying forested wetlands from uplands. The spectro-temporal approach accurately discriminated forested wetlands from uplands. This approach allowed us to tease out subtle differences that would not have been detectible using single image or even multiple images in a year.

In the third chapter, we assessed the predictive power of topographic variables derived from a high resolution lidar DEM in detecting wetlands. The study showed that the topographic variables from lidar data alone can detect wetland accurately 72% of the time, which are comparable to present wetland classification techniques using optical and microwave data. This automated wetland map accuracy compares favorably with the labor-intensive NWI map accuracy reported for the region. The use of topography alone for wetland mapping is justified as movement of water in the landscape is governed in large part by the local topography. The study also showed that the topographic wetness indices derived from a more distributed flow routing is better at predicting wetland location than channelized flow routing. We theorize that the combination of the temporal Landsat metrics discussed in the second study with lidar DEM and distributed flow routing data can significantly improve mapping of wetlands, especially forested wetlands in flat, low lying areas, which are difficult to map using optical data alone. The lidar DEM and distributed flow routing data can be used to identify depressions that do not appear on traditional topographic maps, and thus were likely overlooked in the production of NWI maps. The lidar data also provided information on various micro-topographic features. These features are mainly man-made, such as drainage features in Fig. 6 (Chapter 4) and man- made elevation patterns such as berms to facilitate water accumulation, which are indicative of wetland disturbance or restoration activities. The lidar data is able to identify depressions created by truncation or restriction of draingeways by infrastructure such as roads and railroads. In addition

to mapping the current wetland extent, the use of lidar data can also provide information on areas that were likely wetlands before conversion to the current land use, but do not occur on NWI maps. These locations can be used for identifying logically-successful wetland restoration sites. With the increasing availability of high resolution and accurate lidar based DEM, lidar data should be used in the operational wetland mapping activities.

Wetland vegetation and hydrology in an area may change, but the topography remains same. Integration of topographic information derived from lidar data in the operational mapping of wetlands should significantly improve the accuracy of wetland map products. The accuracy of optical or radar data in wetland mapping will depend on availability of optimal data. Data acquired during abnormal weather condition such as drought or excessive rainfall will affect their usefulness. However, topographic information from lidar is not affected by such limitations. Utility of lidar for wetland mapping will be especially high in areas where the availability of optical data will be limited due to clouds. Although we did not investigate in our study, synergistic use of multi-temporal Landsat and lidar may provide a superior approach to wetland mapping.

Overall, the results of this study demonstrated that both lidar and Landsat time series data can significantly improve wetland mapping and monitoring. Landsat data because of its spatial coverage (swath width of 185 km), spatial resolution of 30 m, spectral bands in visible and near infrared region and free availability is best suited for operational mapping and monitoring of wetland over larger geographic regions. Since highly processed Landsat data is now freely available, the multi-temporal approach presented in this study can be an integral aspect for wetland mapping and monitoring framework of various concerned stakeholders such as the state environmental agencies and the NWI program. Although compiling the initial set of images is

time-consuming, the archive can be archived for future uses and expanded over time. Although lidar data is expensive and is not systematically collected at the same location, it is becoming more available with time and should be utilized by wetland regulatory agencies.

Findings of this study opens avenue for numerous potential researches that will further contribute to mapping and monitoring of wetlands. Some future research direction could include:

- Use the temporal trajectory to classify different disturbance events and identify magnitude of disturbance. This will help provide information on major stressors to wetlands.
- Use of temporal trajectory to monitor restored wetland site. A framework can be developed to compare the trajectory of reference wetland sites to that of restored or created site to compare biophysical properties such as biomass, leaf area index, woody canopy estimate.
- Testing of our methods on coniferous wetland vegetation. Due to limitation of field data, we only assessed the classification accuracy of broadleaf forested wetland and upland. Coniferous forested wetlands are most difficult to map as they have canopy throughout the year. Our method of using temporal information from time series Landsat data should also be assessed to see how well it can classify coniferous forested wetlands.
- Use of time series information from Landsat can be combined with data on long term hydrology to investigate how changes in soil saturation/flooding affects the reflectance properties of Landsat. This information can be used to identify wetlands with different level of flooding and saturation.
- Use of the multi-temporal approach to assess the long term trend in wetlands. A characteristic curve for wetlands area can be generated by combining Landsat data from

multiple years. Deviations from these curves can be analyzed to assess the response against events such as drought.

- Use of lidar data can be extended beyond mapping of wetlands. Different research questions that will provide insight into the functioning of wetland can be explored; such as can the topographic information explain the spatial pattern of vegetation in wetland and upland? Can the lidar data classify wetland area with different hydroperiods?